Titre: Title:	Targeted derivatization of rhodamine B isothiocyanate-chitosan for the study of its interaction with cells
Auteur: Author:	Odette Ma
Date:	2006
Type:	Mémoire ou thèse / Dissertation or Thesis
Référence: Citation:	Ma, O. (2006). Targeted derivatization of rhodamine B isothiocyanate-chitosan for the study of its interaction with cells [Mémoire de maîtrise, École Polytechnique de Montréal]. PolyPublie. https://publications.polymtl.ca/7723/

URL de PolyPublie: PolyPublie URL:	https://publications.polymtl.ca/7723/
Directeurs de recherche: Advisors:	Caroline D. Hoemann, & Michael D. Buschmann
Programme: Program:	Non spécifié

UNIVERSITÉ DE MONTRÉAL

TARGETED DERIVATIZATION OF RHODAMINE B ISOTHIOCYANATE-CHITOSAN FOR THE STUDY OF ITS INTERACTION WITH CELLS

ODETTE MA
INSTITUT DE GÉNIE BIOMÉDICAL
ÉCOLE POLYTECHNIQUE DE MONTRÉAL

MÉMOIRE PRÉSENTÉ EN VUE DE L'OBTENTION
DU DIPLÔME DE MAÎTRISE ÈS SCIENCES APPLIQUÉES
(GÉNIE BIOMÉDICAL)
MARS 2006

Your file Votre référence
ISBN: 978-0-494-17954-3
Our file Notre référence
ISBN: 978-0-494-17954-3

UNIVERSITÉ DE MONTRÉAL
ÉCOLE POLYTECHNIQUE DE MONTRÉAL

Ce mémoire intitulé:

TARGETED DERIVATIZATION OF RHODAMINE B ISOTHIOCYANATE-CHITOSAN FOR THE STUDY OF ITS INTERACTION WITH CELLS

presenté par: MA, Odette
en vue de l'obtention du diplôme de : Maîtrise ès sciences apliquées
a été dûment accepté par le jury d'examen constitué de :

M. DECRESCENZO Gregory, Ph.D., président
Mme HOEMANN Caroline, Ph.D., membre et directrice de recherche
M. BUSCHMANN Michael, Ph.D., membre et codirecteur de recherche
Mme HEUZEY Marie-Claude, Ph.D., membre

Dedications

I would like to dedicate this thesis to Dr. Pierre Savard. Thank you for all you have done to make my experience at École Polytechnique more pleaseant

Acknowledgements

I would like to extend my thanks and appreciation to the numerous people who have contributed to the project that is presented here in this thesis. First on my list, is my research director, Dr. Caroline Hoemann. She has provided countless hours of support through her lightening fast revisions of reports and protocols and improvement on laboratory skills and techniques. It is difficult to find this kind of dedication in the busy schedules of researchers today, and for that, I am greatful. I would also like to thank my co-director, Dr. Michael Buschmann, for his support and advice, and also for the free access he gave to his personal library.

From the Buschmann laboratory, I am indebted to my wonderful collegues and especially to Marc Lavertu, Nicolas Tran-Khanh, Tan-Dat Tran, Anne Gigout, Marc Thibault, Pei-Lian Ma, Julie Tremblay, Jun Sun, Dominic Filion, Stephane Methot, Anik Chevrier, Daniela Martens, Sophie Nguyen, and Monica Iliescu who have always created a lively and stimulating environment in which to work. Their sense of humor and helpful discussions and suggestions on experiments have been invaluable for my experience here at École Polytechnique. I am thankful also for the collaborators (Dr. Piotr Kujawa at the Winnik Lab, Patrick Lajoie at the Nabi Laboratory, McKee Laboratory, and Henderson Laboratory) that have offered their helping hands in the completion of this project.

And without Josée-Christine Levesque and Diane Giroux to point me in the right direction in the administrative shuffle, I would have been forever lost. I am eternally grateful for several faculty and my friends both here and abroad who provided me moral support throughout my studies here. I am grateful to the Canadian Arthritis Network and Biosyntech Ltd, for providing financial support and inspiration.

Finally, I am grateful for the works of S. Fiedler et al. in J. Chem. Phys. 117, 8867 (2002) and J. Phys. Chem. A 109, 4512 (2005). They are encouraging and a fascinating read.

Summary

Cartilage protects the ends of bones in healthy joints and is responsible for absorbing shock and allowing bones to glide over one another during movement. In joints with osteoarthritis this protective covering is damaged and worn away -- permitting bones to be exposed to each other resulting in pain, swelling, and the loss of joint motion. Since cartilage is avascular, damaged cartilage resulting from disease or injury has limited spontaneous healing abilities and regeneration capabilities. Other than monetary cost, arthritis can have a great impact on the mental and emotional health due to limitations of joint function. The prevalence of osteoarthritis increases with age. Therefore, there are clear financial and health incentives to solve this problem.

It has been shown that cartilage lesions can be repaired using chitosan and surgical bone marrow stimulations. In this study, our aim is to further the understanding on how chitosan can stimulate cartilage lesion repairs. Our hypotheses are: (1) chitosan's degree of deacetylation and molecular weight can affect cell binding and uptake, and (2) fluorescent chitosan can be used to quantify and therefore compare cell binding and uptake, given that the chitosans are similary derivatized. The objectives are thus to synthesize 6 chitosans originating from 3 degree of deactyaltions and 2 molecular weights at the same labeling efficiency and to determine their effects on cells. After their effects are established, they can be used to study the interactions of chitosan on cells involved in cartilage repair.

Gathered details on the synthesis of fluorescent chitosan from literature lead us to develop a protocol where medical grade chitosan that were well characterized for their degree of deacetylation and molecular weight are dissolved overnight in an acidic medium followed by an addition of an equal volume of methanol to the chitosan solution. The mixture is homogenized for three hours under constant stirring and degassed for 15 minutes prior to the addition of rhodamine B isothiocyanate, the fluorescent compound, which is suspended in methanol at a concentration of 4mM. The reaction is allowed to proceed for a period of 3 hours to overnight.

Several variables are optimized to achieve acceptable labeling conditions, which include the type and concentration of acid used to dissolve chitosan, number of additions of fluorphore to the reaction, reaction time, and product recovery method. Since the coupling of an isothiocyanate group to a primary amine is optimal at a pH greater than 9 and chitosan can only be soluble under a pH of 6.5, a series of experiments were initiated in order to determine the type of acid to use and at what quantity. This was necessary since sysnthesis of a homogenously labeled fluorescent chitosan can only be achieved under solution.

With the introduction of an equal volume of methanol to the chitosan solution, a phenonom we termed *cross over* behavior was observed, where the pH would increase after the *cross over point*, which refers to a concentration of [acid]/[glucosamine] expressed as percentages. The *cross over points* for acetic acid are found in the low 60% [acetic acid]/[NH_2] for all degree of deacetylations tested. For lactic and hydrochloric acid, the *cross over points* exist in the 90% [acid]/[NH2] range. The implication of the cross-over points is that when experiements are carried out at acid concentrations greater than the concentrations indicated at the *cross over points*, a higher labeling efficiency than expected is achieved. In order to achieve a targeted labeling efficiency faster and with less material, it is recommended that the experiements be carried out in this range. However, the pH must stay as close to 6.5 as possible. Therefore, our experiments have suggested that acetic acid at 70% [acetic acid]/[NH_2] is optimal for chitosan labeling conditions.

Serveral kinetics experiements were also conducted to establish the reaction time since literature suggests that the reaction can take place from as little as one hour to as much as 24 hours. From our experiments, we have determined that 18 hours would be the most pratical and optimal reaction time. Using a stock solution of fluorescent chitosan product at 1 mg/mL, we have diluted the solution to 0.1, 0.05 and 0.025 mg / mL for the measurement of its absorbance and fluorescence and have shown a linear relationship between these two variables. We have found that the final chitosan products follow the fluorescence curve as a function of absorbance of rhodamine B rather than the reactive rhodamine B isothiocyanate which was used to synthesize the fluorescent

chitosan. Therefore, rhodamine B was used to calibrate the concentration of fluorphore in the final chitosan product using an extinction coefficient of 90100 $(M \cdot cm)^{-1}$ that we have determined from experiments.

Using the optimal labeling conditions determined from the experiements, we have synthesized 6 RITC bound chitosans at a labeling efficiency of 0.97 +/- 0.06% mol RITC/mol chitosan. The results of their interaction with human embryonic kidney cells (HEK293) suggest that chitosan particle size decreases with increasing degree of deacetylations. However, no particle size differences are visible when molecular weights are varied. We were able to show that HEK293 and rabbit bone marrow cells were not affected vitally even in the prescence of a high concentration of RITC-chitosan and that chitosan is responsible for mediating cellular uptake rather than the fluroscent molecule, rhodamine B. Futhermore, our experiements suggest that chitosan are recycled and incorporated into the cell within a two-week period

Abstract

Crustaceans, mollusks, and insects have a common component in their exoskeleton, a linear polysaccharide called chitin, which is similar to cellulose by the beta (1-4) linkages between monomer units of N-acetyl glucosamine. Chitin is insoluble in aqueous solvents; however, the N- deacetylation of chitin yields a chitosan derivative with positively charged glucosamine subunits that render chitosan acid-soluble. Since chitosan is a natural product, and because deacetylation gives an irregular distribution of N-acetyl glucosamine and glucosamine, the degree of deacetylation (DDA) and molecular weight (MW) of chitosan are variable, and this variablility can have an effect on biological activity. For example, chitosan biodegradability is proportional to its acetyl content, with faster degradation for lower deacetylation levels. Chitosan has been found to stimulate cartilage repair in animal models when mixed into whole blood and deposited as an implant in surgically treated defects. To understand the influence of chitosan on wound repair, we took the approach of labeling chitosan with a fluorescent tag, in order to follow the binding and uptake of chitosan by repair cells. We coupled chitosan of different DDA and MW to a fluorophore rhodamine B isothyocyanate. The labeled chitosans formed large micron-size aggregates when added to culture media for all DDAs and molecular masses tested, including 71%DDA to 95%DDA and 50,000 to 200,000 Da. RITC-chitosan aggregates using 80%DDA to 83%DDA chitosan were internalized by HEK293 cells and the label retained in intracellular vesicles up to 2 weeks after internalization and cell passage, suggesting that the RITC-chitosan is metabolized and the rhodamine-glucosamine monomer recycled into intracellular structures.

Condensé en Français

Introduction de la problématique

L'arthrite fait partie d'un groupe de maladies dont le nom provient du Grec, et qui signifie inflammation des articulations. Elle inclut des maladies auto-immunes telles que l'arthrite rhumatoïde et psoriasique, des infections telles que l'arthrite septique, et le type d'arthrite le plus commune, l'ostéoarthrite, qui est une maladie dégénérative (Felson, 1998). Dans une articulation saine, le cartilage protège les extrémités des os, amortit les chocs et permet le glissement des os lors des mouvements. Les os et le cartilage baignent dans le liquide synovial et sont entourés par la membrane synoviale, elle-même encerclée par la capsule, qui ferme l'articulation (Figure 1, à gauche). Dans un cas d'ostéoarthrite (Figure 1, à droite), le cartilage protecteur est endommagé et érodé. Les os sont alors exposés l'un à l'autre, entraînant l'apparition de symptômes tels que la douleur, l'enflement et la perte de mobilité de l'articulation.

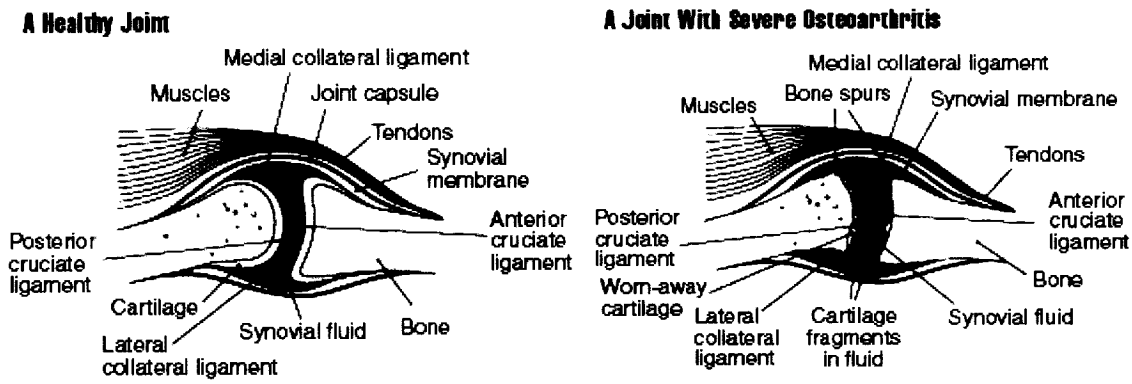

Figure 1. Une articulation saine (gauche) et une articulation atteinte d'ostéoarthrite (droite).

Le cartilage est un tissu avasculaire composé de 60-78% d'eau. Les trois autres composants majoritaires de ce tissu sont les chondrocytes, le collagène et les protéoglycanes. Le collagène et les protéoglycanes constituent la matrice, tandis que les chondrocytes sont les cellules qui synthétisent et maintiennent l'intégrité du cartilage. Lorsque le cartilage est endommagé, suite à un blessure, ou à une maladie, celui-ci ne peut se régénérer à cause de l'absence de vascularisation.

L'ostéoarthrite touche à la fois les hommes et les femmes. Cependant, en moyenne, plus d'hommes souffrent d'ostéoarthrite avant l'âge de 45 ans que de femmes. Par contre, entre 45 et 55 ans, l'ostéoarthrite est détectée avec une fréquence égale chez les hommes et les femmes. Enfin, au delà de 55 ans cette maladie affecte plus de femmes que d'hommes (Moskowitz et al., 1992). Selon Statistiques Canada (2005), 48% des femmes de plus de 65 ans étaient affectées par l'arthrite ou les rhumatismes en 2000-2001, cela représentait environ 5% de la population canadienne en 2002. Selon le NIAMS (National Institute of Arthritis and Musculoskeletal and Skin Disease), 21 milliards de personnes étaient touchées par l'ostéoarthrite aux Etats-Unis en 2002, soit 10% de la population. De plus, les estimations prévoient qu'en 2040, 20,4% de la population des États-Unis (U.S. Census Bureau, 2004) et 22,6% de celle du Canada atteindront un âge de 65 ans ou plus (Statistics Canada, 2005).

L'arthrite était la cause principale d'environ 744 000 hospitalisations en 1997, ce qui représentait 3% de toutes les hospitalisations (Lethbridge-Cejku, 2003). Dans la même année, le nombre de consultations en soins ambulatoires s'est élevé à 36,5 milliards pour l'arthrite et les problèmes rhumatismaux, c'est à dire 4% de toutes les consultations en soins ambulatoires (Hootman, Helmick et Schappert, 2002). Le coût médical s'élevait alors à 86 milliards de dollars pour l'arthrite et les maladies rhumatismales dont 51,1 milliards de dollars en coûts médicaux directs, et 35,1 milliards de dollars en coûts indirects tels que les pertes de salaires (CDC, 2004). D'autre part, l'arthrite peut également avoir un grand impact sur la santé mentale et émotive des patients. En cas d'arthrite, le risque de dépression majeure est de 18,1%. La limitation des mouvements due à la maladie est le facteur le plus fortement associé à la dépression (Dunlopp et al., 2004).

Les traitements les plus courants dans les cas de l'ostéoarthrites incluent le contrôle du poids, les exercices, la thérapie par la chaleur et le froid, les anti-inflammatoires, les anti-douleurs et d'autres suppléments, la gestion du stress, les injections dans l'articulation, et la chirurgie telle que le remplacement du genou ou de la hanche (Lethbridge-Cejku, 2003). Récemment, des chercheurs du groupe du Professeur M. Buschmann de l'École Polytechnique de Montréal ont étudié la réparation des lésions

du cartilage en combinant la stimulation de la moelle osseuse par chirurgie et l'injection d'un gel dans la lésion. Ce gel se compose de chitosane, de glycérol phosphate et de sang entier autologue[1] (Hoemann et al, 2005, 2006 ; Chevrier et al, 2006). L'objectif du travail présenté, était d'améliorer la compréhension du mécanisme par lequel le chitosane stimule la réparation du cartilage, lors d'un traitement basé sur la stimulation de la moelle osseuse. En particulier, nous avons voulu étudier l'effet de la structure du chitosane sur l'interaction et l'intégration du chitosane par les cellules impliquées dans la réparation de cartilage.

Le chitosane

La chitine (Figure 1a) a pour nom chimique, la 2-amino-2-déoxy-ß-D-glcopyranose. C'est un produit organique naturel extrait de crustacés, de mollusques, ou de l'exosquelette des insectes. La chitine est constituée d'une chaîne linéaire de groupes acétylglucosamine. En tant que matériel organique, son abondance naturelle est classée en deuxième place, juste après la cellulose (Figure 1c), découverte 30 ans avant la chitine. L'utilisation de la chitine comme produit biologique est devenue populaire dans les années soixante dix (Roberts, 1992). En 1811, Braconnot l'avait isolée pour la première fois (Braconnot, 1811). La chitine s'est avérée être biocompatible, biodégradable (Tokura et autres, 1983), et bioactive (Prudden et al., 1970 ; Yano et al., 1985 ; Nakajima, Atsumi et Kifune, 1985) et ne crée pas de réponse de rejet chez l'hôte (Palapura et Kohn, 1992 ; Zhao et autres, 1990 ; Nakajima et al. 1986 ; Sapelli et al. 1986). La chitine a une solubilité limitée dans trois catégories de solvants : les solutions aqueuses de sels neutres (Clark et Smith, 1936 ; Von Weimarn, 1927), les acides forts concentrés (Lee, 1974 ; Austin, 1984), les solvants organiques comme certains acides carboxyliques ou des mélanges de solvants organiques spécifiques. Non seulement la dissolution de la chitine se fait rarement à température ambiante, mais en plus, après dissolution, une modification ou une hydrolyse du polymère est observable (Capozza,

[1] Autologue -- Se dit de toute substance organique prélevée sur le sujet lui-même

1975). Le nombre limité de solvants utilisables et la difficile dissolution de la chitine restreignent son champ d'application.

Le chitosane, ou 2-acétamido-2-déoxy-ß-D-glucopyranose est un produit dérivé de la chitine, par déacétylation. (Figure 1b). Le chitosane est une base qui est facilement soluble dans des solutions d'acides diluées, et qui forme des sels hydrosolubles avec une grande variété d'acides organiques (Roberts, 1992). Comme la chitine, le chitosane est également biocompatible, biodégradable, et bioactif. Il a également été testé pour la mutagénicité, la toxicité aiguë et subaiguë, la toxicité chronique, la pyrogénicité, l'hémolyse[2] et la sensibilisation (Seo, 1990) et s'est avéré être une matière biologique sûre.

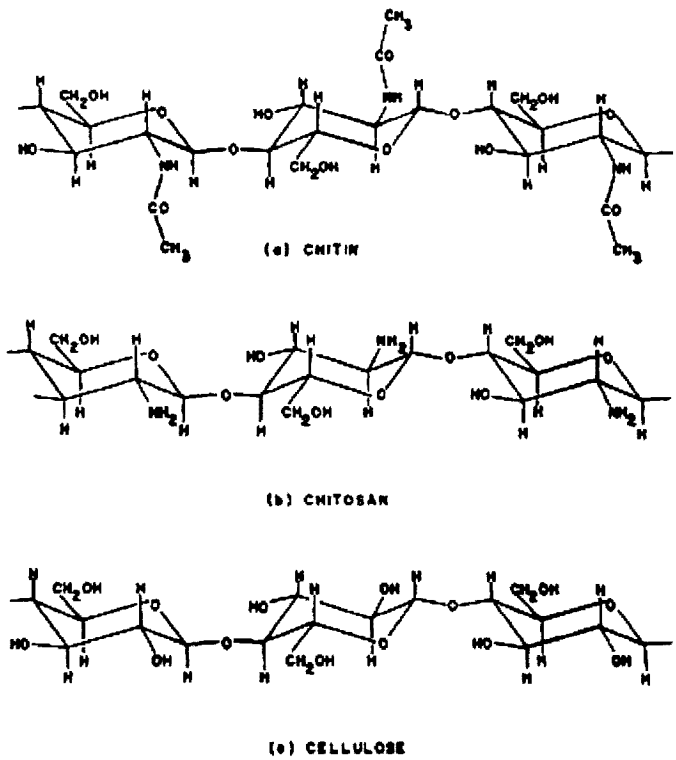

Figure 2. Structure chimique (a) de la chitine, (b) du chitosane et (c) de la cellulose. Courtoisie de Marc Lavertu (2005).

[2] Hémolyse -- Destruction des globules rouges provoquant la libération de l'hémoglobine

Le degré de déacétylation et le poids moléculaire du chitosane

Pour décrire le chitosane, trois paramètres sont d'une importance critique pour des applications biomédicales. Ces paramètres sont : la pureté, le Degré de DéAcétylation (DDA) et le Poids Moléculaire (PM).

La pureté : La chitine peut être obtenue à partir de sources diverses et peu contenir des impuretés telles que le calcium, le phosphore, et des caroténoïdes. Les propriétés physico-chimiques de la chitine et du chitosane sont fortement liées à leurs origines. Dépendamment de la source de chitine, certains DDA ou PM (Shepherd, Reader, and Falshaw, 1997; Rhazi et al., 2000) peuvent être atteints. La chitine pure est un polymère composé d'une chaîne de monomères de N-acétyle-D-glucosamine, tandis que le chitosane est un polymère composé d'unités de D-glucosamine et de N-acétyle-D-glucosamine.

Le Degré de DéAcétylation : Le DDA décrit la fraction du polymère qui est sous forme de D-glucosamine. Quand le DDA est proche de 1, la propriété de la molécule est plus proche du chitosane pur, et la plupart des monomères dans le polymère sont des unités de D-glucosamine. Le poids moléculaire du chitosane, mesuré en Daltons (Da) ou kilo-Daltons (kDa), permet de déterminer la longueur de la molécule si le poids moléculaire monomérique moyen est connu. Le degré de déacétylation et le poids moléculaire sont des paramètres importants à considérer puisqu'ils déterminent les applications particulières des chitosanes.

Le Poids Moléculaire : le PM monomérique moyen d'une molécule de chitosane déacétylée à un certain degré, est déterminé par l'addition de deux produits : le produit de la masse moléculaire de la chitine pure (N-acétyle-D-glucosamine, 203 g/mole) avec la fraction du polymère acétylée, plus le produit de la masse moléculaire du chitosane pur (D-glucosamine, 163 g/mole) avec le degré de déacétylation, comme indiqué dans la formule suivante :

$$MW_{avg} = 203\,\text{g/mol}\,(1 - \text{DDA}) + 161\,\text{g/mol}\,(\text{DDA}),$$

où le DDA représente la fraction du polymère déacétylée.

Le chitosane est une base qui forme un sel avec les acides. La solubilité des polyélectrolytes de chitosane dépend de la nature des anions impliqués. Dans les cas où le sel de chitosane a une solubilité aqueuse limitée, le PM, le DDA, et la quantité d'acide présent sont des facteurs importants qui doivent être pris en considération. Bien que le chitosane n'est pas connu pour être très soluble dans les solvants organiques, l'addition de volumes considérables de solvants polaires aux solutions de chitosane dissous dans l'acide acétique, ne fera pas précipiter le polymère (Roberts, 1992). Ceci implique que l'ajout jusqu'à 70%, en volume, d'alcools tels que le méthanol, le butanol, l'éthylène-glycol, le glycol diéthylène, le glycol triéthylène, l'acétone, et le formamide peut être toléré par la solution du chitosane dissous dans l'acide acétique. En ce qui concerne le 2-propanol et le glycérol seulement 40% et 80 % respectivement, en volume, peuvent être ajoutés (Roberts, 1992).

Le marquage du chitosane

Le marquage du chitosane avec un fluorochrome est un outil qui a été très utilisé lors d'analyses de la fixation et de l'intégration du chitosane ou de particules chitosane-ADN par des cellules. La distribution et le métabolisme du chitosane chez certains organismes ont également été étudiés de cette manière (Ishii et al., 2001 ; Huang et al., 2002 ; Qaqish et Amiji, 1999 ; Yamada et al., 2001 ; Onishi et Machida, 1999). Le marquage comprend deux étapes. La première étape est une dérivatisation chimique utilisant un ratio chitosane : fluorochrome particulier et un temps de réaction fixé. La deuxième étape consiste à enlever le fluorochrome n'ayant pas réagi. Afin de comparer le comportement de molécules de chitosane structurellement distinctes, la technique de marquage étudiée devait permettre d'atteindre des efficacités de marquage semblables dans tout les cas. Les conditions de marquage doivent également permettre de supprimer les contaminations. Par exemple, la présence d'endotoxines microbiennes a un effet toxique sur la viabilité des cellules et induit l'expression de marqueurs inflammatoires dans les leucocytes. Ces toxines sont très difficiles à éliminer,

Les objectifs

Notre groupe de recherche de l'École Polytechnique a découvert que le mélange chitosane- phosphate de glycérol/ caillot sanguin stimule la réparation du cartilage lors d'une stimulation de la moelle (Hoemann et al., 2005). Les mécanismes impliqués dans la réparation du cartilage par le mélange chitosane phosphate de glycérol/ sang incluent la stimulation de l'os sous-chondral et l'angiogenèse (Chevrier et al., 2005). Pour comprendre comment l'implant de chitosane mélangé avec du sang exerce une influence sur les cellules de la moelle, des dérivés de chitosane fluorescents peuvent être employés. En exposant les cellules de la moelle à ce chitosane marqué, *in vitro* ou *in vivo*, l'effet de la fixation et de l'intégration du chitosane sur les réponses cellulaires pourraient être éclairci. Nous avons choisi de marquer le chitosane avec le dérivé IsothioCyanate de la Rhodamine B (RITC), un marqueur qui maintient ses propriétés fluorescentes à pH 5.0, le pH des endosomes. Ainsi, cela permet de détecter l'intégration du chitosane dans les cellules vivantes. Avant d'étudier les cellules de la moelle, nous avons utilisé une lignée de fibroblastes HEK293 pour déterminer si la fixation et l'intégration du chitosane marqué pourraient être affecté par le DDA ou le poids moléculaire. Pour cette finalité, nous avons développé un protocole de production de chitosane avec des DDA et des poids moléculaire distincts, mais avec un degré identique de marquage.

Les résultats

Dans cette étude, des expériences de marquages préliminaires avec la rhodamine B isothiocyanate (RITC) et le vert Orégon (OG) nous ont permis de déterminer qu'une procédure de marquage efficace nécessite un contrôle de la protonation des monomères de glucosamine du chitosane. La protonation est contrôlée par le type et la quantité d'acide employé pour solubiliser le chitosane avant les différentes étapes de marquage. Au début de l'expérience, notre hypothèse était que l'augmentation du pH dû à l'ajout de bêta phosphate de glycérol augmenterait l'efficacité du marquage. Cependant, la présence de ce sel divalent entraîne la précipitation du chitosane, après l'addition d'un volume de méthanol dans la solution. Malheureusement, l'ajout de méthanol est nécessaire pour la solubilisation du fluorophore, qui est hydrophobe. Le chitosane

précipité re-dissout dans l'acide acétique avec du bêta phosphate de glycérol, et du méthanol donne une efficacité de marquage inférieure (0,3% mole/mole dérivé, 2,8% rendement ciblé) en comparaison du même mélange sans phosphate de glycérol (0,8 % mole/mole obtenu, 2,9% rendement ciblé). Ces données pilotes ont suggéré que les groupes amines du chitosane sont plus réactifs avec l'isothiocyanate quand le pH de la réaction est supérieur à 4,8 et quand le chitosane est dissout. D'autres recherches sur la dérivatisation du chitosane avec l'isothiocyanate ont été exécutés à pH 6.5 (Yamada, Onishi, et Machida, 2001), pH 6.9 (Onishi et Machida, 1999), et pH 7.2 (Ishii, Okahata, et Sato, 2001) avec des rendements de marquage correspondant à 0,3%, 2,7%, et 0,01% mole/mole avec un rendement visé de 1,3%, 3%, et 3,2% respectivement.

En raison de la possibilité de la formation de dimères de fluorophores (Ali, Moghaddasi, et Ahmed, 1991), le fluorophore a été ajouté à la réaction par injections séquentielles pour éviter la dimérisation. En plus, la réaction de marquage a été stoppée après trois heures, et le chitosane marqué récupéré par dialyse. Tous ces paramètres proviennent de réactions exécutées précédemment par notre collaborateur Dr. Kujawa. Le rendement de marquage a été comparé lorsque le fluorophore RITC est ajouté en trois injections décalées ou une injection simple. Deux méthodes de récupération du produit final ont également été testées ; par dialyse ou par précipitation dans des conditions alcalines. Enfin, la réaction a été arrêtée à deux temps, 4 heures et 18 heures. Les résultats ont montré qu'une injection au lieu de trois produit un rendement plus élevé. En outre, si un marquage ciblé est désiré, la méthode de précipitation est préférable à la dialyse qui permet à la réaction de continuer, bien que très lentement. La précipitation du RITC-chitosane, quant à elle, permet d'arrêter complètement la réaction. Nous avons également prouvé que la réaction est loin d'être complète après 4 heures. Cependant, après 18 heures, la réaction semble être terminée. Nous avons atteint (Table 1), des rendements de 0,5% mole/mole (4 heures, 3 injections), 1,0% (18 heures, 1 injection), et 1,3% mole de RITC/mole chitosane (18 heures, 3 injections) avec une concentration initiale de 3,2% [rho B]/[chitosane] mole/mole et en utilisant la méthode de récupération par précipitation. En utilisant la dialyse, nous avons atteint des rendements de 0,8% (4

heures, 3 injections), 0,9% (18 heures, 3 injections), et 1,3% mole de RITC/mole chitosane (18 heures, 1 injection).

Table 1. Comparaison du chitosane synthétisé en fonction: du nombre d'injections, du temps de réaction et de la méthode de rétablissement
FDAA signifie la fraction du degré de déacétylation ; Ppt signifie precipitation ; eff signifie efficacité

Chitosane				Fluorophore		calcul du rendement			
Chitosane	FDAA	Qqt. chito (g)	Acide Acetique (mM)	Qqt.fluor (mg)	Temps react. (h)/ # injections	Recup.	Abs	eff mol fluor - mol chito%	cibl mol fluor/ mol chito %
EPRC05	0.802	0.150	33.2	15.37	4h/3inj	Ppt	0.1339	0.5	3.2
EPRC06	0.802	0.150	33.2	15.25	18h/3inj	Ppt	0.2521	1.0	3.2
EPRC07	0.802	0.150	33.2	15.23	18hr/1inj	Ppt	0.3287	1.3	3.2
EPRC08	0.802	0.150	33.2	15.37	4h/3inj	Dialyse	0.1924	0.8	3.2
EPRC09	0.802	0.150	33.2	15.25	18h/3inj	Dialyse	0.2338	0.9	3.2
EPRC10	0.802	0.150	33.2	15.23	18hr/1inj	Dialyse	0.316	1.3	3.2

Nous avons également déterminé le type et la quantité d'acide permettant de solubiliser le chitosane, et de réaliser un marquage ciblé et efficace. Nous avons mesuré le pH de solutions de chitosane avec des quantités variables d'acides acétique, lactique, ou chlorhydrique pour des chitosanes de DDA allant de 77,1 à 94,6%. Toutes les courbes de pH (tous les DDA examinés) fusionnent en une même courbe quand la concentration en acide est normalisée en utilisant le ratio [acide]/[NH_2]. Ce ratio est un facteur important. Il est exprimé en pourcentage, où [acide] est la concentration molaire de l'acide et [NH_2] est la concentration molaire des monomères de glucosamine dans un chitosane particulier et ceci pour une solution du chitosane de 1% poids/volume. Nous avons constaté que le chitosane en solution dans certain acides (70% -230% [acide]/[NH_2]) ne précipite pas après l'addition d'un volume égal de méthanol. Dans ce cas, il existe un ratio [acide]/[NH_2] 'charnière' pour lequel le pH baisse, au lieu d'augmenter après addition du méthanol, ce point est appelé «point charnière». Ce *point charnière* se trouve autour de 90% [acide]/[NH_2] pour les solutions de chitosane dans les acides lactique et chlorhydrique, mais il est autour de 60% [AcOOH]/ [NH_2] pour l'acide

acétique. Le *point charnière* est le point pour lequel l'efficacité de marquage prévue peut être atteinte, car le pH ne varie pas, après l'ajout de méthanol.

Pour cibler le marquage, la cinétique de réaction a dû être déterminée afin d'établir le temps de réaction optimum. Plus tôt, nous avons démontré que 4 heures ne sont pas suffisantes pour que la réaction soit complète mais que 18 heures le sont. Nous avons également étudié si le niveau de déacetylation avait un effet sur l'efficacité du marquage. Pour cela, nous avons exécuté des expériences de cinétique de réaction sur du chitosane de DDA variés. Nous avons conclu que la fraction de RITC incorporée pendant les premières 7 heures augmente considérablement et que le marquage ciblé est difficile pendant cette période. Après 18 heures, la fraction de RITC incorporée varie peu, ceci jusqu'à 72 heures. Après 18 heures, ~50% du RITC utilisé dans la réaction a été incorporé aux chitosanes ayant des DDA de 80,2% et 98,4%, tandis que pour le chitosane avec un DDA de 71,7% seulement 40% avait été incorporé Afin d'atteindre la même efficacité, la quantité de RITC utilisée avec le chitosane ayant un DDA de 70% devrait être augmentée de 10%.

Nous avons aussi constaté que la dérivatisation molaire du chitosane avec le RITC peut être extrapolée des solutions diluées (5 à 50 µg/ml) de pH 5,0 à pH 6,0 en absence de sel, en utilisant le coefficient d'extinction de la rhodamine établi à 90100 $(M \cdot cm)^{-1}$ à λ_{abs} = 556 nm absorbance maximale. Bien que la fluorescence diminue à pH 2,5, en présence de 150mM de NaCl, le RITC-chitosane est encore fluorescent. Ceci suggère que l'internalisation du RITC-chitosane dans les endosomes ou les lysozomes pourraient toujours être détectée par microscopie confocale.

Le travail présenté dans ce mémoire explique qu'un marquage ciblé du chitosane avec le RITC peut être réalisé. Nous avons synthétisé six chitosanes, marqués avec le RITC, ayant trois DDA (71,7%, 80%, et 92,7% DDA) et deux PMs (~40 et ~140kDa) différents, avec des rendements très semblables (0,9-1,0 % de mole RITC /mole chitosane). Le marquage visé a été réalisé en utilisant des quantités limitées d'acide acétique pour dissoudre le chitosane, et en contrôlant le pH de la réaction, la température et le temps de réaction. Ces six chitosanes marqués ont été utilisés pour déterminer si le DDA ou le PM ont une influence sur l'internalisation du polymère par les cellules.

Avec une concentration finale 50 µg/ml, le chitosane fortement marqué avec le RITC n'était ni toxique aux cellules stromales (BMSC) de la moelle de lapin, ni aux cellules embryonnaires humaines du rein (HEK293). Le RITC-chitosane a été détecté dans la membrane cytoplasmique et à proximité du noyau. Nous avons pu vérifier notre hypothèse de départ, qui supposait que les particules se trouveraient dans des vésicules d'endocytose ou les lysosomes et nos données suggèrent que le RITC-chitosane est co-localisé avec LAMP-2 (marqueur de lysosome). Deux semaines après la première incubation avec du RITC-chitosane, des particules fluorescentes étaient encore observées dans les cellules, et ceci après plusieurs passages. Cela prouve que le RITC-chitosane a été métabolisé et que les produits de décomposition, fluorescents, ont été incorporés aux structures cellulaires. Par contre, le RITC-chitosane, s'il est résistant à la dégradation dans les lysosomes, pourrait être transmis aux cellules filles par division des lysosomes pendant la mitose. Nos résultats obtenus avec la lignée cellulaire HEK293 montre que les chitosanes ayant un DDA plus élevé, ont une dimension de particules plus petite. Par contre le PM n'influence pas la taille des particules.

Table of Contents

List of Tables

List of Figures

List of Abbreviations and Acronyms

β-GP	beta glycerol phosphate
AcOOH	acetic acid
ATCC	The American Type Culture Collection
CDC	Centers for Disease Control and Prevention
COX II	cyclo-oxygenase II
CCF-STTG1	human brain tumor astrocytoma cell line, model for multiple sclerosis
Da	Daltons
DNA	deoxyribonucleic acid
DDA	degree of deacetylation
DMSO	dimethylsulfoxide
ECM	extracellular matrix
FACS	fluorescence activated cell sorting
FDAA	fraction of deacetylation
FITC	fluorescein isothiocyanate
GH	growth hormone
Gluc	glucosamine
HCl	hydrochloric acid
HEK293	human embryonic kidney 293 cell line
HeLa	cervical cancer cells isolated from and Henrietta Lacks
IFN-γ	interferon- γ
IL	interleukin
kDa	kilo Daltons
LacOOH	lactic acid
LPS	lipopolysaccharide
MW	molecular weight
NaCl	sodium chloride
NF-κB	nuclear factor κB

NIAMS	National Institute of Arthritis and Musculoskeletal and Skin Disease
NSAID	nonsteroidal anti-inflammatory drugs
OD	optical density, same as absorbance
OG-itc	Oregon green isothiocyanate
OG-chitosan	Oregon green chitosan
PDGF	platelet derived growth factor
PFA	Parafomaldahyde
PLLA	Poly(L-lactic acid)
RFU	relative fluorescence unit
RITC	rhodamibe B isothiocyanate
rho B	rhodamine B
Rxn	reaction
SW756	cell line derived from primary squmaous carcinoma of uterine cervix
TGF-β1	transforming growth factor β1
TNF-β	tumor necrosis factor-β
TRAIL	TNF-related apoptosis inducing ligand

List of Equations

Chapter 1: Osteoarthritis

Arthritis is a group of disease whose name originates from Greek, meaning inflammation of the joints. It encompasses autoimmune diseases such as rheumatoid and psoriatic arthritis, joint infections such as septic arthritis, and the degenerative joint disease osteoarthritis, which is the most common type of arthritis (Felson, 1998). Cartilage protects the ends of bones in healthy joints and is responsible for absorbing shock and allowing bones to glide over one another during movement. Both bones and cartilage are surrounded by synovial fluid, enclosed within the synovial membrane which lines the joint capsule (Figure 1-1, left). In joints with osteoarthritis (Figure 1-1, right), this protective covering is damaged and worn away -- permitting bones to be exposed to each other resulting in pain, swelling, and the loss of joint motion. Bone spurs may form at the edge of the bones and there is an increase in synovial fluid.

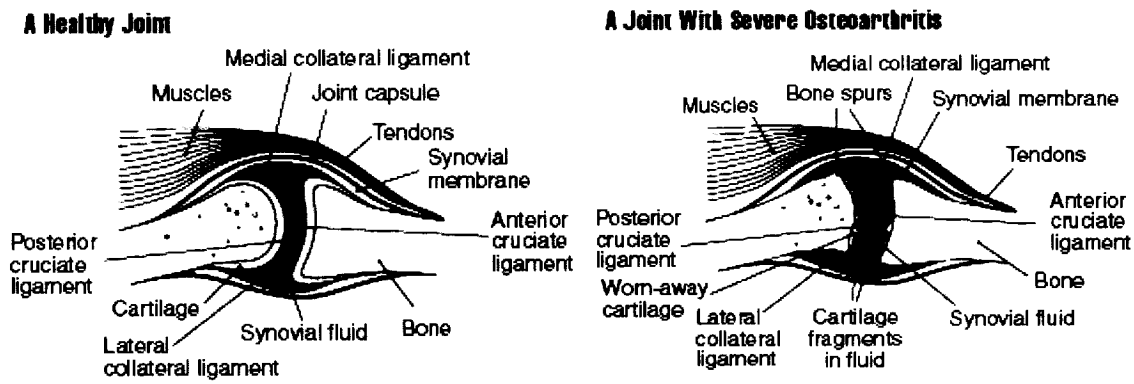

Figure 1-1. Cartilage in healthy joint (left) and in joints with osteoarthritis (right)
Source: NIAMS (National Institute of Arthritis and Musculoskeletal and Skin Disease). 2002. "Handout on Health: Osteoarthritis."
http://www.niams.nih.gov/hi/topics/arthritis/oahandout.htm

Cartilage, an avascular tissue, consists of 60-78% water and three other principle components – chondrocytes, collagen, and proteoglycans, where the latter two being part of the cartilage matrix. Chondrocytes are cartilage cells that maintain the cartilage. It is

due to its avascularity that damaged cartilage resulting from disease or injury has limited spontaneous healing abilities and regeneration capabilities.

The prevalence of osteoarthritis increases with age, to which both men and women are susceptible. However, on the average, more men have osteoarthritis before age 45 than women. Between 45-55 years old, osteoarthritis is found at an equal frequency in men and women, while over the age of 55, this disease affects more women than men (Moskowitz et al., 1992). According to Statistics Canada (2005), 48% of women over the age of 65 years old were affected by arthritis or rheumatism in 2000-2001 (Figure 1-2), which is about 5% of the Canadian population in 2002 (Figure 1-3). 21 million people, according to the National Institute of Arthritis and Musculoskeletal and Skin Disease (NIAMS), were affected by osteoarthritis in the United States in 2002, which is 10% of the population. In the near future, with the event of population aging, it is estimated that in 2040, 20.4% of the population in the United States (Table 1-1, U.S. Census Bureau, 2004) and 22.6% of the Canadian population (Table 1-2) will be 65 years or older (Statistics Canada, 2005).

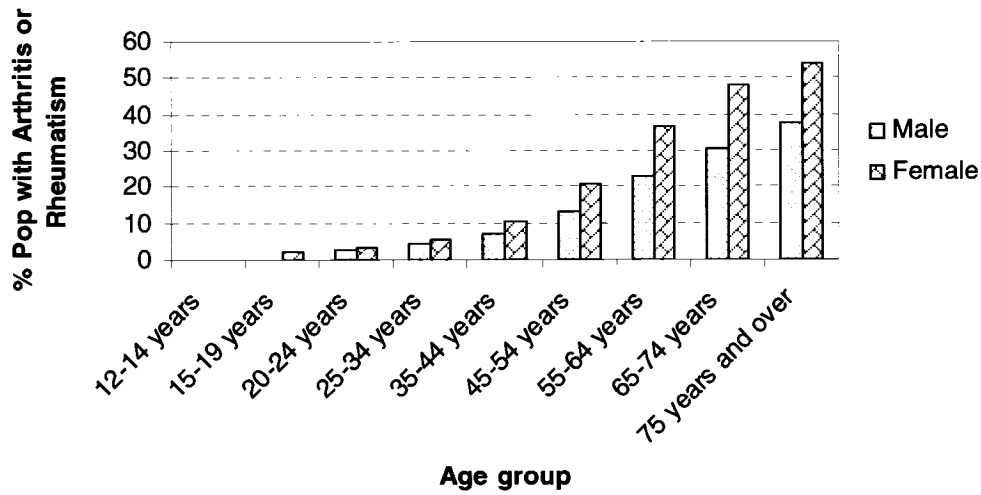

Figure 1-2. Percentage of people affected with arthritis or rheumatism in 2000-2001
Source: Stastics Canada. 2005. "Persons with arthritis or rheumatism by age and sex". http://www40.statcan.ca/l01/cst01/health51a.htm?sdi=arthritis. Accessed 31 January 2006.

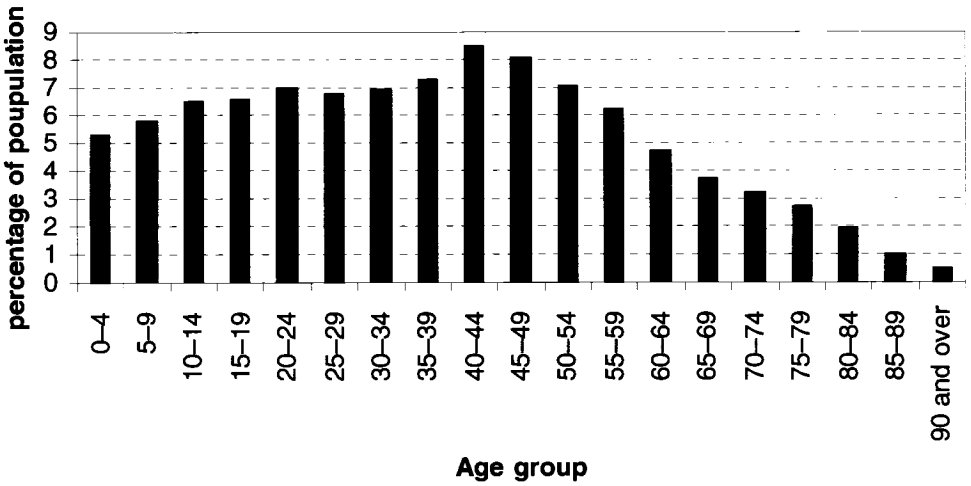

Figure 1-3. Age demographics for 2005
Source: Statistics Canada. 2005. "Population by sex and age group". [Online]. http://www40.statcan.ca/l01/cst01/demo10a.htm?sdi=age%20sex. Accessed 6 February 2006.

Table 1-1. Projected population of the United States by age and sex for 2001-2050.
The numbers are in thousands unless indicated otherwise. As of July 1. Resident population

Population or percent, sex, and age	2000	2010	2020	2030	2040	2050
PERCENT OF TOTAL						
TOTAL						
TOTAL	100.0	100.0	100.0	100.0	100.0	100.0
0-4	6.8	6.9	6.8	6.7	6.7	6.7
5-19	21.7	20.0	19.6	19.5	19.2	19.3
20-44	36.9	33.8	32.3	31.6	31.0	31.2
45-64	22.1	26.2	24.9	22.6	22.6	22.2
65-84	10.9	11.0	14.1	17.0	16.5	15.7
85+	1.5	2.0	2.2	2.6	3.9	5.0
MALE						
TOTAL	100.0	100.0	100.0	100.0	100.0	100.0
0-4	7.1	7.2	7.1	6.9	7.0	6.9
5-19	22.7	20.8	20.4	20.3	20.0	20.1
20-44	37.8	34.7	33.3	32.5	31.9	32.0
45-64	21.9	26.0	24.8	22.7	22.8	22.4
65-84	9.5	9.9	12.9	15.7	15.3	14.8
85+	0.9	1.3	1.5	1.9	2.9	3.8
FEMALE						
TOTAL	100.0	100.0	100.0	100.0	100.0	100.0
0-4	6.5	6.7	6.6	6.4	6.4	6.4
5-19	20.8	19.2	18.9	18.7	18.5	18.6
20-44	36.0	32.9	31.4	30.7	30.2	30.3
45-64	22.3	26.4	25.0	22.5	22.4	22.0
65-84	12.2	12.1	15.2	18.3	17.6	16.5
85+	2.1	2.7	2.9	3.4	4.9	6.1

Source: U.S. Census Bureau, 2004, "U.S. Interim Projections by Age, Sex, Race, and Hispanic Origin," <http://www.census.gov/ipc/www/usinterimproj/>
Internet Release Date: March 18, 2004

Table 1-2. Aging of the population in Canada
Source: Public Health Agency Of Canada. 1999. "Canada's Seniors A growing population". [Online] http://www.hc-sc.gc.ca/seniors-aines/pubs/factoids/1999/pdf/entire_e.pdf.

Population aged 65 and over

Year	People aged 65 and over			As a % of the Canadian population
	Men	Women	Total	
	000s			
1921	215.0	205.3	420.2	4.8
1931	294.6	281.5	576.1	5.6
1941	390.9	376.9	767.8	6.7
1951	551.3	535.0	1086.3	7.8
1961	674.1	717.0	1391.1	7.6
1971	790.3	972.0	1762.3	8.0
1981	1017.2	1360.1	2377.3	9.6
1986	1147.6	1589.3	2737.0	10.4
1991	1349.8	1867.4	3217.2	11.4
1996	1515.3	2066.7	3582.0	12.1
1998	1588.5	2147.2	3735.7	12.3
Projections				
2016	2591.2	3302.9	5894.3	15.9
2021	3050.7	3840.6	6891.1	17.8
2026	3558.1	4438.8	7996.9	20.0
2031	3976.5	4960.1	8936.5	21.7
2036	4166.6	5261.0	9427.6	22.4
2041	4244.8	5424.6	9669.6	22.6

Source: Statistics Canada

Arthritis was the main cause for an estimated 744,000 hospitalizations in 1997, which is 3% of all hospitalizations (Lethbridge-Cejku, 2003). In the same year, ambulatory care amounted to 36.5 million visits for arthritis and rheumatic problems or 4% of all ambulatory care visits (Hootman, Helmick, and Schappert, 2002). 86 billion dollars was incurred due to arthritis and rheumatic conditions, where 51.1 billion dollars were as a result of direct medial costs, while 35.1 billion dollars was due to indirect costs such as lost in wages (CDC, 2004). Other than monetary cost, arthritis can have a great impact on the mental and emotional health and has a risk of 18.1% for major depression,

where the limitation of joint function due to the disease is the factor that is most strongly associated with depression (Dunlopp et al, 2004).

Current treatments for osteoarthritis include weight control, exercise, heat and cold therapy, pain medication and other supplements, stress control, injection into the joint, and surgery such as knee replacements and hip replacements (Lethbridge-Cejku, 2003). Weight control is used as a treatment since being overweight is an osteoarthritis risk factor. Overweight people risk developing osteoarthritis in the knee with increasing age (Felson et al., 2000 Part1). By reducing weight, stress is reduced on the hips, knees, back, and feet. Exercising can strengthen the muscles around the joint to reduce damage and improve joint function.

Heat and cold therapy is used to relieve pain or relax muscles. Others use pain medication for its relief. Such drugs can include acetaminophen, nonsteroidal anti-inflammatory drugs (NSAID), COX II inhibitors (Felson et al., 2000 Part 2), and muscle relaxants. Acupuncture has also been used to relieve pain in osteoarthritc patients (Rao et al, 1999). Some patients report that glucosamine sulfate and chondroitin sulfate supplements relieve their arthritis pains and enjoy an increase in joint movements. Both glucosamine and chondroitin sulfate are molecules that are produced in the body for the manufacture and repair of cartilage (Uebelhart et al., 1998; Bassleer, Rovati and Franchimont, 1998). Another alternative is to treat the joint through medication injected directly into the joint. Although corticosteroids are not generally used for osteoarthritis, it can significantly reduce swelling of soft tissues and inflammation in the joints to reduce pain (Stahl et al, 2005). Hyaluronic acid is a substance found normally in joint fluid and acts as lubrication. Currently, treatment where hyaluronic acid is injected into the joints is available to relieve the discomfort of arthritis (Stahl et al, 2005; Roth et al, 2005). Nevertheless, none of these treatments actually stops or cures arthritis.

Surgery is used as the last option for osteoarthritis patients. Simpler treatment must be tried before this option is considered, especially for young people. Four types of surgery are possible: Arthrodesis, osteotomy (Millis, 1996), arthroscopy, and finally total joint replacement. Unfortunately, surgery cannot permanently correct the problem. Arthrodesis or fusing the joints requires that the surfaces of the joint be removed and the

bone ends are joined, thus inhibiting movement. In osteotomy, the bone below the affected join is cut, realigned, and reset so that load-bearing now occurs on the remaining intact surfaces of the joint. Arthroscopy is a minimally invasive surgical approach used to remove damaged cartilage or loose cartilage fragments that cause irritation. Microsurgical tools are inserted through small incisions in the skin along the affected joint. This however does not stop osteoarthritis progression and can last for only 1-6 months. Finally, total joint replacement involves the removal of the affecting joint, which is often replaced by stainless steel, cobalt-chromium alloy, titanium, high-density polyethylene, or silicon artificial joints. Joint replacements are available and common for the hip and knee, and less commonly replaced for shoulder and elbow.

Recently, our research group showed that cartilage lesions can be repaired by a combination of surgical marrow-stimulation, and application of an implant consisting in chitosan-glycerol phosphate mixed into whole autologous blood (Hoemann et al, 2005; Chevrier et al, 2006; Hoemann et al, 2006). The aim of the studies presented here were to further our understanding of how chitosan can stimulate bone marrow-based repair of cartilage lesions. In particular, we wanted to test the effect of chitosan structure on the binding and uptake of chitosan by cells involved in cartilage repair.

Chapter 2: Chitosan

Also known by its chemical name as 2-amino-2-deoxy-ß-D-glucopyranose, chitin (Figure 2-1a) is a naturally occurring organic material extracted from crustacean, mollusk, and insect exoskeletons. Its abundance in nature as an organic material is second only to cellulose (Figure 2-1c), which was discovered 3 decades after chitin's discovery. The use of chitin as a biomaterial has attained popularity during the 1970s (Roberts, 1992) -- since Braconnot had first isolated it in 1811 (Braconnot, 1811) -- due to its biocompatibility, biodegradability (Tokura et al., 1983), and bioactivity (Prudden et al., 1970; Yano et al., 1985; Nakajima, Atsumi and Kifune, 1985) with no adverse response from the host (Palapura and Kohn, 1992; Zhao et al, 1990; Nakajima et al.,1986; Sapelli et al, 1986). Chitin has limited solubility in three categories of solvents -- aqueous solutions of neutral salts (Von Weimarn, 1927), concentrated strong acids (Austin, 1984), a few organic carboxylic acids, and few mixtures of organic solvents – often requiring that the dissolution occur not at room temperature and with modification or hydrolysis of the polymer (Capozza, 1976). The limited number of solvents and methods available to solublize chitin, restricts its application.

Fortunately, the deacetylated derivative of chitin – chitosan -- or 2-acetamido-2-deoxy-ß-D-glcopyranose (Figure 2-1b) is a base, which can be easily solubilized in dilute acid solutions and forms water-soluble salts with a great variety of organic acids (Roberts, 1992). Like chitin, chitosan is also biocompatible, biodegradable, and bioactive. Chitosan has been tested for mutagenicity, acute and subacute toxicity, chronic toxicity, pyrogenicity, hemolysis, and sensitization (Seo, 1990) and was found to be a safe biomaterial.

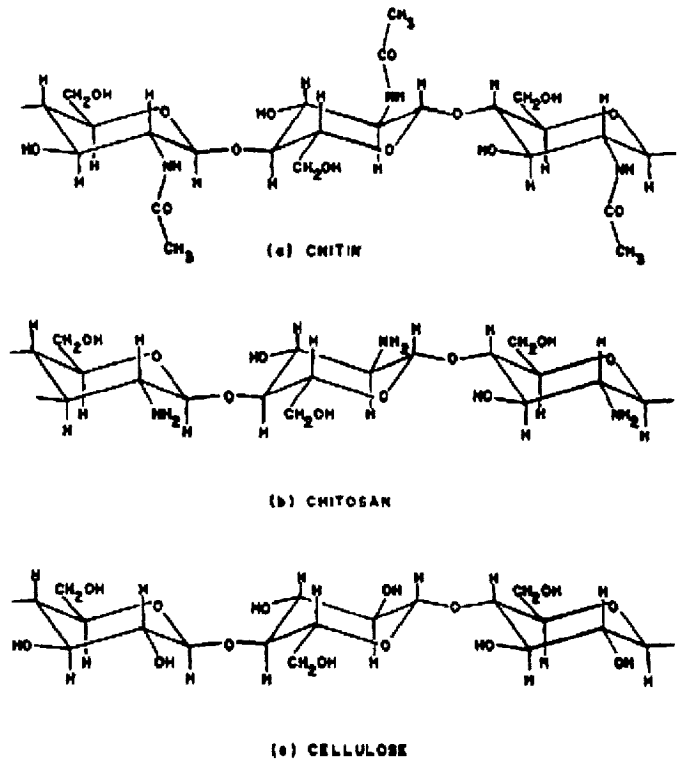

Figure 2-1. Chemical structures of chitin, chitosan, and cellulose.
Courtesy of Marc Lavertu (2005).

2.1 Degree of Deacetylation and Molecular Weight

To describe chitosan, three main characteristics are of critical importance for biomedical applications. These parameters are purity, the degree of deacetylation (DDA), and molecular weight (MW). Chitin can be obtained from various sources and can contain impurities such as calcium, phosphorous, and carotenoids. The physicochemical properties are highly related to their source. This is because depending on the source of chitin, one can achieve a certain DDA or MW (Shepherd, Reader, and Falshaw, 1997; Rhazi et al., 2000). Pure chitin is a polymer consisting of repeating N-acetyl-D-glucosamine monomers, while chitosan is a polymer composed of D-glucosamine and N-acetyl-D-glucaomine units. The degree of deacetylation describes the fraction of the polymer that is D-glucosamine monomers. When the degree of de-

actylation is near 1, it is closer to pure chitosan, where most of the monomers in the polymer are of D-glucosamine units. The molecular weight of chitosan, measured in Daltons (Da) or kilo-Daltons (kDa), determines the total length of the molecule when the average monomeric molecular weight is known. Both the degree of deacetylation and molecular weight are important parameters to consider since they determine chitosan's particular application.

The average monomeric molecular weight of a chitosan deacetylated to a certain degree, is determined by the summation of two products – the product of the molecular mass of pure chitin (N-acetyl-D-glucosamine, 203 g/mol) and the fraction of the polymer that is acetylated, plus the product of the molecular mass of pure chitosan (D-glucosamine, 161 g/mol) and its degree of deacetylation, or simply stated as,

$$MW_{avg} = 203\,g/mol\,(1 - DDA) + 161\,g/mol\,(DDA)$$

Equation 2-1. Determination of the average monomeric molecular mass of chitosan

where DDA represents the fraction of the polymer that is deacetylated. Note that hydrolysis of the chitosan polymer yields monomers D-glucosamine and N-acetyl-D-glucosamine with molecular masses of 179.15 g/mol and 221 g/mol, respectively.

The chitosan degree of deacetylation (DDA) can affect chitosan charge state and its ability to complex with negatively charged molecules. Chitosan DDA has been evaluated for its effect on nanoparticle formation and DNA binding, its effect on cell morphology, as well as *in vivo* and *in vitro* gene transfection efficiency (Kiang, 2004). Köping-Höggård et al. (2001) showed that transfection efficiency depends on charge density rather than molecular weight where the degree of deacetylation cannot be lower than 65%. They argued that the shape of the complex was more important than specific DDA or MW (Köping-Höggård et al., 2003). Kiang (2004), however, found that the chitosan : DNA binding efficiency depended on chitosan DDA, where a greater N:P ratio (chitosan amino group to DNA phosphate group charge ratio, or +/- ratio) was necessary with decreasing DDA for efficient chitosan-DNA complexation. The nanoparticles formed with varying N:P ratios and variable DDA were not significantly different in

terms of size and morphology (Kiang, 2004), although overall luciferase expression was higher for higher DDAs for HEK293, SW756, and HeLa cells, while intramuscular luciferase expression was greater with decreasing DDAs. Other than transfection efficiency, the chitosan DDA is known to affect flocculation (Sheherd, Reader, and Falshaw, 1997). Likewise, chitosan's emulsion properties are dependant on DDA and can be tested for specific pharmaceutical and industrial uses (Mun, Decker, and McClements, 2005). For the purpose of chitosan derivatization by rhodamine B isothiocyanate, it was therefore important to demonstrate the potential influence of chitosan DDA on parameters that could influence derivatizaiton efficiency such as chitosan solubility and solvent pH.

2.2 Chitosan Solubility in Different Acids

Just as chitin's use is restricted due to its insolubility in common solvents, chitosan's use also has limitations since it is insoluble at neutral pH (Sashiwa and Shigemasa, 1999). However, researchers have found ways to modify chitosan for their particular purpose. Chitosan's biodegradability, for instance, can be controlled by adding hydrophobic side chains (Luckachan and Pillai, 2006) for time controlled drug delivery. Amphiphilic features were added for use in localized, time-release drug delivery (Zhu, Liu, and Ye, 2006).

While the biological properties of chitosan are well known, it also has a good film and gel forming characteristics that is relative to its molecular β(1→4) D-glucosamine backbone, which gives it a semi rigid character that also allows it to form a hydrogen bond network (Rinaudo et al., 2005). This hydrogen-bonding capability plays an important role on the gelation process of this material, as well as in its hydrophobic, biodegradability properties (Vachoud, Zydowicz, and Domard, 1997).

In an acidic media, chitosan becomes a polyelectrolyte due to the protonation of the NH_2 groups where an equilibrium is established between the protonated and

unprotonated forms according to Equation 2-2, where the dissociation constant is obtained from Equation 2-3.

$$\text{Chit-NH}_3^+ + \text{H}_2\text{O} \rightleftharpoons \text{Chit-NH}_2 + \text{H}_3\text{O}^+$$

Equation 2-2. Chitosan chemical equilibrium in acidic media

$$k_a = \frac{[chit - NH_2][H_3O^+]}{[chit - NH_3^+]}, \text{p}K_a = \text{-log } K_a$$

Equation 2-3. Dissociation constant of chitosan

pK_0 is the intrinsic dissociation constant for the monomeric unit, when the net charge nears zero. The absolute value differs depending on chitosan DDA, acid, charge state, and presence of salt (Domard, 1987; Park and Choi, 1983; Filion, Lavertu, and Buschmann, 2005). Chitosan pK_0 was found to be 6.5 (Domard, 1987) in the absence of salt and 6.4 in 0.1M NaCl (Park and Choi, 1983), or 6.9-7.5 depending on DDA in the absence of salt and 6.7 -6.9 in salt (Filion, Lavertu, and Buschmann, 2005). Rinaudo, Pavolv, and Desbrières (1999) have investigated the solubility of chitosan in the presence of acetic acid and hydrochloric acid. When chitosan is protonated to 50%, the pK_0 was found to be 6 (Rinaudo, Pavlov, and Desbrières, 1999).

Since chitosan is a base that forms salts with acids, the solubility of chitosan polyelectrolytes depends on the nature of the anions involved. For cases where the chitosan salt has limited aqueous solubility, molecular weight, DDA, and amount of acid present are important factors that should be taken into consideration. Although, chitosan is not known to be very soluble in organic solvents, the addition of a considerable volume of polar solvents to chitosan solutions in acetic acid will not precipitate the polymer (Roberts, 1992). Chitosan can remain soluble in up to 70% by volume of various organic solvents including methanol, butanol, ethylene glycol, diethylene glycol, triethylene glycol, acetone, and formamide. Chitosan is also soluble in up to 40% v/v 2-propanol, or 80% v/v glycerol (Roberts, 1992).

2.3 Chitosan Labeling Procedures with Fluorophores

The labeling of chitosan with a fluorescent marker is a very useful tool in analyzing the binding and uptake of chitosan or chitosan-DNA particles by cells, and the distribution and metabolism of chitosan in organisms (Ishii et al., 2001; Huang et al., 2002; Qaqish and Amiji, 1999; Yamada et al., 2001; Onishi and Machida, 1999). Labeling is a 2-step process involving chemical derivatization with a particular chitosan:dye ratio for a set reaction time, followed by removal of unreacted fluorochrome. In order to compare the behavior of structurally distinct chitosans, targeted labeling of chitosan with the fluorescent dye should be carried out to yield similar labeling efficiencies. The labeling conditions should also suppress contamination with microbial endotoxins, which are difficult to remove, and are cytotoxic *in vitro* and inflammatory *in vivo*.

The molar level of derivitization must be sufficient to detect the labeled chitosan using fluorimetry, fluorescence microscopy, and flow cytometry, but not so high as to significantly alter the degree of deacetylation and molecular mass. Since the molecular mass of rhodamine B isothiocyante (RITC) is equivalent to over three monosaccharide units, 30% derivitization of free amino groups will double the molecular mass of the labeled chitosan, which will influence chitosan solubility, particle size, charge density, and consequentially cell uptake. It is therefore important to be able to accurately determine the average molecular mass of the chitosan starting material, the labeling efficiency (mg fluorophore per mg chitosan), and the average molecular mass of the derivatized chitosan, to be able to produce qualified, fluorescently labeled chitosan with a verified degree of derivitization and molecular mass. The affinity of free fluorochrome (no reactive group) for chitosan should be determined.

The amine reactive group isothiocyanate is preferable to use when derivitizing chitosan, which can only be solubilized at pHs less than 6.5 (Sashiwa H. and Sigemasa Y., 1999). The problem with using succinimidyl ester-reactive fluorophores is that the reaction is much more pH sensitive and should be performed with the most stability at pH

7.7-8.5 (Panchuk-Voloshina et al., 1999), which is not very practical for chitosan. Moreover, the reaction with succinimidyl ester requires an additional step (with hydroxylamine to remove the protective group from the dye). Therefore, it is more complicated, and more difficult to obtain purified derivative (Molecular Probes, 2005).

An amine's reactivity for isothiocyanate derivatization is significantly higher when in the free base form. The kinetics for isothiocyanate derivatization of an amine group is therefore pH dependant. Molecular Probes amine-reactive fluorophores are commonly used to label proteins. It is suggested that to modify lysine residues, an optimal pH of 8.5-9.5 is required. At lower pH, the fluorophore has a tendency to degrade. (Molecular Probes, 2005).

Fluorophore coupling with succinimidyl esters as reactive groups should be performed at pH 8.5, while those with isothiocyanate groups should usually take place at pH > 9 for optimal reactivity. Isothiocyanates that react with primary amines form thioureas (Figure 2-2), which is reasonably stable. However, antibody conjugates with fluorescent isothiocyanates have been reported to deteriorate over time. Thiorureas from fluorescein isotihocyanate (FITC) conjugated amines are predisposed to convert to a guanidine in concentrated ammonia (Molecular Probes, 2005).

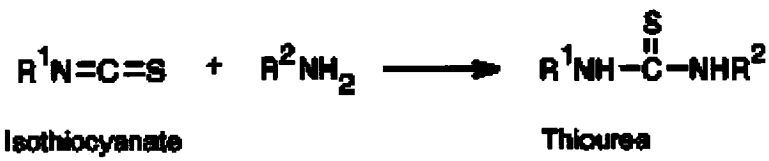

Figure 2-2. Reaction of isothiocyanate with primary amine to form thiourea

In Table 2-1, we compared the labeling of chitosan from several research groups where chitosan was derivatized with fluorophores fluorescein isothiocyanate (FITC), Texas Red, or 9-anthraldehyde. The chitosans that were derivatized ranged from 50% to 99.9%DDA and were solubilized in either hydrochloric acid or acetic acid. The reactions times extended from 1 hour to 24 hours and the labeling efficiency was highly variable

(Table 2-2). From Table 2-1 and Table 2-2, it is difficult to determine which factors contribute to a more efficient labeling. The variables that could contribute are concentration of chitosan, concentration of fluorophore, type and amount of acid used, reaction time, and recovery method. In Table 2-3, the labeling efficiencies were calculated using the same unit of measure such that they can be compared. From Table 2-3, Onishi and Machida (1999) were able to achieve the best labeling efficiencies out of the articles presented here. This achievement is followed by Huang et al. (2004 then 2002). However, this group does not always attain the same labeling efficiencies using the same protocols. Furthermore, Huang et al. (2002;2004) did not use the same method for determining labeling efficiency as the others. They have used fluorescence as a basis while the other researchers have used absorbance to determine the labeling efficiency. Qaqish and Amiji (1999) obtained greater than 50% labeling efficiency while Yamada (2001) and Ishii (2001) obtained less than 50% labeling efficiency. As it was mentioned before, fluorophore molecular mass are rather large compared to the average molecular weight of one chitosan monomer. Adding as many fluorophores as Onishi and Machida (1999) could possibly alter the chitosan properties that interest researchers.

Table 2-1. Comparison of chitosan fluorophore conjugates from literature

Author of article	Chitosan MW and source	DDA%	Acid used to dissolve chitosan	fluorophore	Fluorophore conc.	Chitosan conc	rxn time chito and fluorophore
Qaqish, Amiji (1999)	70k,750k,2M Fluka	82-85	100mL 0.1M acetic acid, then dehyd MeOH 100mL slowly	FITC in methanol 1mg/ml	0.2 mg/ml FITC	5mg/ml	1 hr in dark
Yamada, Onishi, Machida (2001)	Daichitosan H MW = 650,000 Dainichiseika Color & Chemicals Mfg. Co Ltd.	82	Chito dissolved with water adjust ph to 3 with HCl. pH of soln adjust to 6.5	30 mg FITC in 60 mL water (0.5 mg/ml)	0.028 mg/ml	9.4g/ml	24 hour in dark room
Huang, Ma, Khor, Lim (2002)	Chitosan hydrochloride Protosan CL113 Pronova Biopolymer MW = 180,000+/- 7683	90.21 ±0.88	dehydrated methanol (100mL) then + 1% (w/v) chito hydrochloride + 0.1M acetic acid (100 mL)	2.0 mg/mL FITC in 50 mL methanol	0.4 mg/ml	4 mg/ml	3 hr rxn in dark ambient temperature
Tommeraas, Strand, Tian, Kenne, Varum (2001)	Pronova	39-99.9	(2-5mmol gluc) 1g chito in 2% acetic acid (120mL) methanol added (120mL)	9-anthraldehyde in 120mL MeOH	Unkwn	4.2mg/ml	stir 24 hr, add sodium cyanoboro-hydride 4.5 mg stir for 12 hr
Onishi, Machida (1999)	Random deacetyl 1×10^4 1×10^6 DaAjinomoto Co, Ltd., Japan	50	300 mg chito dissolved in 10 mL water in 1N HCl pH adjusted with 1N NaOH to pH 6.9	21 mg FITC sigma added to mixture (didn't first dissolve in anything)	2 mg/ml or less	30 mg/ml or less	Room temp 24 hour
Ishii, Okahata, Sato (2001)	Chitosan hydroacetate Yaizu Suisankaguku Industry Co., Ltd 40,84,110 kda	85+	154 mg chitosan hydrochloride (40 kDA) w/ Texas Red dissolved in water 1.5mL	5 mg texas red dissolved in 1.5 mL miliQ water Adjust pH 7.2 w/ 0.1 N NaOH, add chito soln.	1.7 mg/ml	51.3 mg/ml	Rxn carried out overnight at 20°C under stirring

Table 2-2. Comparison of chitosan recovery after derivatization with fluorophore

Author of article	method used to remove unreacted fluorophore	How product (chito-fluo) was washed	Extent of derivatization
Qaqish, Amiji (1999)	Wash w/DI H_2O dissolve in 0.1M acetic acid 2x ppt w 0.1 M NaOH, freeze dry	DI water	1 fitc to 70 d-gluc
Yamada, Onishi, Machida (2001)	Dissolve with 1N HCl, ppt with 1 M NaOH pH to 9 centrifuge 3000rpm 5 min	wash with water, lyophilize	0.6% (w/w) FITC to chitosan
Huang, Ma, Khor, Lim (2002)	ppt in 0.2M NaOH	Separated with free fluorophor w/ sephadex column 1/15 M phosphate buffer/0.2 M NaCl (pH5.5). Dialyzed in 4 liters distelled water 3 days darkness, freeze dry	FITC:chitosan 2.7%(wt fitc/wt chito)
Tommeraas, Strand, Tian, Kenne, Varum (2001)	evap under vacuum <30°C until volume 100 mL. Extract with EtOAc (3 x 100mL) to remove excess reagent	Water phase dialyse against 0.2M NaCl then against DI water adjust to pH 4.5 with HCl before lyophiolize	85%DDA-0.02-1.4 mol% 99.1%DDA-0.008-2.7 mol% 39%DDA – 0.02-1.6mol% 99.9%DDA -0.04-1.6mol%
Onishi, Machida (1999)	pH 5.5 Filtered, sephadex G50 column	not mentioned	6.4% (w/w) fitc to chito
Ishii, Okahata, Sato (2001)	Purify product with 5 mL ethanol added to rxn, then few drops of 1N NaOH, centrifuge ppt at 6000rpm for 10 minute	five mL miliQ few drops of 1N HCl added to dissolve product. Repeated 5 x until texas red fluorescence not detected in supernatant. Freeze dried	Determined to be 1/40 per chitosan molecule

Table 2-3. Comparison of labeling efficiencies from literature
The labeling efficiencies of six articles are listed here using the same unities. Both intended and effective labeling efficiencies are listed for both weight fluorophore to weight chitosan percent and mole fluorophore to mole chitosan percent. Huang et al (2002 and 2004) was the only author who have determined their labeling efficiencies based on fluorescence. The other articles reported using absorbance to determine labeling efficiencies.

Chitosan	% DDA	amt chito (g)	recovery method	amt fluoro-phore (mg)	Rxn time (hours)	Intended mol fluor / mol chito%	Intended wt fluor / wt chito %	Eff mol fluor/mol chito %	Eff wt fluor/wt chito %
Fluorescein-ITC MW = 389.4 g/mol									
Yamada 2001	82	1	ppt	30	24	*1.3*	*3*	0.3	0.6
Qaqish 1999	82-85	1	ppt	100	1	*2*	*4.6*	1.2	2.7-2.8
Huang 2002	80	1	ppt	100	3	*4.4*	*10*	1.2	**2.7**
Huang 2004	46	1	ppt	100	3	*4.4*	*10*	2.7	**5.7**
Huang 2004	61	1	ppt	100	3	*4.4*	*10*	1.8	**4**
Huang 2004	88	1	ppt	100	3	*4.4*	*10*	0.8	**2.3**
Onishi 1999	50	0.3	Seph coln	21	24	*3*	*7*	2.7	6.4
Texas Red MW=625.16 g/mol									
Ishii 2001	85	0.154	ppt	5	ovnt	*0.9*	*3.2*	0.01	0.04

One interesting aspect of the labeling procedures found in literature is that most of the groups used methanol in their labeling protocol. According to Molecular Probes (2006), Texas Red sulfonyl chloride (Figure 2-3) is very unstable in water at higher pHs and can hydrolyze at room temperature within 2-3 minutes at pH 8.3. It is recommended that conjugation take place at low temperatures. However, once the conjugation is formed, the products are rather stable. It does, however produce hydrochloric acid as byproduct (Figure 2-4). FITC is only sparingly soluble in water at less than 0.1 mg/mL. It is, however, soluble in ethanol at 20 mg/ml, in 2-methoxyethanol at 9 mg/ml, and in DMSO at 5mg/mL (Sigma Aldrich, 2006). FITC decomposes in water, therefore, an organic solvent is recommended for stocking the solution. Between these two fluorophores, FITC would be more suitable conjugate for chitosan since Texas Red is so unstable in water and at high pHs and must be derivatized in low temperature conditions. Instability of FITC in aqueous solvents could partly explain the low chitosan derivatization efficiency obtained by Ishii et al (2001).

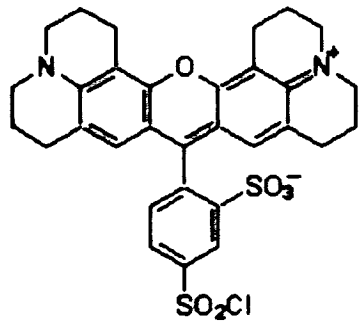

Figure 2-3. Texas Red or sulforhodamine 101 acid chloride
$C_{31}H_{29}ClN_2O_6S_2$, (625.16g/mol)

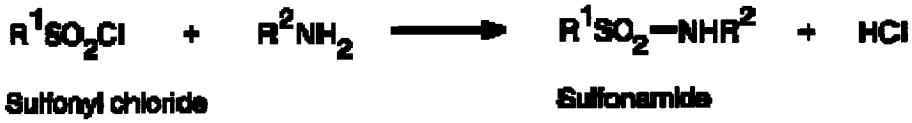

Figure 2-4. Reaction schematic of primary amine with sulfonyl chloride
This reaction produce HCl as byproduct.

To use a fluorophore as an investigative tool, one must be able to detect it. Since FITC (Figure 2-5, left) signals quench at pH 5 (where the pH of endosomes and lysosomes are found), a similar tool which is relatively insensitive to pH is preferred. Rhodamine B isothiocyanate (RITC, Figure 2-5, right) with the same reactive group has been determined to be less pH-sensitive, and less bleachable than FITC (Lakowicz, 1983; Nairn, 1976). However, Verhaegh and Blaaderen (1994) found it just as bleachable in their confocal comparison study. RITC has been used as an anterograde and retrograde marker for retinal neurons in rats with no detection of extracellular leakage for more than 30 days (Thanos, Vidal-Sanz, and Aguayo, 1987). It has also been used to detect proteoglycan core proteins in polyacrylamide gels (Fernàndez-Busquets and Burger, 1995) and conjugated to chitosan. RITC has been used as a demonstration tool for confocal microscopy (Lamprecht, Schäfer, and Lehr, 2000). Rhodamine B, the free fluorophore, has been used as a probe for acidic organelles in skeletal muscles (Vult Von Steyern, Josefsson, and Tågerud, 1996). Although rhodamine B has been reported to

dimerize in ethanol at temperatures below zero (Ali, Moghaddasi, and Ahmed, 1991), similar conditions reported for room temperature settings have not been found. Technical support at Sigma Aldrich suggested that dimerization could possibly occur, which is not covalent and can be resolved by working at a lower concentration.

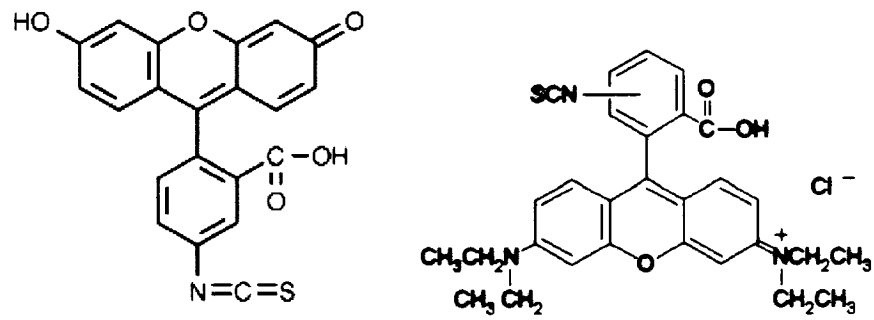

Figure 2-5. Fluorescein isothiocyanate (left) and, Rhodamine B isothiocyanate (right) FITC, 389.4 g/mol. RITC, 536.1g/mol.

In order to determine the labeling efficiency with RITC, the extinction coefficient should be determined. From literature, the extinction coefficient for RITC has been reported as ranging from 11000 to 106000M $^{-1}$cm^{-1} at maximal absorbances from 532 - 580 nm in ethanol, or solvents not mentioned (Du et al., 1998; Caldentey et al., 1999; Forouhar et al, 2003; Kang and Gapinski, 2005). Depending on what RITC is coupled with, this value can possibly vary. RITC being similar in structure to FITC is likewise hydrophobic. Therefore, it is no wonder most of the researchers added methanol, a polar organic solvent, to increase fluorophore solubility in their chitosan coupling reactions. Fluorophores are normally sensitive to light and should be manipulated in the dark.

2.4 The Effects of Chitosan on In Vitro Cultured Cells

A lot of research has been conducted on chitosan *in vitro.* For instance, both chitosan and D-glucosamine were found to induce Th1 cytokine gene expression in porcine spleen cells (Lee et al., 2002), specifically, IL-2 and IFN-γ. The Th1 subset of T lymphocyte cells are responsible for cytokine secretion such as interleukin-2, interferon-γ

(IFN- γ), tumor necrosis factor-β (TNF-β), and granulocyte and macrophage colony-stimulating factors for cell-mediated immune responses (Lee et al., 2002). On the same note, chitin and chitosan inhibits nitric oxide production in activated RAW 264.7 macrophages (Hwang, et al, 2000). In a host system, macrophages that are activated by inflammatory agents such as IFN- γ and bacterial lipopolysaccharide (LPS) produce nitric oxide as a cytotoxic mediator to prevent invading microorganisms and tumor cell growth (Moncada and Higgs, 1993; Stuehr and Nathan, 1989), but this same response provoke damage to neighboring cells around the wound site and hamper the healing process (Beckman et al., 1990; Laskin and Pendino,1995; Bauer, Rao, and Smith, 1998). Thus, although a low concentration of nitric oxide production is necessary in the early wound healing process, excess nitric oxide in the later phases of wound healing can become unfavorable for fibroblast regeneration and collagen accumulation (Shearer et al, 1997). Chitosan also accelerates wound cleaning by infiltrating polymorphonuclear leukocytes, which are involved in the early phase of wound healing to clean the wound site (Ueno et al., 2001a).

Kim et al. (2002) have shown that water soluble chitosan has anti inflammatory effects on human astrocytoma cell line CCF-STTG1, which is an active cytokine mediator for Alzheimer's disease. For osteoarthritis, transforming growth factor β1 (TGF-β1) was proposed as a promoter of cartilage regeneration due to its positive effects on the synthesis of matrix molecule and cell proliferation (Ignotz, RA and Massague, J., 1986; Frenkel SR et al., 2000). These results were confirmed by other researchers who found that chitosan stimulates TGF- β1, PDGF as well as ECM production (Badgett, Bonner, and Brody, 1996; Ueno et al., 2001b). Other effects that may be useful for osteoarthritis treatment exist. Poly(L-lactic acid) or PLLA surfaces that were modified with chitosan by two methods were both able to enhance chondrocyte adhesion, proliferation and function for cartilage repair (Cui et al., 2003; Guo et al., 2006). Lu et al. (1999) had injected a 0.1% chitosan solution at near neutral pH into rat knees and had shown that it induced chondrocyte proliferation, dampened the decrease in epiphyseal cartilage thickness with time, and maintained the intra-articular fibrous tissue formation from the first week, which was still present after 6 weeks.

Osteoarthritis is a polygenic disease that is controlled by genetic factors that are expressed. Interleukin-6 (IL-6) is mentioned to be involved in cartilage degradation (Pola et al., 2005) where at elevated levels of this inflammatory cytokine lead to the development of disability, frailty, and mortality in older people, where iflammatory cytokine activities alter the hormones, skeletal muscles, and immune system (Walston et al., 2005). Harper et al. (2001) have reported that TNF-related apoptosis inducing ligand (TRAIL) induces the activation of nuclear factor κB (NF-κB) in HEK293 cells, along with pro-inflammatory cytokine IL-8 production. According to Seo et al., (2003) chitosan inhibits NF-κB under hypoxic conditions which is a transcription factor responsible for many inflammatory gene expression such as IL-1, IL-4, IL-6, IL-8, and IL-13.

Our research group has discovered that chitosan-glycerol phosphate/blood clots stimulate cartilage repair by surgical bone marrow stimulation techniques (Hoemann et al., 2005). The mechanisms behind chitosan-glycerol phosphate/blood implant-based cartilage repair involve stimulation of subchondral bone remodeling and angiogenesis (Chevrier, 2005). Fluorescent chitosan derivatives could be used to understand how the chitosan clot implant exerts an influence on bone marrow cells, by exposing bone marrow cells to fluorescent chitosan *in vitro* or *in vivo*, and by studying the relationship between cell binding and uptake on cellular responses. We have chosen to derivatize chitosan with rhodamine B isothiocyanate (RITC), a fluorophore that retains its fluorescent properties, at endosomal pH 5.0, in order to be able to detect internalized chitosan in live cells. Prior to studying the binding and uptake of RITC-chitosan by bone marrow cells, we used the HEK293 fibroblast cell line to determine whether binding and uptake could be affected by DDA or molecular weight. The HEK293 cell line is a permanent line derived from primary human embryonal kidney and transformed by human adenovirus type 5 DNA with an Ad 5 insert from the left end of the viral genome (ATCC, 2006). These cells are hypotriploid and turmorgenic in nude mice (Graham et al, 1977) and express receptors for growth hormone (GH) and IL-6 (Von Laue et al., 2000). To determine the effect of chitosan structure on uptake by HEK293 cells, a protocol was

developed to produce chitosans of distinct DDA and molecular weight, with an identical degree of derivatization with rhodamine B isothiocyanate.

Chapter 3: Molecular Absorption Spectroscopy

(Skoog et al., 1999)

Spectroscopy is a technique used for quantitative analysis for the study of electromagnetic radiation absorbed or emitted by a chemical species. The quantity of chemical species present is related to the radiation absorbed or emitted. Electromagnetic radiation includes a wide range of energies, encompassing X rays, ultraviolet, infrared, visible light, and microwaves -- among others, therefore numerous spectroscopic techniques exists. Here, we will focus on only one technique, which is based on the absorption of visible light in the 400nm to 700nm range.

In molecular absorption spectroscopy, measurements of transmittance (T) or absorbance (A) are obtained from the solutions held in transparent cells of path length b, which usually measures 1 cm. The concentration (c) of the absorbing species is linearly related to the absorbance according to Equation 3-1, where P_0 and P are the radiant power of the incident and emergent beam, respectively, and ε is the molar absorptivity. Both absorbance and transmittance are unitless values, while concentration is measured in [mol/L] or [M] and the molar absorptivity has units of [L/mol·cm] or [$(M \cdot cm)^{-1}$].

$$A = -\log T = -\log \frac{P}{P_0} = \varepsilon b c$$

Equation 3-1. Mathematical representation of Beer's law

The transmittance and absorbance of an analyte held in a transparent container or cell undergoes a substantial beam attenuation due to reflection losses at the air/wall, the wall/solution interfaces, and can also occur due to scattering losses by large molecules or absorption by the container walls (Figure 3-1). To compensate these effects, the radiant power of the beam transmitted in the solution is compared to that of the beam transmitted

by an identical cell holding only the solvent. This assures that the true absorbance and transmittance is obtained from Equation 3-2.

$$T = \frac{P_{solution}}{P_{solvent}} = \frac{P}{P_0}$$

Equation 3-2. Definition of transmittance

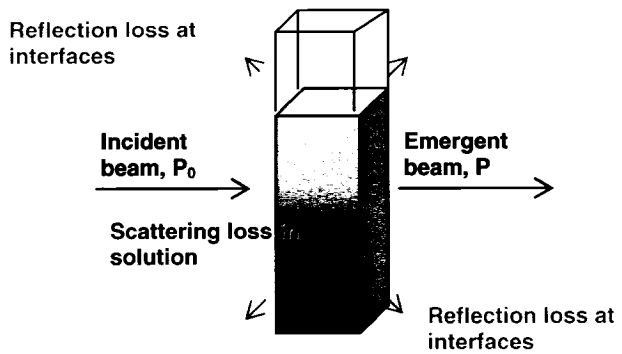

Figure 3-1. Reflection and scattering loss of measured transmittance or absorbance

There are few exceptions to the linear relationship between absorbance and path length. However, the linear relationship does not always hold for absorbance and concentration when *b* is kept constant. Deviations from Beer's law can occur due to instrumental deviations defined by the manner in which the measurements are made or due to chemical deviations where a chemical change is associated with concentration change. Some deviations are fundamental, representing the real limitations of the law.

The real limitations to the law include the restriction that analyte concentration must be relative low. At concentrations greater than 0.01 M, the charge distribution of neighboring molecules is affected due to the reduced distance between the molecules responsible for absorption, which modifies the capacity of the molecule to absorb a given wavelength of radiation. This effect is also observed where analyte concentrations are low, but high concentrations of other species are present – particularly electrolytes. When ions and absorbers are in close range, the molar absorptivity of the absorber is altered by electrostatic interactions. This effect is reduced through dilution. Since ε is dependant on the refractive index of the solvent, deviations from Beer's law can also

occur if the concentration change significantly alters the refractive index (*n)* of a solution. Corrections for this effect is made through substitution of $\varepsilon n/(n^2+2)^2$ for ε in Equation 3-1, which is often insignificant for concentrations less than 0.01 M.

Chemical deviations occur when the analyte dissociates, associates, or react with a solvent, where the product has different absorption spectra compared to the analyte such as with aqueous solutions of acid/base indicators. Instrumental deviations occur when instead of monochromatic radiation, polychromatic radiation is used, where more than one wavelength is applied to the solution containing analyte. If the molar absorptivity differs greatly for the different wavelengths, a stronger deviation from Beer's law is observed. Normally, the Beer's law deviations due to polychromatic light is not significant unless the radiation used includes spectral regions where the analyte exhibits large change in absorption with respect to wavelength as depicted in Figure 3-2.

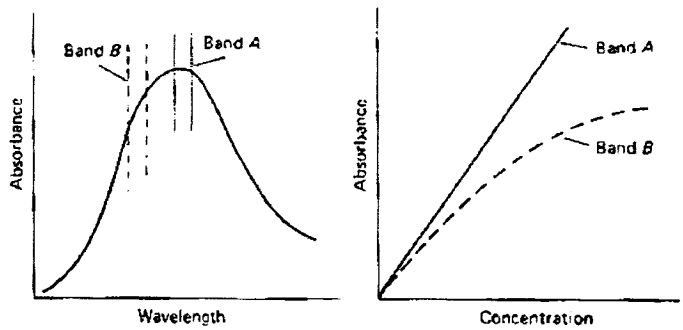

Figure 3-2. Instrumental deviation from Beer's law due to polychromatic radiation.
Band A does not deviate significantly since ε does not vary greatly through the band. Band B significantly deviates due to the drastic change of ε within this region.
Source: Skoog et al, 1999.

To determine the labeling efficiency or the level of derivitization of our final RITC-chitosan product, we have employed the visible spectroscopic measurements at λ_{abs}= 556nm. According to our scan of several RITC-chitosan, wavelengths between 550 -560nm do not possess great changes in absorbance with respect to wavelength. This is true regardless of the concentration of acid used to solubilize the fluorescent chitosan

(Figure 3-3). Our labeling efficiencies were determined using solubilized RITC-chitosan in 100% HCl at ~pH 5.

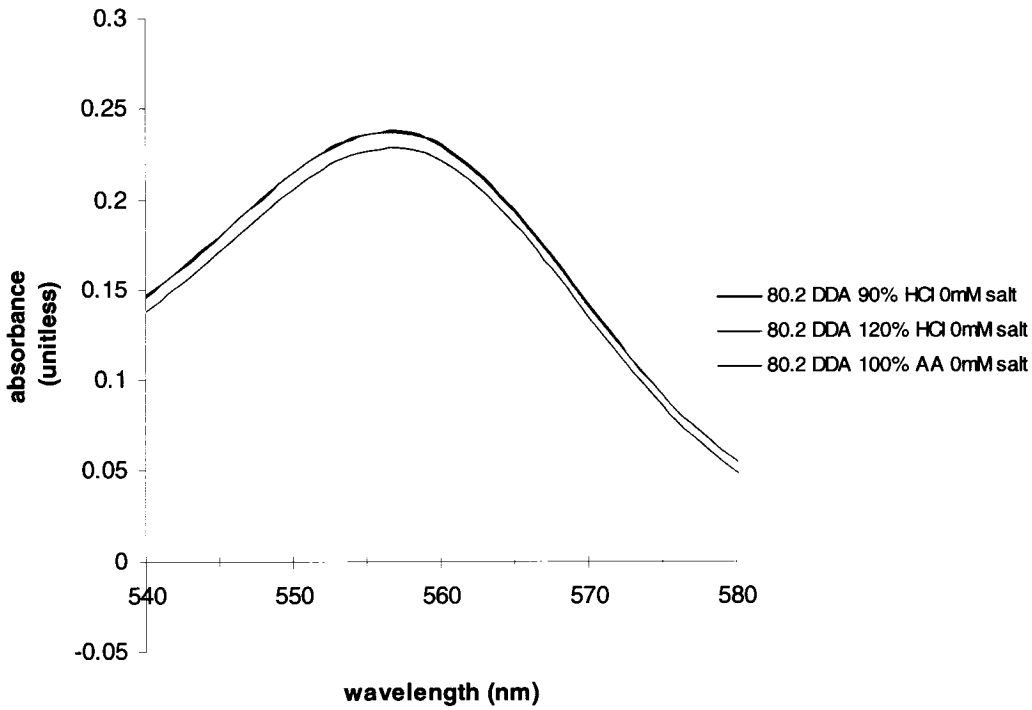

Figure 3-3. RITC-chitosan scan of absorbance with respect to wavelength.
The ε in the range 550-560nm does not deviate significantly. We have conducted all of our RITC-chitosan derivitization measurements at λ_{abs}= 556nm, where the wavelength of maximal absorbance lies.

Chapter 4: Methods

4.1 Materials and Preliminary Chitosan Derivitization

Medical-grade chitosan was obtained from BioSyntech (Laval, Quebec, Canada). We have derivatized the RITC-chitosan product according to Section 4.3, with the chitosans listed in Table 4-1. The reagents purchased from Sigma-Aldrich (Oakville, Ontario, Canada) include rhodamine B (rhoB, Product No. 25242-5), rhodamine B-isothiocyanate (RITC, mixed isomers, Product No. R1755, 283924, or 83692), tissue culture grade 1N HCl (Product No. H9892) and PBS with calcium and magnesium (Product No.D-1283). From VWR, we purchased DriSolv® HPLC grade anhydrous methanol (Mississagua, ON, Canada, Product No. 322415). Gibco Dulbecco's Modified Eagles Medium (high glucose DMEM) was purchased from Invitrogen (Burlington, ON, Canada, Product No. 12100-046). Fetal Bovine Serum was purchased from Atlantic Biological; (Norcross, GA, USA). Sodium hydroxide pellet was purchased from Fisher (Ottowa, ON, Canada, Product No. S-320-1). Hoeschst 33342 was purchased from Molecular Probes (Burlington, ON, Canada, Product No. H-1399).

Table 4-1. Chitosan specifics for preliminary chitosan labelings
Fluorescent chitosan are synthesized at the Université de Montréal (UM) or École Polytechnique de Montréal (EP) and are either Oregon Green Isothiocyanate chitosan (OGC) or Rhodamine B Isothiocyanate chitosans (RC). They are recovered through dialysis or precipitation (ppt).

Supplier	Chitosan lot	New lot number	DDA	MW (kDa)	Post treatment	recovery
Biosyntech	CH10064	UMOGC	82.6	367	n/a	dialyze
Sigma	Gift of Piotr	UMRC01	~85	~300	n/a	dialyze
Wako10	DWG2169	UMRC02	81.4	78	n/a	dialyze
Biosyntech	CH10064	EPRC01	82.6	367	Autoclave	dialyze
Biosyntech	CH10064	EPRC02	82.6	367	n/a	ppt
Biosyntech	CH10064	EPRC03	82.6	367	β-GP	ppt
Biosyntech	PCCH00061	EPRC04	94.6	333	n/a	ppt

4.2 Chitosan Behavior with Acid

Table 4-2. Chitosan specifics for behavior with acid study

Supplier	Chitosan lot	DDA	MW (kDa)	post treatment	recovery
Biosyntech	PCCH00025	77.1	300	n/a	n/a
Biosyntech	CH10086	81.7	300	n/a	n/a
Biosyntech	CH10064	82.6	367	n/a	n/a
Biosyntech	PCCH10061	94.6	357	n/a	n/a

We used medical-grade chitosans (Ultrasan from Biosyntech, Table 4-2) PCCH00025, CH10086, CH10064, and PCCH10061, which are 77.1%, 81.7%, 86.2% and 94.6% DDA, respectively. Chitosan solutions were prepared by dispersing chitosan powder in autoclaved sterilized water (9 mL total volume) and 1 mL of ten-fold concentrated acid was added to the chitosan solution, which was stirred overnight. All experiments were carried out on one percent w/v chitosan solutions, with quality control of solution preparation by using calibrated Metler balances, calibrated pipettes, pH solution verification of acid stock solutions, and visual inspection of solutions for complete dissolution of chitosan particles.

A Neslab RT-111 instrument (NesLab Inc., Runcorn, UK) with temperature-controlled water bath equipped with a pH electrode (Accumet, Model 20, Fisher, Ottowa, ON, Canada) calibrated with pH 4.0, pH 7.0, and pH 11.0 standards and temperature probe was used to measure the pH and temperature of the solutions held in a 50 mL Kontes beaker. The temperature was controlled at 20°C $\pm$ 0.5. No precipitation was observed for any of the solutions. A series of 1% chitosan solutions were prepared at targeted starting molar ratios of acid : glucosamine (70%, 80%, 90%, and 100%) and 60mM and 100mM acid..

Calculations of percent chitosan solution took in account the chitosan loss on drying for chitosans not dried by SpeedVac. The acids tested were hydrochloric acid, acetic acid, and lactic acid. We then monitored pH and temperature during additions of methanol in 0.2 to 2.5 mL aliquots every 2 minutes with a 20 mL piston burette dispenser

to achieve a final 0.5% wt/vol chitosan solution with 50% vol/vol methanol over a ~40 minute time period and a 2 to 20 minute wait for final pH equilibration.

4.3 Chitosan RITC Labeling Comparison of Time, Injection, and Recovery

Table 4-3. Chitosan specifics for chitosan labeling comparisons study

Supplier	Chitosan lot	new lot number	DDA	MW (kDa)	recovery
Biosyntech	PCCH10075	EPRC05	80.2	205	dialyze
Biosyntech	PCCH10075	EPRC06	80.2	205	dialyze
Biosyntech	PCCH10075	EPRC07	80.2	205	dialyze
Biosyntech	PCCH10075	EPRC08	80.2	205	ppt
Biosyntech	PCCH10075	EPRC09	80.2	205	ppt
Biosyntech	PCCH10075	EPRC10	80.2	205	ppt

Care was taken to minimize potential endotoxin contamination when possible, through the use of autoclave-sterilized solutions, and glassware baked overnight at 220°C in a Pasteur Oven. Medical grade 1% w/v chitosan solutions (10 to 35 mL) were prepared by dispersing chitosan powder (Table 4-3) in autoclaved MilliQ water either in a 50 mL 3-neck round-bottom flask (VWR CanLab, Mississauga, ON) or in 25-150 mL erlenmeyer flasks. Ten-fold concentrated acid was added to the chitosan dispersion to yield, in the first set of experiments, a final concentration of 60 mM, 95 mM, or 100 mM acetic acid. In other experiments, chitosan was dissolved in acetic acid to give an acid : glucosamine ratio of 70%. Chitosan solutions were allowed to solubilize overnight with stirring. An equal volume of anhydrous methanol, 35 mL (VWR DriSolv®) was added to the solutions and let homogenize for 3 hours. The flasks were sealed with rubber spetums or parafilm wrap and the solutions were de-gassed with N_2 (g) for 15 minutes. RITC powder (at a mass varying from ~2-3% mol/mol RITC/chitosan) was dissolved in 5 to 13 mL anhydrous methanol to generate a 4 mM RITC solution before addition to the chitosan solution. Either the entire volume of RITC was injected into the chitosan-methanol solution with agitation or one third volume was injected every hour for 3 hours. The reaction was allowed to proceed for 4 hours or 18 hours in the dark. To remove unreacted RITC, the solution was either dialyzed against 100 mM acetic acid in the dark

using MWCO 1000 dialysis tubing (Spectra/Por, SpectrumLab, CA), or precipitated with 0.25-0.5 mL 10 N NaOH and rinsed with MilliQ water and centrifuged with a Jouan Benchtop CR422 centrifuged at 4500 rpm repeatedly. Dialysis or washing of precipitates were continued until the dialysate or supernatant was clear (< 0.01 absorbance OD_{556}, with water as blank). Final products were frozen and lyophilized for 3 days, and later analyzed for their RITC content.

4.4 Chitosan RITC Labeling Kinetics

Table 4-4. Chitosan specifics for the labeling kinetics study

Supplier	Chitosan lot	new lot number	DDA	MW (kDa)	recovery
Biosyntech	PCCH00023	EPRC21-26	71.7	330	ppt
Biosyntech	PCCH10075	EPRC11-20	80.2	205	ppt
Biosyntech	PCCH0009	EPRC27-32	98.4	189	ppt

(Biosyntech Ultrasan) PCCH10075 (80.2% DDA), PCCH0009 (98.4% DDA) and PCCH00023 (71.7%DDA), were prepared by dispersing chitosan powder (Table 4-4) in autoclaved MilliQ water. Ten-fold concentrated acid was added to the chitosan solution to achieve a final acid: glucosamine ratio of 70% and soubilized overnight. An equal volume of anhydrous methanol, 35 mL (VWR DriSolv®) was added to the solutions and let homogenize for 3 hours. Prior to the addition of (2 %mol RITC/mol chitosan for 98.4% and 71.7% DDA, and 3%mol RITC/mol chitosan for 80.2% DDA) rhodamine B isothiocyanate (RITC) (Sigma) to chitosan, solutions were de-gassed with N_2 (g) for 15 minutes. The reaction proceeded in the dark. 5mL (98.4% and 71.7% DDA) or 10 mL (80.2% DDA) of the resulting solution was withdrawn at various time-points, from 0.5 to 72 h. RITC-chitosan and precipitated with 200-300 µL 10N NaOH (Fisher). The precipitates were rinsed with MilliQ water and centrifuged with a Jouan Benchtop CR422 centrifuged at 4500 rpm repeatedly until the supernatant was clear (< 0.01 absorbance with water as blank). Supernatants were collected for analysis of RITC content and final products were frozen and lyophilized for 3 days, and later analyzed for their RITC content.

4.5 Labeling Efficiency of RITC-Chitosan

Labeling efficiency was determined from the absorbance of RITC-chitosan solutions using a Beckman DU-600 Spectrophotometer (Thermo Electron Corporation, MA) in 2 mL plastic cuvettes,using MilliQ water as blank. To do this, 4-5 mg of lyophilized RITC-chitosans were solubilized at 100% [HCl]/[NH_2] (Sigma-Aldrich) and autoclaved MilliQ water overnight at 1mg/mL. The solution was diluted to 0.1, 0.05, and 0.025 mg/mL. Standard curves were generated for rhodamine B (rho B) (Sigma) and RITC (Sigma). Absorbance was measured at 556nm. The relative fluorescence of these solutions was determined by measuring the relative fluorescence units (RFU) of 200 µL test solution in duplicate with a water blank, at λ_{exci} = 543 nm and λ_{emiss} =580 nm, emission cutoff = λ_{570nm}.with a SpectraMax Gemini XS fluorometer plate reader (Molecular Devices Corp., Sunnyvale, CA, USA) and black FluoroNunc 96-well plates (Fisher,Scientific, Ottawa, ON, Canada).

4.6 Synthesis of Six RITC-labeled Chitosans at Similar Labeling Efficiency

Table 4-5. Chitosan specifics for targeted labeling of 6 chitosans

Supplier	Chitosan lot	depolymerized	new lot number	DDA	MW (kDa)	recovery
Biosyntech	PCCH00060	D-BST-60-40-1	EPRC33	92.7	40.7	Ppt
Biosyntech	PCCH0057	D-BST-57-40-1	EPRC34	80	38.9	Ppt
Biosyntech	PCH00023	D-BST-23-40-1	EPRC35	71.7	36.8	Ppt
Biosyntech	PCCH00060	D-BST-60-150-1	EPRC36	92.7	152	Ppt
Biosyntech	PCCH0057	D-BST-57-150-1	EPRC37	80	142.2	Ppt
Biosyntech	PCH00023	D-BST-23-150-1	EPRC38	71.7	149.4	Ppt

15 mL of medical grade 1% chitosan solutions were made using Biosyntech chitosan degraded to specific molecular mass ranges by researchers from our group. Six chitosans of distinct %DDA and molecular mass were used (Table 4-5), including PCCH00060 (40.7 kDa and 152kDa at 92.7% DDA), PCCH0057 (142.2 kDa and 38.9

kDa at 80.0% DDA) and PCCH00023 (149.4 kDa and 36.8 kDa at 71.7%DDA). Chitosan powder was dispersed in autoclaved MilliQ water. Ten-fold concentrated acetic acid was added to the chitosan solution to achieve a final acid to glucosamine ratio of 70% and solubilized overnight. An equal volume of anhydrous methanol, 15 mL (VWR DriSolv®) was added to the solutions and let homogenize for 3 hours. Prior to the addition of (2 mol% for 92.74% and 80.0% DDA, and 2.3% for 71.7% DDA) rhodamine B isothiocyanate (RITC) (Sigma) to chitosan, solutions were de-gassed with N_2 (g) for 15 minutes. The reaction proceeded in the dark. RITC-chitosan was precipitated with 1-2 mL 10N NaOH (Fisher). The precipitates were rinsed with 30 to 40 mL MilliQ water and centrifuged with a Jouan Benchtop CR422 centrifuged at 4500 rpm for 5 to 6 times until the supernatant was clear (< 0.01 absorbance with water as blank). Supernatants were collected for analysis of RITC content and final products were frozen and lyophilized for 3 days, and later analyzed for their RITC content.

4.7 Cell Interaction with Chitosan

Primary Bone Marrow Stromal cells and Immortalized HEK293 cells

Immunohistofluorescence for LAMP-2, a lysosomal protein, was carried out by washing cells thrice with PBS with calcium and magnesium. The 6 time passaged (P6) cells on coverglass seeded at 750,000 cells per well in a 24-well plate were fixed in 3% PFA for 15 minutes at room temperature followed by rinsing 5 times with PBS. We used PBS containing 0.2% BSA to block non-specific binding and 0.7% triton X 100 to permeabilize the cell membrane. The LAMP 2 antibody (a generous gift from Dr. Robert Nabi) was diluted by 1000 times in blocking solution and centrifuged at 15,000 rpm for 10 minutes. The cells were incubated with secondary antibody (anti mouse Alexa 488) for 30 minutes and washed in PBS, followed by couterstaining with using 2μg/mL of Hoechst 33258 and rinsed again. Mowiol was then applied onto the glass slide and allowed to solidify in the dark.

Uptake of various RITC-chitosans was observed for primary rabbit bone marrow stromal cells (BMSC), passage 3 (kindly given by Marc Thibault) and passage 41 HEK293 cells (generously provided by Marc Lavertu). BMSC cells were cultured in DMEM low glucose (Gibco), DMEM + 10% fetal bovine serum (FBS), or DMEM + 10% heat-inactivated FBS. UMRC01 (acetic acid conjugate) was dissolved in doubly de-ionized H_2O at 5 mg/mL, filter-sterilized, and deposited in Petri dishes carrying rabbit BMSC cells at 650 mg/mL RITC-chitosan final concentration, or 50μg/mL RITC-chitosan for HEK293 cells in DMEM high glucose (Gibco), DMEM + 10% fetal bovine serum (FBS), or DMEM + 10% heat-inactivated FBS. The cells were exposed for 18 hours after which the RITC-chitosan was removed by washing with DMEM. Cells were cultured an additional 4 days in DMEM with 10% FBS. Uptake was documented with an inverted fluorescent microscope (Zeiss Axiolab, 20x and 40x magnification), digital camera, and Northern Eclipse Imaging software (Empix, Mississauga, ON, Canada).

HEK293 cells were cultured in DMEM with 10% FBS (Gibco or Sigma) in 24-well plates, or 60 mm or 100 mm Petri dishes. RITC-chitosan (UMRC01 or EPRC02) was added by pipetting filter-sterile solutions at 5 mg/mL directly into the Petri dish to a final concentration of 50 μg/mL to 200 μg/mL. Cells were exposed to RITC-chitosan for 4 to 18 hours prior to washing the cells with media and photodocumentation of cell uptake.

For examining interaction of cells with the depolymerized chitosan labeled with rhodamine, HEK293 cells were seeded at 25,000 cells/well in flat-bottom 96-well plates in a total of 100 μL high glucose DMEM with 10% FBS (Atlantic Biological) in a 96 well plate. Chitosan solutions solubilized overnight with HCl at a 95% HCl : glucosamine ratio and autoclaved MilliQ water, at 2.5mg/mL. Solutions were filtered with a 0.45μm syringe filter and diluted to 0.25mg/mL in sterile autoclaved MilliQ water. Chitosans were incubated with the cells at 5μg/mL by pipetting 2 μL of the 0.25 mg/mL stock into 100 μL of media. Cultures were protected from light in the 37°C, 5% CO_2 incubator for 20 hours. To control for the effects of acid, cells were incubated with a final concentration of 0.224 mM HCl, the same final concentration of HCl that was used to solubilize the 80% DDA RITC-chitosan For negative viability control, cells were

incubated with 50% v/v hydrogen peroxide in complete media by replacing 50 μL of the media with hydrogen peroxide. Cells were photographed under phase contrast or fluorescent excitation using a digital camera and Northern Eclipse software (Empix, Missisauga, ON) and Zeiss inverted Axiolab fluorescent microscope at 4x to 20x original magnification.

Chapter 5: Results

5.1 Preliminary RITC-Chitosan Experiments

We have labeled RITC-chitosan according to a modified Qaqish labeling protocol (Qaqish and Amjii, 1999). Our first labeled product, EPRC01 (Table 5-1), was synthesized by solubilizing chitosan in 100mM acetic acid, adding an equal volume of methanol, followed by three injections of RITC suspended in methanol and a reaction time of 4 hours. The labeling efficiency was 0.3% mol/mol and similar to the labeling efficiency obtained by our collaborator, Dr. Piotr Kujawa of the Winnik Laboratory at the Université de Montréal. Residual RITC was removed by dialysis against 100 mM acetic acid. Therefore, trace acetic acid was present when adding this preparation of RITC-chitosan to live cells. Since Cl^- ions, and not acetate ions, are a normal component of cell culture media and plasma, we aimed to generate fluorescent chitosan as a chloride salt conjugate. To do this, we synthesized Oregon Green chitosan by dissolving chitosan in 100mM HCl in lieu of acetic acid, followed by reaction with RITC and dialysis against dilute HCl. The labeling efficiency of this experiment was very low (0.1% mol OG /mol chitosan) and had required a lot more material in order to detect the chitosan using a fluorimeter. The reaction pH using 100 mM acetic acid to dissolve chitosan was around pH 4.0 while the reaction pH using 100 mM HCl was ~ pH 2.5. These data suggested that the labeling efficiency was suppressed by low pH.

We next tested the hypothesis that increasing the reaction pH above pH 4.0 would increase the labeling efficiency. In an article by Chenite et al. (Chenite et al, 2000), beta-glycerol phosphate (β-GP) was shown to raise the pH of chitosan higher than the pKa of chitosan without precipitation. For EPRC02, we increased the solution pH by lowering the concentration of acetic acid from 100 mM to 60mM. For EPRC03, using the same concentration of acetic acid, we added a final concentration of 90mM β-GP to further raise the pH, where the results were unexpected. Chitosan stayed in solution when the β-

GP was added, however the chitosan precipitated when an equal amount of methanol was added to the solution. The labeling efficiency of EPRC03 was less than half as labeled as EPRC02. For EPRC04, we have used a higher DDA chitosan. Using 97 mM of acetic acid to solubilize chitosan and an overnight reaction time, we obtained a labeling efficiency of 1.1% mol RITC/mol chitosan. This suggested that the labeling efficiency was dependent upon chitosan DDA, type and quantity of acid (determinant of pH), and reaction time. Two other parameters that could affect labeling efficiency were tested, including product recovery method and the necessity of three staggered injections of the fluorophore in the reaction. Although we dialyzed our first few batches of labeled chitosan, precipitation and centrifugation of the labeled chitosan proved to be a faster method to recover the product as a free base.

Table 5-1. Preliminary chitosan experiments
to test the effect of reaction pH, reaction time, fluorophore injection method, and recovery method on labeling efficiency. UMOGC is an Oregon green derivativatize chitosan synthesized by Dr. Piotr Kujawa of the University of Montreal according to the listed conditions. EPRC01 was autoclaved for 20 minutes on the liquid cycle to reduce the molecular weight of the polymer after overnight solubilization. Both UMOGC and EPRC01 were dialyzed against 100mM HCl and acetic acid, respectively. The initial chitosan of EPRC02 and EPRC03 were synthesized side by side, we used 60mM of acetic acid, but for EPRC03, we included a final concentration of 90mM β-GP. The final products EPRC02-EPRC04 were precipitated with NaOH and centrifuged for recovery. EPRC05-07 are the same RITC chitosan products as EPRC08-EPRC10. However, they were recovered differently, where the first set was precipitated and the latter was dialyzed against deionized water. Efficiency determinations of RITC-chitosans were derived from a 0.05mg/mL chitosan solution (UMOGC at 0.5mg/mL) and determined using 85,000 $(M \cdot cm)^{-1}$ as extinction coefficient at λ_{abs} =556nm. For UMOGC, we used 78,000 $(M \cdot cm)^{-1}$ at λ_{abs} =494nm. Abbreviations: FDAA: fraction deacetylated; amt: amount; eff: efficiency; fluor: fluorochrome; ppt: precipitate; abs: absoption; rxn: reaction; chito: chitosan.

Chitosan				Fluorophore		Efficiency calculations			
Chitosan	FDAA	amt chito (g)	Acetic acid (mM)	amt fluor (mg)	rxn time (hours)/ # injections	Recovery	Abs	eff mol fluor - mol chito%	intend mol fluor/ mol chito %
UMOGC	0.826	0.170	100 HCl	5	3h/3inj	Dialyze	0.116	0.1	1.2
EPRC01	0.826	0.200	100.0	20.8	3h/3inj	Dialyze	0.0875	0.3	3.3
EPRC02	0.826	0.146	60.0	13.58	17h/3inj	Ppt	0.1918	0.8	2.9
EPRC03	0.826	0.152	60.0+βGP	13.76	17h/3inj	Ppt	0.0749	0.3	2.8
EPRC04	0.946	0.211	97.0	24.28	18h/3inj	Ppt	0.2738	1.1	3.5
EPRC05	0.802	0.150	33.2	15.37	4h/3inj	Ppt	0.1339	0.5	3.2
EPRC06	0.802	0.150	33.2	15.25	18h/3inj	Ppt	0.2521	1.0	3.2
EPRC07	0.802	0.150	33.2	15.23	18hr/1inj	Ppt	0.3287	1.3	3.2
EPRC08	0.802	0.150	33.2	15.37	4h/3inj	Dialyze	0.1924	0.8	3.2
EPRC09	0.802	0.150	33.2	15.25	18h/3inj	Dialyze	0.2338	0.9	3.2
EPRC10	0.802	0.150	33.2	15.23	18hr/1inj	Dialyze	0.316	1.3	3.2

Our collaborators at the Université de Montréal suggested that injecting RITC in three equal portions over three hours would ensure a more uniform labeling due to suppression of potential RITC-RITC dimer formation (Ali, Moghaddasi, and Ahmed, 1991). To directly compare the effect of reaction time, fluorophore addition, and precipitation versus dialysis for free fluorophore removal, three distinct labeling reactions were carried out on a preparation of chitosan that was dissolved in 33 mM acetic acid and divided into three equal portions. One portion was labeled for four hours using three

staggered injections of RITC. The second portion was labeled for 18 hours using three staggered injections of RITC, while the third portion was labeled for 18 hours using one injection of RITC. At the end of the reaction period each portion was split in half with one half dialyzed and the other half precipitated under alkaline conditions and rinsed exhaustively with water (Table 5-1, Figure 5-1).

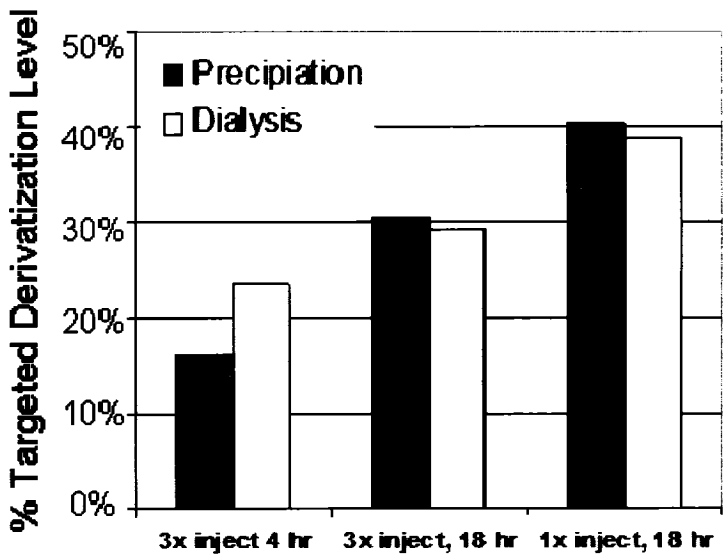

Figure 5-1. Comparison of the labeling efficiency
varying RITC injection, reaction time and method of recovery. We have achieved the highest labeling efficiency with 18 hours reaction time, 1 injection using the precipitation method of recovery. Data are represented as percent fluorophore reacted with chitosan relative to initial fluorophore added to chitosan.

These results demonstrated that the highest labeling efficiency was obtained with one injection of fluorophore and a reaction time of 18 hours (EPRC07, 1.3% mol/mol, Table 5-1). The slightly higher labeling efficiency obtained for the 4-hour labeled, dialyzed preparation (EPRC08 = 0.8% mol/mol, Table 5-1) compared to 4-hour labeled, precipitated preparation (EPRC05 = 0.5% mol/mol, Table 5-1), suggested that the reaction could proceed in an uncontrolled manner during dialysis when the reaction time was limited to 4 hours.

5.2 Chitosan Solution pH

A Function of Acid Type, Acid Concentration, and Dilution in 50% Methanol

The conditions for covalently bonding rhodamine B isothiocyanate (RITC) to chitosan involve the addition of an equal amount of methanol to maintain solubility of hydrophobic RITC. Chitosan is soluble at solution pH lower than pH 6.5 (Sashiwa H. and Sigemasa Y., 1999). It also could be predicted that optimal labeling will occur when chitosan is in a soluble state. In previous chitosan-isothiocyanate derivatization reactions, chitosan was initially dissolved at 10 mg/mL in 100 mM acetic acid (pH 4.4~4.6) (Qaqish and Amiji, 1999; Huang, et al., 2002). However, the reaction of the isothiocyanate group with a primary amine is optimal at a pH greater than 9. Therefore, we tested the hypothesis that higher labeling efficiency could be achieved using chitosan-methanol solutions in which the pH was kept close to, but not greater than pH 6.5. Chitosan dissolved in minimal amounts of acid will have a higher pH, but may precipitate after addition of methanol. To determine the lowest concentration of acid necessary to maintain chitosan solubility near pH 6.5, after addition of an equal amount of methanol, we have monitored chitosan solubility and pH after dissolving chitosan at various concentrations using three acids that could potentially be used for chitosan derivatization reactions : acetic acid, lactic acid, and hydrochloric acid.

Chitosan is completely soluble when the glucosamine residues are fully protonated. Therefore, proportionally more acid is required to fully protonate 100% deacetylated chitosan (100% glucosamine), compared with 77% deacetylated chitosan (77% glucosamine, 23% N-acetyl glucosamine). It should be noted that each 10 mg/mL chitosan solution has a glucosamine concentration that varies according to the fraction of N-acetyl glucosamine (Mw 203 g/mol) and glucosamine (Mw 161 g/mol) monomer, given by the Equation 5-1, where FDAA is the fraction of deacetylated residues, or glucosamine monomer. Molar concentration of chitosan also varies for chitosan with different deacetylation level (Table 5-2).

$$MW(\frac{g}{mol}) = FDAA \times 161\frac{g}{mol} + (1 - FDAA) \times 203\frac{g}{mol}$$

Equation 5-1. Determination of chitosan average molecular weight from FDAA

Table 5-2. Molar concentration of chitosan of various deacetylation levels in terms of total monomer, and total glucosamine, dissolved at 10 mg/mL in varying ratios of mM acid : mM glucosamine. FDAA= fraction of deacetylated residues in chitosan; NR: Not relevant because 0% acetylated is chitin, which is insoluble in aqueous solution.

FDAA	Mw chitosan all monomers	Total mM monomer in a 10 mg/mL solution	Total mM glucosamine in a 10 mg/mL solution	mM acid to yield 100% acid: glucosamine 10 mg/mL solution	mM acid to yield 90% acid: glucosamine 10 mg/mL solution	mM acid to yield 80% acid: glucosamine 10 mg/mL solution	mM acid to yield 70% acid: glucosamine 10 mg/mL solution
0.00	203	49	0	NR	NR	NR	NR
0.77	171	59	45	45	41	36	32
0.83	168	59	49	49	44	39	35
0.94	164	61	57	57	52	46	40
1.00	161	62	62	62	56	50	43

To generate chitosan solutions of pH approaching pH 6.5, decreasing concentrations of acid were used to dissolve chitosan at 10 mg/mL, giving between 100% acid : glucosamine to 70% acid : glucosamine ratios (Table 5-2). To determine whether chitosan dissolved in limiting amounts of acid would precipitate after addition of an equal volume of methanol, a titration apparatus equipped with a 20°C water bath, injection nozzle, and pH electrode was used to measure solution pH with incremental addition of methanol up to 50% v/v. Chitosan solubility in the final solution composed of 0.5% w/v chitosan, varying acid concentrations, and 50% v/v methanol, was determined visually.

5.2.1 Chitosan Solution pH in Acetic Acid With or Without Methanol

We measured the pH of distinct 1% w/v chitosan solutions dissolved in decreasing concentrations of acetic acid (Figure 5-2, AcOOH). Chitosan solution pH increased with decreasing amounts of acetic acid (filled symbols). After addition of an equal volume of methanol, the final solution pH increased by nearly 1 pH unit at 100mM acetic acid (Figure 5-2). A similiar trend of higher pH in chitosan solutions containing

methanol was observed for all of the different degree of deacetylation (DDA) tested, which were 94.6%, 82.6%, and 77.1% DDA. Note that the pH values in Figure 5-2 compared the solution pHs for two distinct chitosan solutions: 10 mg/mL chitosan with 25 - 100 mM acetic acid (filled symbols), and 5 mg/mL chitosan with 12.5 - 50 mM acetic acid, 50% vol/vol methanol (open symbols).

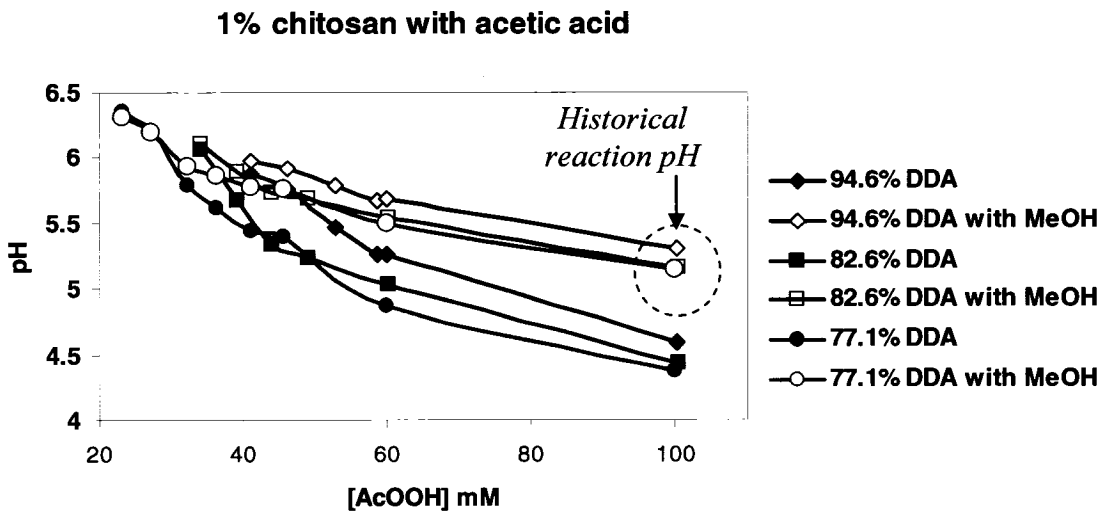

Figure 5-2. pH change of chitosan in initial acetic acid concentration (mM).
An equal amount of methanol was added to each solution for cases with methanol (MeOH). The concentration of acetic acid for solutions containing MeOH was therefore half as much as those solutions dissolved in aqueous acid alone. Note that previous labeling of chitosan with FITC was carried out at 100 mM acetic acid in 50% methanol around pH 5.5 (Qaqish and Amiji, 1999).

To compare the solution pH for different %DDA chitosans, the data were expressed as the molar ratio of acid : glucosamine for each solution (Figure 5-3). When the data were expressed in this manner, it was discovered that similar pH values were obtained for chitosan solutions dissolved at the same ratio of acid : glucosamine, irrespective of deacetylation level. These data suggested that RITC coupling to chitosan could potentially be similar for different deacetylation levels, provided the acid concentration were adjusted according to the concentration of glucosamine in a 10 mg/mL solution.

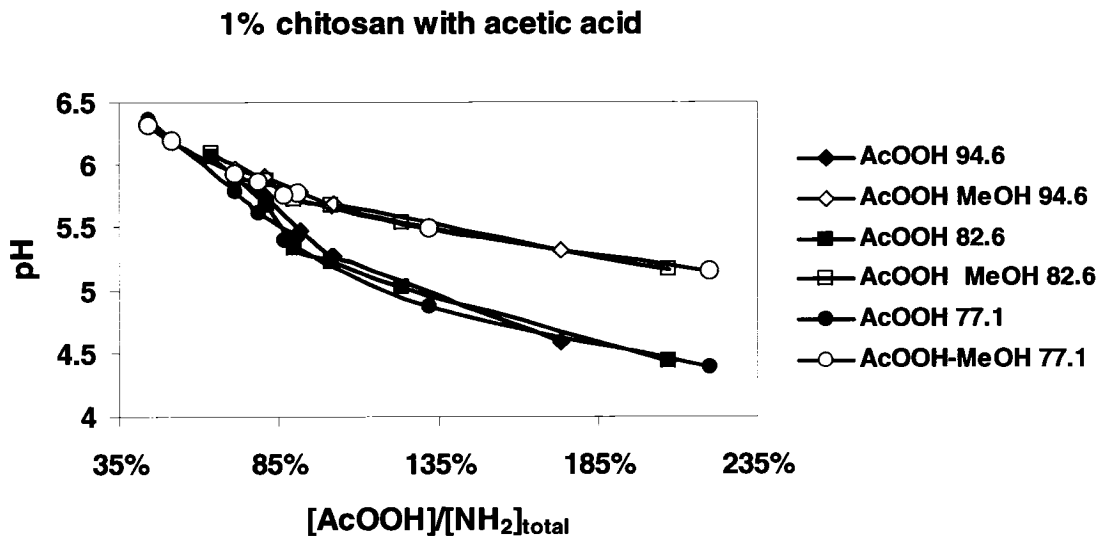

Figure 5-3. pH variation of chitosan in normalized acetic acid concentration

An interesting phenomenon manifests itself upon further inspection. It appears that at a particular normalized acid concentration, the pH remained the same even after the addition of methanol It was observed that below a certain pH for each chitosan solution analyzed, that the addition of methanol no longer resulted in an increase in final solution pH.

In Figure 5-4, we took a closer look at 77.1% DDA chitosan and dissolved it with an acid concentration (60% and 50% [AcOOH]/[NH_2]) less than at the point where the addition of methanol does not change the pH. Indeed the pH was slightly lower after the addition of methanol. The final solution pH was slightly lower after addition of methanol when the acid : glucosamine ratio was less than 61% (Figure 5-5). Overall, the solution pH attained values close to pH 6.4 with no observable precipitation in the presence of methanol, using limiting amounts of acetic acid.

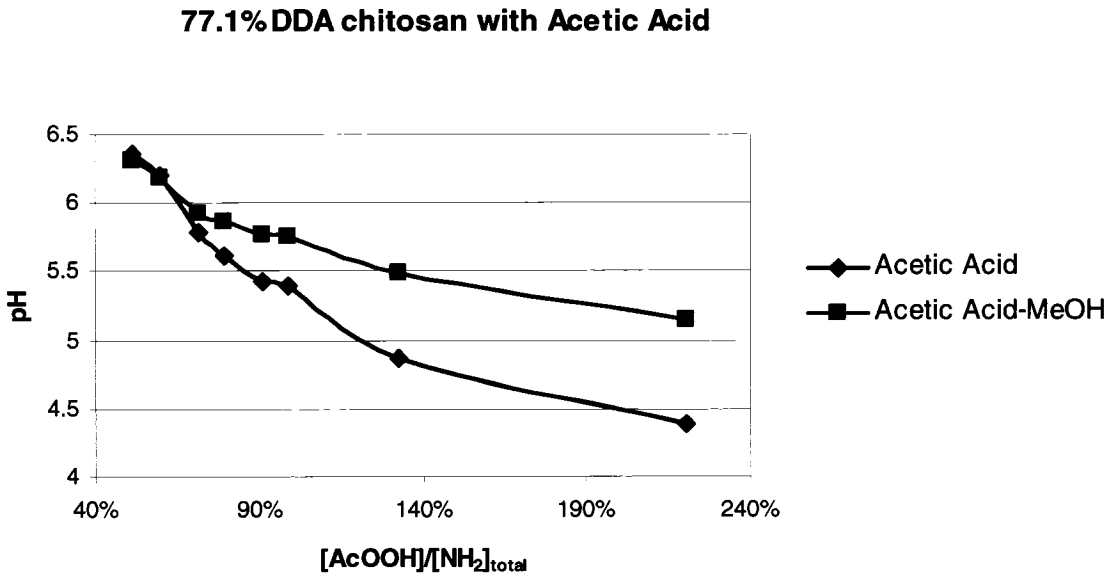

Figure 5-4. 77.1% DDA chitosan in normalized acid concentration in 50% methanol

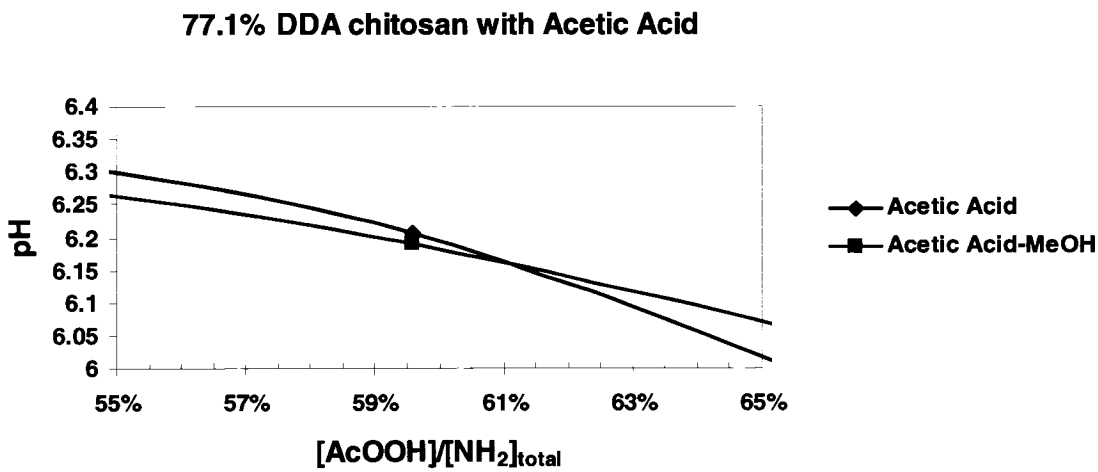

Figure 5-5. Cross over point of 77.1% DDA chitosan in acetic acid
The concentration of acetic acid where addition of methanol would switch from decreasing to increasing pH. Zoom in of Figure 5-4~~Figure 5-4~~ for the 77.1% DDA chitosan with Acetic Acid

5.2.2 Chitosan Solution pH in Lactic Acid With or Without Methanol

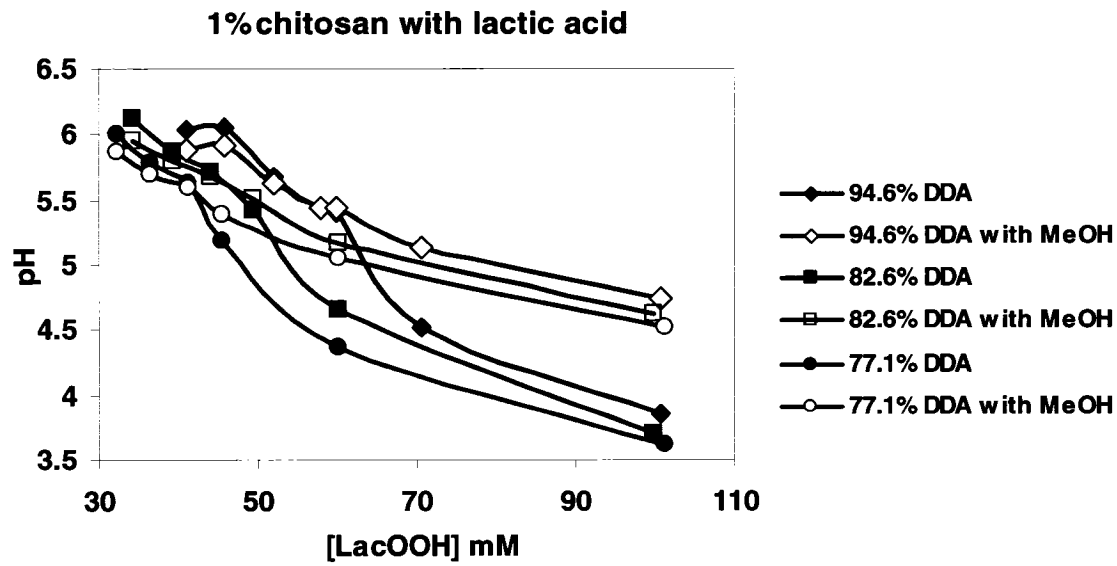

Figure 5-6. pH change of chitosan of varying DDA in lactic acid
An equal amount of methanol was added to each solution for cases with methanol (MeOH). The concentration of lactic acid for solutions containing MeOH was therefore half as much as those solutions dissolved in aqueous acid alone.

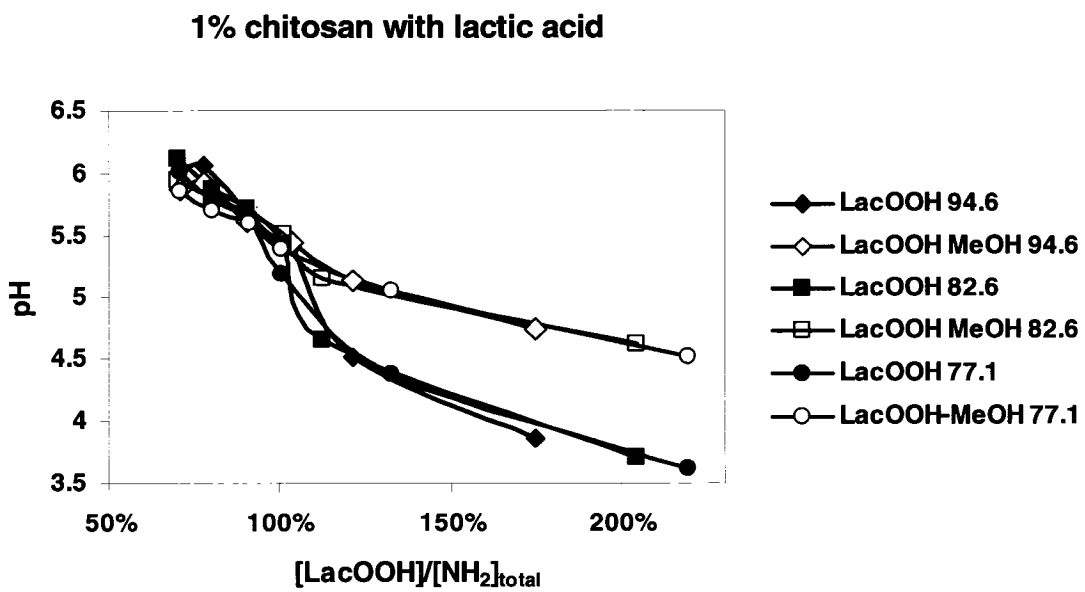

Figure 5-7. pH variation of chitosan in normalized lactic acid concentration

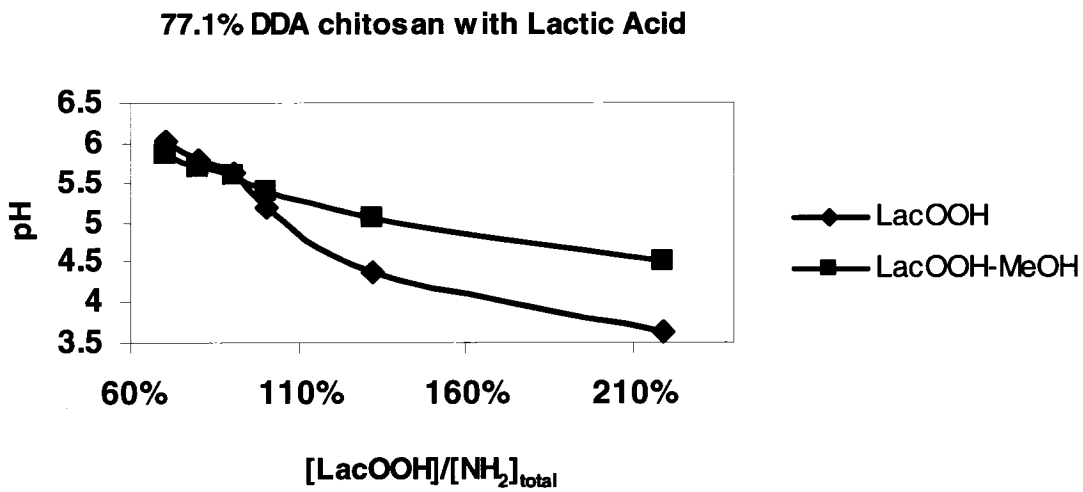

Figure 5-8. 77.1% DDA chitosan in normalized acid concentration in methanol

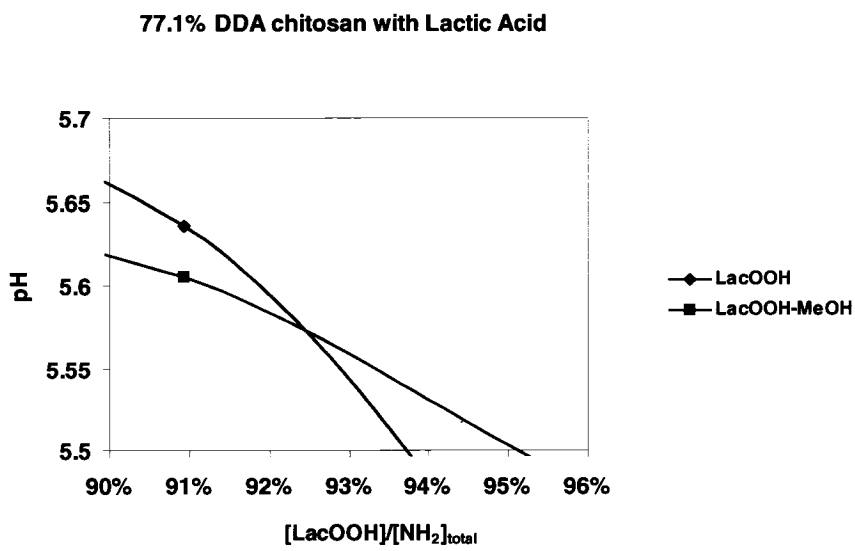

Figure 5-9. Cross over point of 77.1% DDA chitosan in lactic acid
The concentration of lactic acid where addition of methanol would switch from decreasing to increasing pH. Zoom in of Figure 5-8~~Figure 5-8~~ for the cross over point for lactic acid at 77.1%DDA, between 92-93% normalized acid concentration.

Since lactic acid is a common acid found in the body and therefore biocompatible, it is a candidate acid for dissolving chitosan for direct medical applications. The pH decreased in a similar fashion as the acetic acid curves with increasing acid concentration (Figure 5-6). Furthermore, with an addition of equal volume methanol, the also pH rose by nearly 1 pH unit at 100 mM lactic acid. When the data were represented as pH of solutions according to the ratio of lactic acid to glucosamine concentration, similar pH values were obtained for different deacetylation levels of chitosan (Figure 5-7). When chitosan is solublized with lactic acid, the point where pH change from decreasing to increasing is more apparent. Focusing on the same 77.1% DDA (Figure 5-8) chitosan, as was done for acetic acid, we notice that the cross-over point is between 92-93% normalized acid concentration (Figure 5-9). This is in contrast to acetic acid, where the cross-over point was around 60% (Fig. 1-4). Overall, the solution pH attained values

close to pH 6.0 with no observable precipitation in the presence of methanol, using limiting amounts of lactic acid.

5.2.3 Chitosan Solution pH in Hydrochloric Acid With or Without Methanol

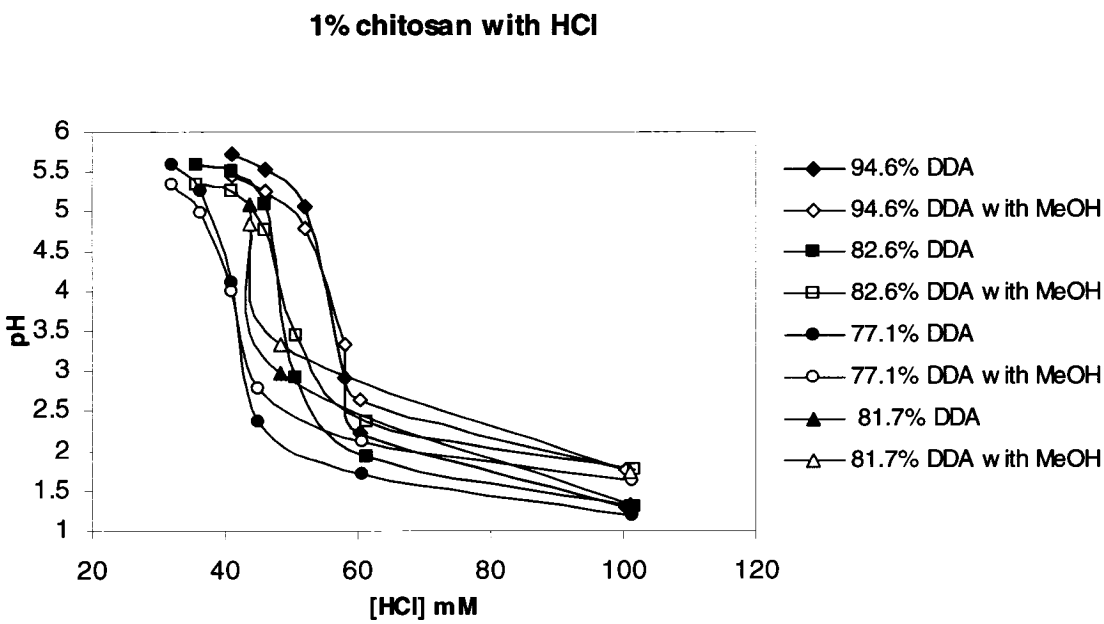

Figure 5-10. pH change of chitosan of varying DDA in hydrochloric acid
An equal amount of methanol was added to each solution for cases with methanol (MeOH). The concentration of hydrochloric acid for solutions containing MeOH was therefore half as much as those solutions dissolved in aqueous acid alone.

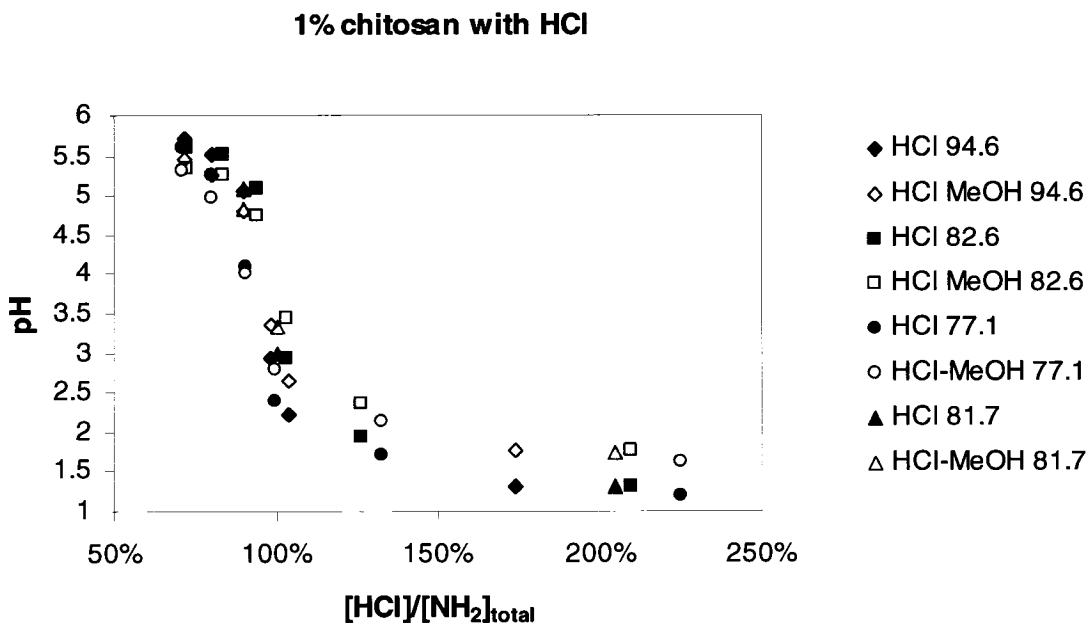

Figure 5-11. pH variation of chitosan solutions of varying DDA
as a function of the molar ratio of hydrochloric acid : glucosamine concentration

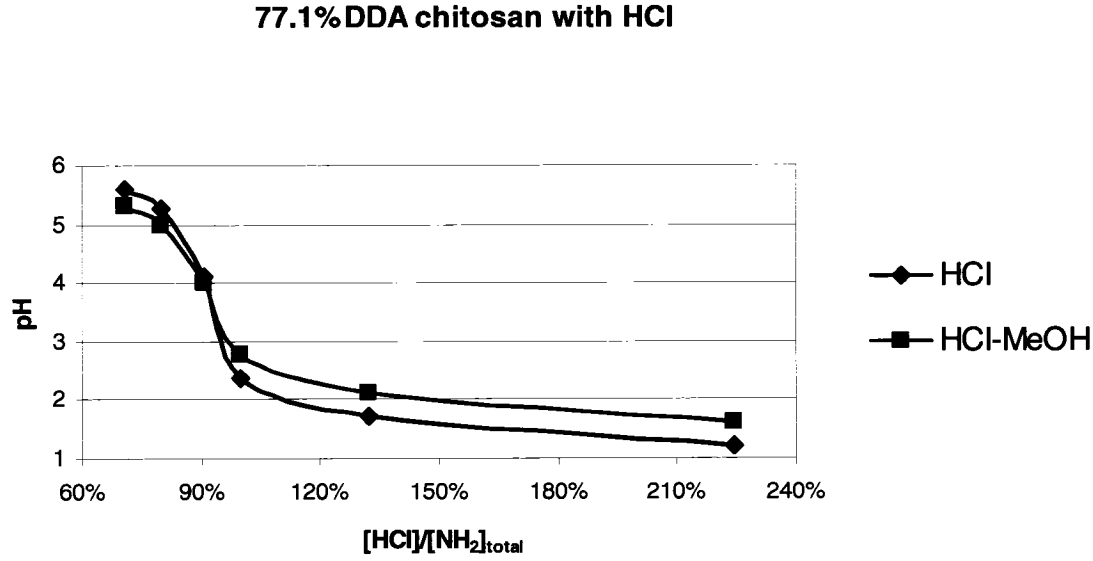

Figure 5-12. 77.1% DDA chitosan in normalized HCl concentration in methanol

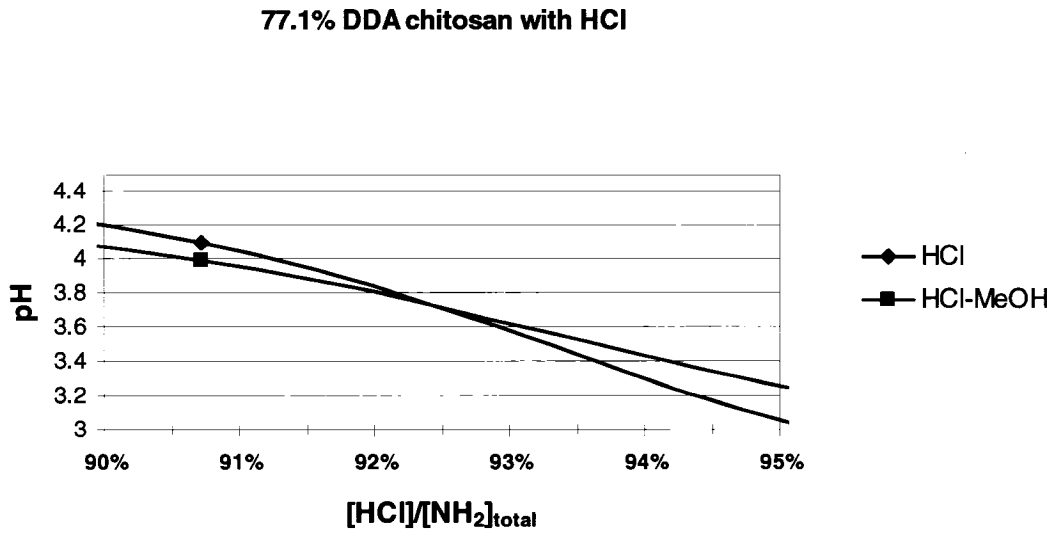

Figure 5-13. Cross over point of 77.1% DDA in hydrochloric acid
The concentration of HCl where addition of methanol would switch from decreasing to increasing pH
Zoom in of Figure 5-12~~Figure 5-12~~ for the cross-over point of HCL for the 77.1% DDA chitosan with HCl

Hydrochloric acid (HCl) was the only strong acid that was used in this study. Chitosan solutions generated with HCl demonstrated a broader pH range, from pH 1-6 (Figure 5-10), compared to the pH of solutions generated with weak acids -- acetic and lactic acid, which generated solutions with pH 4-6 (Figure 5-3, Figure 5-7). When representing the data as the molar ratio of acid : glucosamine, which in this case represents the charge state of the chitosan polymer, comparable solution pH values were obtained for different deacetylated chitosan, as observed using weak acids. Another difference from the weak acids is that with HCl, the pH only rose by 0.5 pH units after adding methanol, and only when the chitosan was over 90% protonated (Figure 5-11). For the weak acids, the change in pH difference increases with increasing acid concentration. However, for HCl, the pH gap is relatively the same at all acid concentrations, with the exception at the cross-over point (Figure 5-12), which was determined to be ~90% for the 77.1% DDA chitosan (Figure 5-13). The results of all the cross-over points are summarized in Table 5-3.

Table 5-3 suggests that the cross over point is a characteristic of the acid used. For acetic acid, that point is ~60% normalized acid; for lactic acid, it is in the ~90%; and for hydrochloric acid, it is in the ~90% range as well. The cross-over point in each acid was similar for all three deacetylation levels measured. It should be noted that the cross-over point for chitosan dissolved in acetic acid was experimentally determined uniquely for the 77.1% DDA chitosan dissolved in 50%, 60% and 70% normalized acetic acid : glucosamine, and extrapolated for 82.6%DDA and 94.6%DDA chitosan dissolved in 70% normalized acetic acid. We have indicated the experimental conditions in parentheses, where under the column chitosan DDA, the concentration of chitosan glucosamine is listed, and under the different acids columns, the concentration of acid is listed.

Table 5-3. Cross-over points for all acids and all DDAs tested
where the addition of methanol would change from decreasing to increasing pH for different acids and different DDAs. The experimental conditions are listed in parentheses. The concentration of glucosamine for a 10 mg/mL solution is listed under chitosan DDA in parentheses and amount of acid concentration for the initial 10 mg/mL solution is listed underneath the percentage of acid : glucosamine for each particular acid. The pH of a chitosan solution diluted in water instead of methanol did not result in increase in solution pH by 0.5 to 1.0 pH units.

Chitosan DDA	Acetic Acid	Hydrochloric Acid	Lactic Acid
77.1% (45mM)	61% (27.6 mM)	92-93% (~42 mM)	93% (42 mM)
82.6% (49mM)	61% (extrapolated) (30 mM)	97-98% (~48 mM)	96% (47 mM)
94.6% (58mM)	60% (extrapolated) (34.8 mM)	94% (54.5 mM)	98-99% (~57 mM)

5.3 Chitosan RITC Labeling Kinetics

The above experiments permitted us to determine which acid to use and at what concentration to obtain the optimal labeling efficiency. An improved labeling efficiency was obtained when using less than 100 mM acetic acid, when using 1 injection to

introduce the fluorophore instead of 3 injections, and by allowing the reaction to proceed for more than 4 hours. Better control over the labeling reaction was obtained when using precipitation instead of dialysis to remove residual free fluorochrome. To determine the maximum labeling over time, we performed three kinetic experiments with chitosans of different %DDA at 71.7, 80.2, and 98.4% DDA. For this experiment, after solubilizing the chitosan overnight in acetic acid with 70% acid : glucosamine ratio (pH around 5.8) adding an equal volume of methanol, and homogenizing for 3 hours, we added 3.1% mol/mol (80.2%DDA) or 2% mol/mol (71.7%DDA and 98.4%DDA) RITC per chitosan. At various time points from 0.5 to 29 hours, we withdrew 5 or 10 mL of sample and precipitated the chitosan to remove the unincorporated RITC. The supernatant and precipitated chitosan from each time point were used to compare the concentration of RITC remaining in the supernatant and RITC incorporated into the final RITC-chitosan product. These data showed the disappearance of RITC from the reaction by analyzing the supernatant washes of the RITC-chitosan product and the incorporation of RITC into the RITC-chitosan product (Figure 5-14). The data were represented as percent total RITC added to the reaction. Our collaborator at the Université de Montréal, suggested that an extinction coefficient of 85,000 $(M \cdot cm)^{-1}$ for RITC be used to determine the RITC concentration in RITC-chitosan. Therefore, the analysis in this section was based on this value.

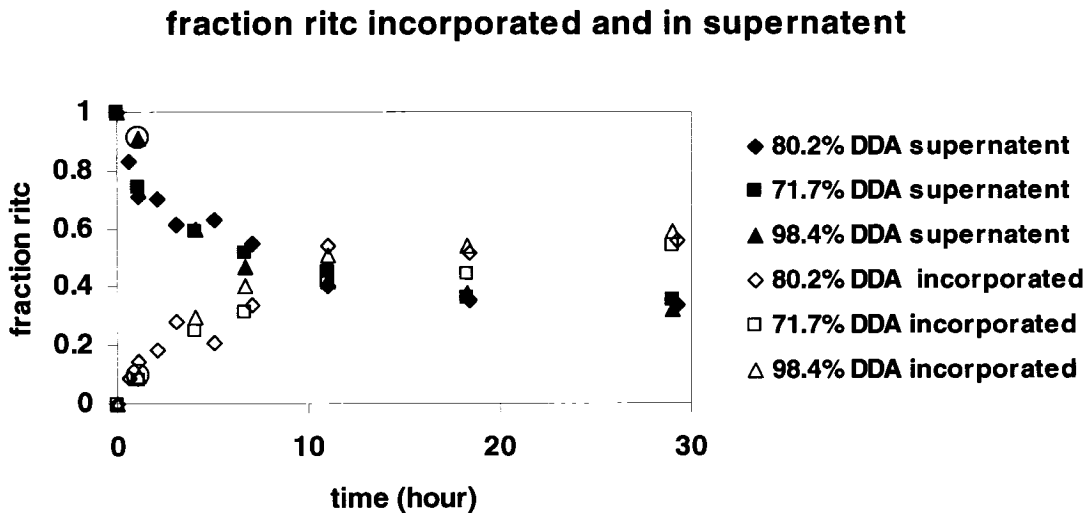

Figure 5-14. Kinetic incorporation and loss of RITC
as a function of time for 3 chitosans of different DDAs. The two circled points are from samples collected from rubber adaptors when the glass centrifuge tubes shattered. Concentration of RITC was measured by absorbance was calculated with $\varepsilon_{556nm} = 85000\ (M\text{-}cm)^{-1}$

Table 5-4. Percentage of RITC covalently bonded to chitosans with time.
For the 80.2%DDA chitosan, the reaction used 350 mg chitosan and 35 mg RITC (3.1% mol RITC/mol chitosan EPRC11-EPRC20). For the 98.4%DDA chitosan, the reaction used 350 mg chitosan and 23 mg RITC (1.9% mol RITC/mol chitosan, EPRC27-EPRC32). For the 71.7%DDA chitosan, 350 mg chitosan and 21 mg RITC (2% mol RITC/mol chitosan, EPRC21-EPRC26) was used. Percentage incorporation was determined by absorbance using the Beer-Lambert law with $\varepsilon_{556nm} = 85000\ (M\text{-}cm)^{-1}$.

time (hour)	DDA	% incorp
1.1	71.7%	8.61%
4.0	71.7%	24.66%
6.7	71.7%	31.17%
11.0	71.7%	42.02%
18.3	71.7%	44.03%
29.0	71.7%	54.24%
0.7	80.2%	9.17%
1.1	80.2%	14.71%
2.1	80.2%	18.96%
3.0	80.2%	28.36%
5.1	80.2%	20.44%
7.0	80.2%	34.39%
11.0	80.2%	54.14%
18.4	80.2%	52.10%
29.2	80.2%	55.78%
72.6	80.2%	63.85%
1.1	98.4%	9.73%
4.0	98.4%	29.85%
6.7	98.4%	40.31%
11.0	98.4%	51.06%
18.3	98.4%	54.71%
29.0	98.4%	59.36%

Figure 5-14 depicts the depletion of RITC (filled symbols) and its incorporation onto chitosan (empty symbols) represented as the change in fraction of RITC with respect to reaction time. The change in RITC depletion and incorporation varied greatly in the first few hours, and then reached a plateau at around 18 hours after which little additional incorporation was observed, even after 72 hours of reaction. These data indicated that the maximal reaction time is 18 hours, where approximately 50% of the initially added RITC

was covalently bonded to the chitosans for all DDAs tested. In Table 5-4, we listed the actual percentage of incorporated RITC, sorted by increasing DDA and increase reaction time for the three chitosans, using 85,000 $(M \cdot cm)^{-1}$ as the extinction coefficient.

Collectively, these data suggested that similar labeling efficiencies of chitosans with different deacetylation levels could be achieved by dissolving chitosan in 70% acetic acid : glucosamine and allowing the reaction to proceed for 18 hours. Additionally, we must note that at 18 hours of reaction, 77%DDA chitosan appeared to incorporate slightly less RITC (44% initial fluorophore) compared with 80%DDA and 95%DDA chitosan (54% initial fluorophore). This result however could be partly due to inaccuracy of the method used to weigh 10 to 13 mg of the toxic fluorophore in a tared cryovial, or to slower incorporation rate since all 3 chitosan were similarly derivatized at 27 hours (Figure 5-14).

5.4 Relative Fluorescence and Absorbance of RITC-Chitosan

To ensure that the precipitation method did not result in quenching of the fluorophore, the peak absorbance at 556nm versus relative fluorescence at 543nm excitation and 580nm emission of each RITC-chitosan derivative was compared. The absorbance of RITC-chitosan had a linear relationship to its relative fluorescence (RFU) for all RITC-chitosan regardless of DDA, MW, chitosan manufacturer, or method of preparation. The dialyzed chitosan showed depressed RFU vs absorbance (Figure 5-15, EPR08). This may be due to the lower pH of this sample solution, since excess acid was added to the dialyzed chitosan to promote solubility. In Figure 5-15, we presented RFU data for a dozen RITC-chitosan synthesized at École Polytechnique de Montréal (EPRC) and Universite de Montreal (UMRC), where the UMRC batches are from different suppliers – Sigma-Aldrich in St. Louis, USA (UMRC01) and Wako Pure Chemical Industries, Ltd. in Osaka, Japan (UMRC02). All of the EPRC batches were derived from chitosan manufactured at BioSyntech, Inc. in Laval, QC, Canada.

We considered two molecules as a candidate calibration tool for concentration – rhodamine B (rho B) and RITC. Rhodamine B is the free fluorophore without the

reactive group, isothiocyanate, while RITC is the fluorophore used to covalently bond to chitosan's amine group. According to Figure 5-15, the derivatized RITC-chitosans strongly followed the rho B set of data. Therefore, we used rho B to determine the extinction coefficient (Fig. 1-15). We noted that EPRC08 followed the RITC curve more strongly than the rho B curve. Yet, it was the only set of data, which followed the RITC curve. In Figure 5-16, we measured the RFU and absorbance of RITC-chitosan for the 80.2% DDA kinetics experiment. It is apparent that as the reaction time increased, the RFU and absorbance increased as well. These data sets also fall on same linear relationship as Figure 5-15.

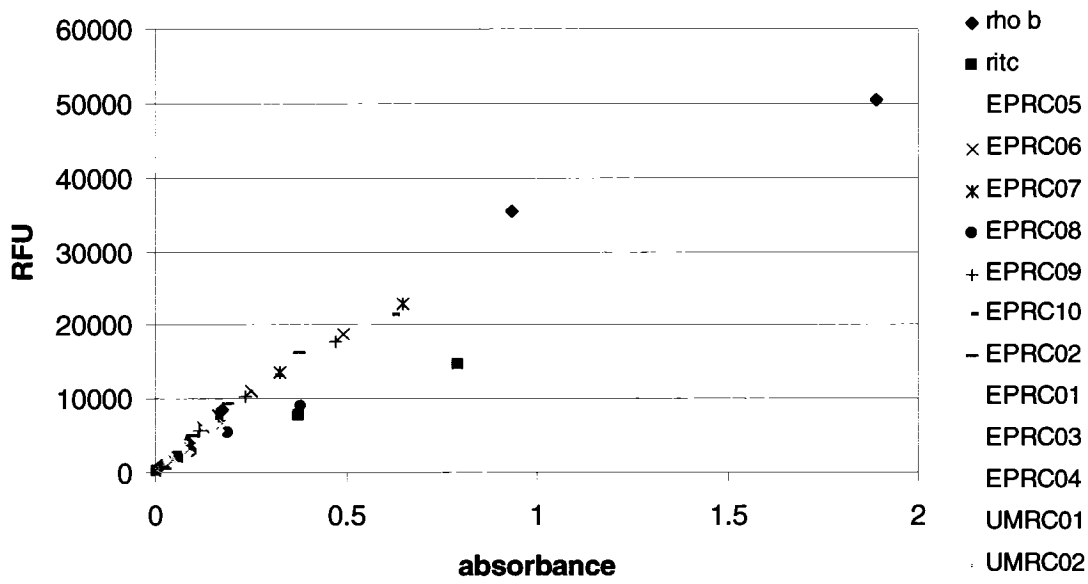

Figure 5-15. Absorbance and relative fluorescence of RITC-chitosans synthesized.
For RFU λ_{exci} = 543nm and λ_{emis} = 580nm. For absorbance measurements were taken at λ_{abs}=556nm.

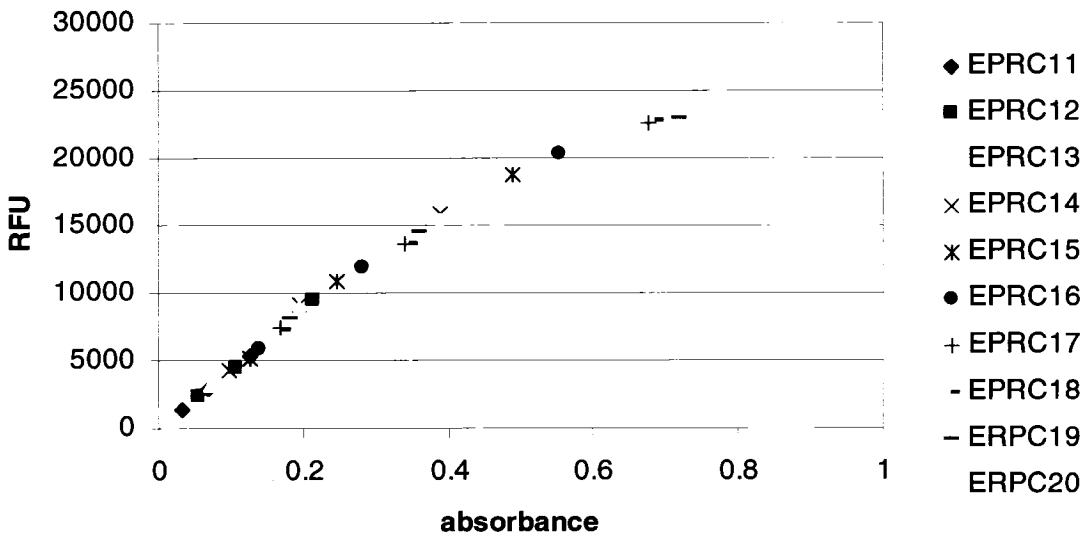

Figure 5-16. Absorbance and relative fluorescence from kinetics experiement
from the 80.2% DDA kinetic experiment. For RFU λ_{exci} = 543nm and λ_{emis} = 580nm. For absorbance measurements were taken at λ=556nm.

5.5 Effects of Salt and pH on RITC-Chitosan Fluorescence and Absorbance

Since we would be using the absorbance and RFU data to determine labeling efficiency, we explored whether RFU and absorbance could be influenced by solution pH, salt concentration, or chitosan DDA level using two RITC-chitosans of similar labeling efficiencies, EPRC04 and EPRC06 (Table 5-1). The range of conditions tested are presented in Table 5-5. We compared the change in absorbance and RFU of rhodamine-labeled chitosans with two distinct DDAs, at 50μg/mL, dissolved in two HCl concentrations (90% and 120% [HCl]:[glucosamine]) in the presence and absence of NaCl salt. The HCl concentrations were chosen in order to generate chitosan solutions with excess acid and low pH, or excess free glucosamine and higher pH.

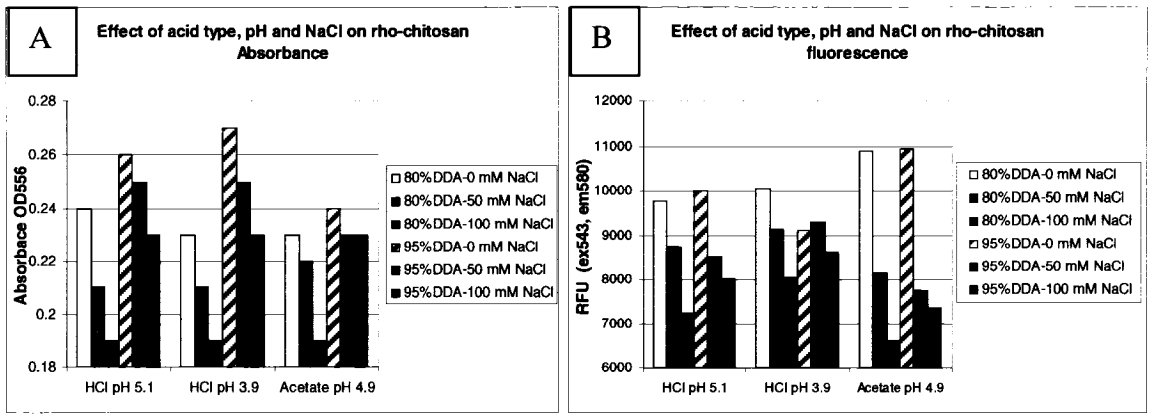

Figure 5-17. Influence on RITC-chitosanabsorbance and fluorescence
(A) Effects of acid type, pH and salt on RITC-chitosan absorbance. (B) Effects of acid type, pH, and salt on RITC-chitosan relative fluorescence.

The results showed that fluorescence was very similar for both 95%DDA and 80%DDA RITC-chitosan, dissolved in two different acids with no salt (Figure 5-17B; Figure 5-5). However, for these same solutions, the absorbance was slightly higher for 95%DDA RITC-chitosan compared to 80%DDA RITC-chitosan (Figure 5-17A; Figure 5-5). When 100mM NaCl was added, both the absorbance and the fluorescence were uniformly suppressed for both 80% and 95%DDA RITC-chitosan (Figure 5-17A&B). The derivatization level for all RITC-chitosans was determined from the absorbance of RITC-chitosan dissolved in HCl, pH 4.0 to pH 5.0, no salt.

Table 5-5. Influence of acid, salt, and pH on absorbance and fluorescence.
A final RITC-chitosan concentration of 50 μg/mL was used to determine absorbance and fluorescence. For RFU λ_{exci} = 543nm and λ_{emis} = 580nm. For absorbance measurements were taken at λ=556nm.

chitosan	DDA	[acid]/[NH_2]	acid	pH	NaCl (mM)	Abs	RFU
EPRC04	0.946	0.9	HCl	5.1	0	0.26	9995
EPRC04	0.946	0.9	HCl		50	0.25	8529
EPRC04	0.946	0.9	HCl		100	0.23	8022
EPRC04	0.946	1.2	HCl	3.9	0	0.27	9105
EPRC04	0.946	1.2	HCl		50	0.25	9312
EPRC04	0.946	1.2	HCl		100	0.23	8608
EPRC04	0.946	1.0	AcOOH	4.9	0	0.24	10936
EPRC04	0.946	1.0	AcOOH		50	0.23	7762
EPRC04	0.946	1.0	AcOOH		100	0.23	7356
EPRC06	0.802	0.9	HCl	4.4	0	0.24	9772
EPRC06	0.802	0.9	HCl		50	0.21	8745
EPRC06	0.802	0.9	HCl		100	0.19	7246
EPRC06	0.802	1.2	HCl	4.0	0	0.23	10044
EPRC06	0.802	1.2	HCl		50	0.21	9143
EPRC06	0.802	1.2	HCl		100	0.19	8038
EPRC06	0.802	1.0	AcOOH	4.9	0	0.23	10900
EPRC06	0.802	1.0	AcOOH		50	0.22	8151
EPRC06	0.802	1.0	AcOOH		100	0.19	6607

5.6 Labeling Efficiency of RITC-Chitosan

The efficiency of chitosan labeling can be determined either from the absorbance (Yamada et al, 2001; Tommeraas et al, 2001; Onishi and Machida 1999; Qaqish and Amiji 1999) or fluorescence of the fluorophore-chitosan solution (Huang et al 2002). To determine the moles RITC present in a RITC-chitosan solution, the Beer-Lambert law can be used to deduce the extinction coefficient based on absorbance of a standard curve of rhodamine B. Alternatively, a calibration curve based on fluorescence can be used to deduce molar concentration of RITC present in a RITC-chitosan solution (Figure 5-18). Absorbance has a direct linear relationship for concentrations up to an absorbance 1.0 using a conventional spectrophotometer. We observed that there is a linear relationship between fluorescence for rhodamine B concentrations for RFU values under 40,000

(Figure 5-18). Absorbance has more frequently been used to determine labeling efficiency of chitosan with fluorophore (Yamada et al, 2001; Tommeraas et al, 2001; Onishi and Machida 1999; Qaqish and Amiji 1999). The simplest method to determine derivatization of RITC chitosan is the Beer-Lambert relationship, where the extinction coefficient for rhodamine B was determined to be 90,100 using rhodamine B standards between 1 to 10 μM (Figure 5-19).

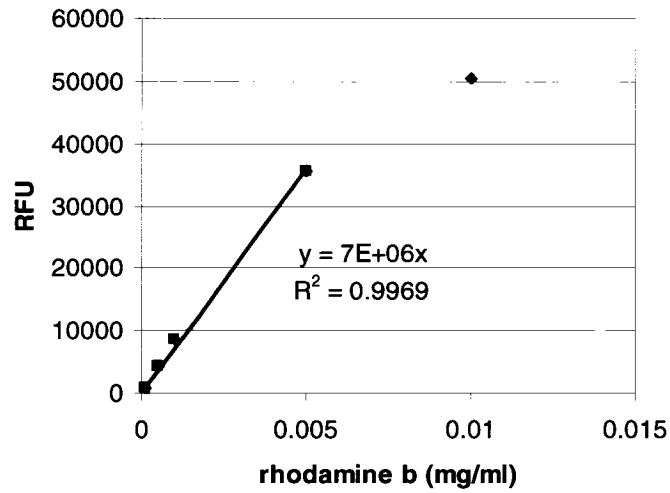

Figure 5-18. Calibration of rhodamine B for relative fluorescence
For RFU λ_{exci} = 543nm and λ_{emis} = 580nm. The RFU is linear up to 40,000 units and becomes non-linear above this value. Therefore, a RFU measurement above 40,000 units is not accurate.

The extinction coefficient of RITC-chitosan is found by determining the slope of the absorbance – rho B concentration curve as indicated by Equation 5-2. In this equation, A is the absorbance of the species measured; ε is the extinction coefficient at maximal absorbance wavelength (λ = 556 nm for RITC-chitosan) in units of $(M \cdot cm)^{-1}$; C is the molar concentration of rho B; and l is the path-length of the cuvette, which is usually 1 cm.

$$A = \varepsilon C l \rightarrow \quad C = A / (\varepsilon l)$$

Equation 5-2. Beer-Lambert relationship for absorbance and concentration
The slope of the Beer-Lambert relationship is the extinction coefficient.

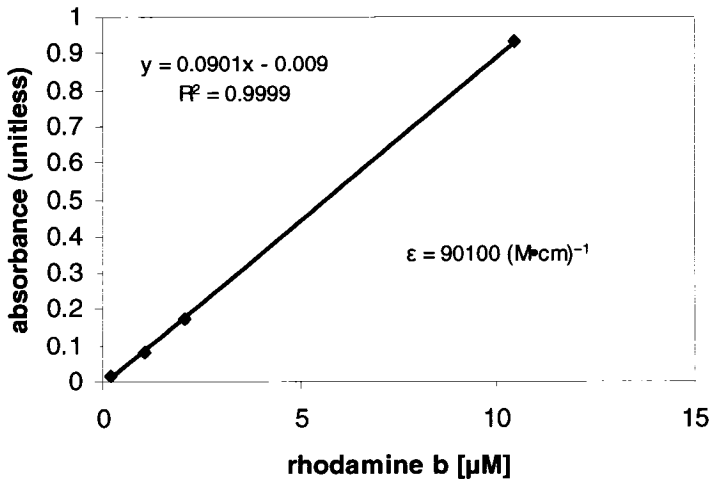

Figure 5-19. Molar extinction coefficient of rho B
determined from the slope of the Beer-Lambert relationship. For absorbance measurements were performed in quartz cuvettes at λ=556nm.

The slope of the curve yields the extinction coefficient. The labeling efficiency determined from the extinction coefficient 85,000 $(M \cdot cm)^{-1}$ (Dr. Piotr Kujawa, personal communication) and the new extinction coefficient (90100 $(M \cdot cm)^{-1}$), are very close.

Table 5-6. Extinction coefficient comparisons
for accuracy of efficiency determinations using the kinetic experiment for the 80.2% DDA chitosan.The efficiency of labeling can be calculated most accurately by absorbance calibration, and can be more easily determined by applying Beer's Law, using an extinction coefficient of 90100$(M \cdot cm)^{-1}$.

	time (hour)	ritc-chitosan (g/L)	abs	rfu avg	mol% by calib rfu	mol% by calib abs	mol% by ε = 85000	mol% by ε = 90100
EPRC11	0.6	0.025	0.0313	1462	0.30	0.24	0.25	0.24
EPRC12	1.1	0.025	0.0545	2350	0.47	0.41	0.43	0.41
EPRC13	2.4	0.025	0.0711	3268	0.66	0.54	0.57	0.53
EPRC14	3.0	0.025	0.0958	4365	0.88	0.73	0.76	0.72
EPRC15	5.1	0.025	0.1257	5247	1.06	0.96	1.00	0.94
EPRC16	7.0	0.025	0.1389	5815	1.17	1.06	1.11	1.04
EPRC17	11.0	0.025	0.1692	7426	1.50	1.29	1.35	1.27
EPRC18	18.4	0.025	0.1719	7325	1.48	1.31	1.37	1.29
EPRC19	29.2	0.025	0.1813	8162	1.65	1.38	1.44	1.36
EPRC20	72.6	0.025	0.1953	8822	1.78	1.49	1.56	1.47
EPRC11	0.6	0.05	0.0674	2868	0.29	0.26	0.27	0.25
EPRC12	1.1	0.05	0.1072	4526	0.46	0.41	0.43	0.40
EPRC13	2.4	0.05	0.1451	6063	0.61	0.55	0.58	0.55
EPRC14	3.0	0.05	0.194	9077	0.92	0.74	0.77	0.73
EPRC15	5.1	0.05	0.2447	10939	1.10	0.93	0.97	0.92
EPRC16	7.0	0.05	0.2812	11969	1.21	1.07	1.12	1.06
EPRC17	11.0	0.05	0.3386	13546	1.37	1.29	1.35	1.27
EPRC18	18.4	0.05	0.3465	13559	1.37	1.32	1.38	1.30
EPRC19	29.2	0.05	0.3596	14455	1.46	1.37	1.43	1.35
EPRC20	72.6	0.05	0.3871	15391	1.55	1.47	1.54	1.45
EPRC11	0.6	0.1	0.1258	5400	0.27	0.24	0.25	0.24
EPRC12	1.1	0.1	0.215	9404	0.47	0.41	0.43	0.40
EPRC13	2.4	0.1	0.2925	12551	0.63	0.56	0.58	0.55
EPRC14	3.0	0.1	0.3873	15889	0.80	0.74	0.77	0.73
EPRC15	5.1	0.1	0.489	18807	0.95	0.93	0.97	0.92
EPRC16	7.0	0.1	0.5546	20298	1.02	1.05	1.10	1.04
EPRC17	11.0	0.1	0.6768	22634	1.14	1.29	1.35	1.27
EPRC18	18.4	0.1	0.6877	22696	1.15	1.31	1.37	1.29
EPRC19	29.2	0.1	0.7175	22978	1.16	1.36	1.43	1.35
EPRC20	72.6	0.1	0.7727	25026	1.26	1.47	1.54	1.45

5.7 Synthesis of Six Distinct Chitosans at Similar Labeling Efficiency

Once the conditions of chitosan reactions with RITC has been optimized and the method of efficiency determination has been established, our goal was to synthesize a fluorescent chitosan library to determine if there are any effects of DDA or MW on chitosan uptake by cells. Chitosan with three DDAs were chosen – 92.7, 80.0, and 71.7% DDA as well as two different MWs (~140kDA and ~40kDA), for a total of six different chitosans. The results of the reactions are presented in Table 5-7. Using the materials provided in the RITC-chitosan reaction, we added an amount of RITC to target a 2% labeling efficiency. The reaction was allowed to proceed for 18 hours, which according to the kinetics experiment predicted a ~50% labeling efficiency. Furthermore, the kinetics experiment also indicated that approximately 10% more RITC would be required to achieve the same labeling efficiency. We obtained a labeling efficiency of 0.9 to 1% labeling efficiency using an extinction coefficient of 90,100 $(M \cdot cm)^{-1}$.

Table 5-7. Efficiency calculations for chitosans of 3 DDAs and 2 MW (batches EPRC33-EPRC38) with $\varepsilon = 90{,}100\ (M \cdot cm)^{-1}$.

Descrp	% DDA	Abs λ=556nm	avg RFU	samp (g/L)	eff mol fluor - mol chito%	eff wt fluor/ wt chito	intend mol fluor/mol chito %	intend wt fluor/wt chito %
152 kDa	92.7	0.1196	6120	0.025	0.9	2.8	2.0	6.5
Centrf	92.7	0.2445	11328	0.05	0.9	2.9	2.0	6.5
18 hours	92.7	0.4809	19631	0.1	0.9	2.9	2.0	6.5
36.5 kDa	92.7	0.1311	6513	0.025	1.0	3.1	2.0	6.5
Centrf	92.7	0.2633	12041	0.05	1.0	3.1	2.0	6.5
18 hours	92.7	0.5249	20263	0.1	1.0	3.1	2.0	6.5
143.3 kDa	80	0.1156	5962	0.025	0.9	2.8	2.0	6.3
Centrif	80	0.2339	11132	0.05	0.9	2.8	2.0	6.3
18 hours	80	0.4634	19412	0.1	0.9	2.8	2.0	6.3
38.9 kDa	80	0.1157	5881	0.025	0.9	2.8	2.0	6.2
Centriff	80	0.2337	10512	0.05	0.9	2.8	2.0	6.2
18 hours	80	0.4608	19073	0.1	0.9	2.7	2.0	6.2
140.4 kDa	71.7	0.1305	6749	0.025	1.0	3.1	2.2	6.8
Centrif	71.7	0.2636	12196	0.05	1.0	3.1	2.2	6.8
18 hours	71.7	0.5255	20995	0.1	1.0	3.1	2.2	6.8
36.5 kDa	71.7	0.1158	6136	0.025	0.9	2.8	2.2	6.7
Centrif	71.7	0.2317	11202	0.05	0.9	2.8	2.2	6.7
18 hours	71.7	0.4625	19186	0.1	0.9	2.8	2.2	6.7

5.8 Bone Marrow Cell and HEK293 Cell Interaction with Chitosan

Our first experiments with RITC-chitosan with cells, involved Sigma RITC-chitosan acetate salt (UMRC01), which gave us a rough idea of chitosan's interaction with the 3rd passage (P3) rabbit bone marrow cells (BMSC) and HEK293 cells. BMSC were exposed 18 hours to RITC-chitosan, rinsed, and cultured for an additional 4 days. We were able to observe red vesicles inside the cell when the culture media contained

FBS serum with or without heat inactivation (Figure 5-20B & C). When cells were cultured with RITC-chitosan in serum-free DMEM media, a diffuse red cytoplasmic red signal was observed (Figure 5-20A). Therefore, at least some rabbit P3 BMSC cells cultured in normal media were phagocytic for RITC-chitosan. Furthermore, exposure to very high concentration of RITC-chitosan (0.625 mg/mL) was not generally toxic to rabbit P3 BMSC cells which reached confluency 4 days after exposure to RITC-chitosan. It is interesting to note the size of the chitosan particles found within the media. In the DMEM media, chitosan were found in large aggregates, followed by a smaller, more digestible size found in the heat-inactivated serum, where most of the chitosan gathered around the nuclues. The smallest chitosan particles were found with the regular serum media. The size of the chitosan particles may influence uptake. We conjectured that a medium size particle, such as the one found in the heat inactivated serum would be an ideal size for quick uptake of chitosan. We also noticed that vortex mixing of RITC-chitosan dissolved in water or media results in various sized aggregates and that it did not acidify the media. The RITC-chitosan aggregates sedimented on the cells during the 2½ hours period of exposure to the cells.

In HEK293 cells exposed to 50 μg/mL chitosan-acetate salt, 80%DDA (UMRC01) for 4 to 18 hours, many cells contained 1 to 2 μm diameter fluorescent red vesicles (Figure 5-20 E through H). Calcein AM and Hoechst 33234 were used as a live cell counter-stain for the HEK293 cells after RITC-chitosan exposure. Calcein AM is a membrane stain for live cells, while Hoechst dye is stain to label all nuclei (dead and live cells). By using both of these stains, we were able to determine if there was co-localization of RITC-chitosan with the cytoplasm or nuclei. We can see that the chitosan appears to be gathering in the cytoplasm (from Figure 5-21) near the nuclear membrane (Figure 5-22).

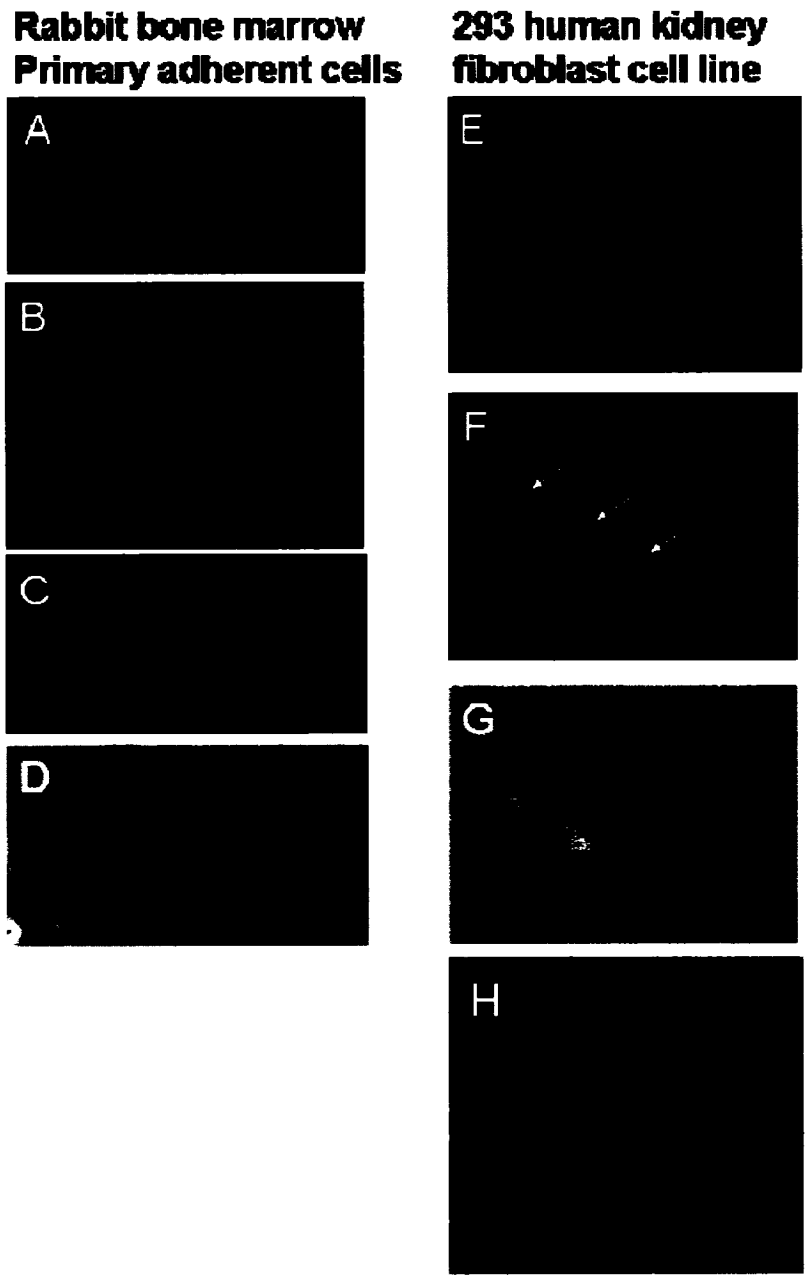

Figure 5-20. RITC chitosan uptake by undifferentiated bone marrow stromal cells
(A)DMEM with no serum; (B)10% heat inactivated serum or (C)10% FBS after 3 days exposure (650μg/mL) washing and 3 days of additional culture. A subset of cells took up the chitosan. (D)Phase contrast image of P3 rabbit bone marrow stromal cells. (E-G) RITC chitosan was taken up by all HEK293 cells in DMEM with 10% FBS after 18 hours exposure with 50 μg/mL. Nuclei of cells are stained in blue by Hoechst dye. RITC-chitosan is visible in 1-3μm diameter red vesicle. (H)HEK293 cells were exposed to RTIC chitosan for 18 hours, washed, and subcultured for 12 days, after which red fluorescent vesicles were still present in some cells. (A-G) 40x original magnification. (H) 20 x original magnification

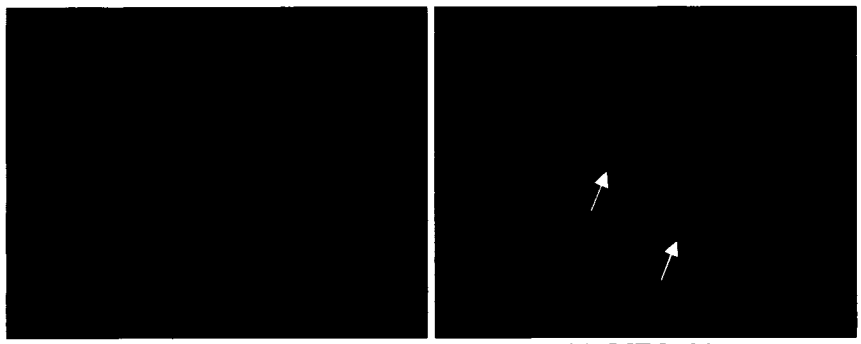

Figure 5-21. Calcein AM stained bone marrow stromal cells with RITC chitosan
40x, Calcein AM is a vital stain based on esterase-modification of calcein AM which produces a fluorescent derivative. The RITC-chitosan (UMRC01) is observed in the vescicles of BMS cells (white arrows) in DMEM + 10% heat inactivated FBS one day after first incubation with cells.

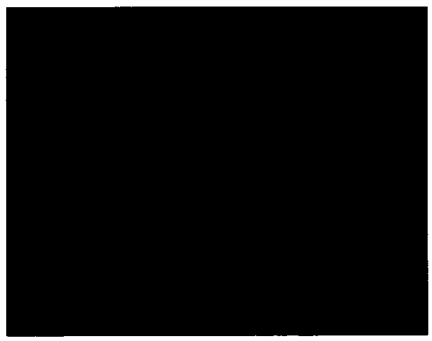

Figure 5-22. Hoescht stained bone marrow stromal cells with RITC chitosan
40x, RITC-chitosan UMRC01 in vesicles close to the nuclear membrane of BMSC cultured for 18 hours with UMRC01 at 650 μg/mL then rinsed and cultured an additional six days.

Since endosomes and phagosomes are routed through the lysosomal compartment, we tested whether any of the RITC-chitosan vescicles observed at 4 hours post-uptake were lysosomes. Cells were fixed and immunostained with an antibody to LAMP2 (lysosomal-associated membrane protein 2, a lysosome-specific protein). In Figure 5-23, we have shown that the RITC-chitosan appears to co-localize with the LAMP2 antibody, due to overlapping fluorescence of the red vesicles with some of the green LAMP2-positive vesicles by inverted fluorescence microscopy. This result was obtained for both UMRC01 and UMRC02 after 4 hours of incubation with HEK293 cells.

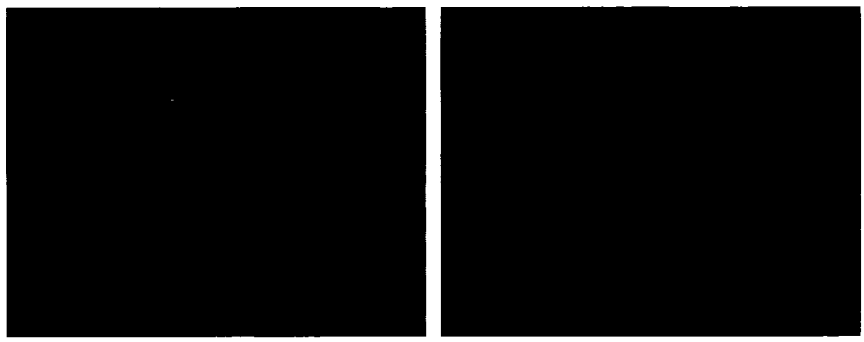

Figure 5-23. HEK 293 cells in 50 μg/mL of different RITC-chitosans
100x, HEK 293 cells in the presence of 50 μg/mL UMRC01 (left, red) and UMRC02 (right, red). Lysosomes were immunostained with LAMP2 and anti-mouse Alexa488 (green, gift from Professor Robert Nabi) and nucleus (blue, labeled with Hoechst 33358) after 4 hours of incubation. The yellow signal indicates potential co-localization of RITC-chitosan and LAMP2.

We have preliminary data on the internalization and retention of RITC-chitosan by HEK293 cells, which were incubated with 82.6% DDA RITC-chitosan (EPRC01) at 50 μg/mL overnight and passaged over 2 weeks. In the first few days, the cells appeared to clump together. However, after several passages, the cells recovered. Two weeks later, fluorescent particles were still seen within the cells (Figure 5-24). Exposure of HEK293 cells to free rho B resulted in a homogenous staining of the cell membrane and a complete lack of vesicular staining (Figure 5-25).

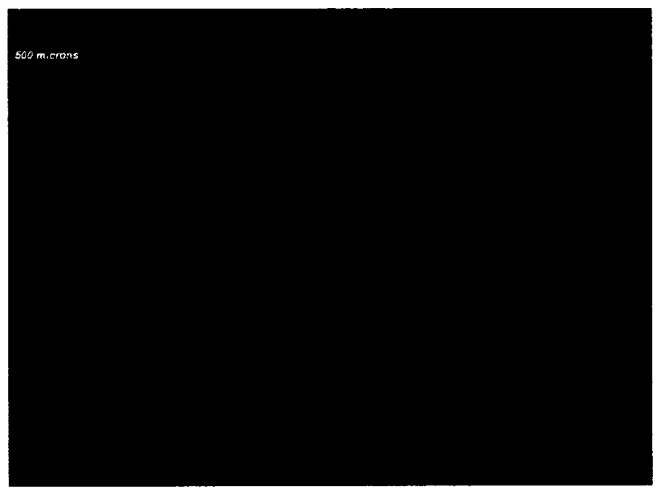

Figure 5-24. HEK293 cells exposed to RITC chitosan and passaged for 2 weeks
4x, Phase contrast with red fluorescent filter. 80% confluent HEK 293 cells exposed for 18 hours to 50μg/mL EPRC01 and then passaged for two weeks after first incubation. Cells proliferated during

passaging but two weeks after first incubation with EPRC01 in DMEM +10% FBS, red markers were still seen within the cells. Scale bar upper left : 500 μm.

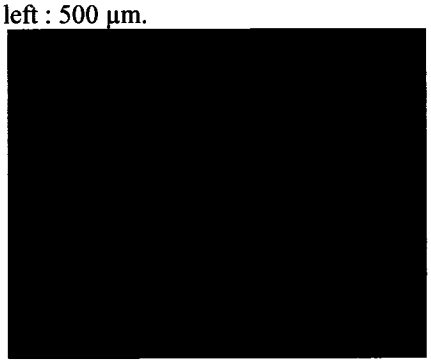

Figure 5-25. 20x, HEK293 cells in complete media with rho B
24 hours after incubation with free rho B fluorophore, a diffuse membrane signal and no vesicle uptake was seen. Scale bar : 100 μm.

To observe the uptake of RITC-chitosan with distinct molecular mass and %DDA, we cultured HEK293 cells for 20 hours in the presence of 5μg/mL RITC-chitosan from the library of 6 chitosans. In Figure 5-26, at 92.7%DDA, chitosans exhibit smaller particle size with many particles seemingly within cellular structures At 80% DDA, RITC-chitosan revealed slightly larger particles under the fluorescent lamp, with few particles within the vesicles, while 71.1%DDA RITC-chitosan resulted in even larger particle size where chitosan particles surround the cells. We observed no noticeable differences between MW at the same DDA. The RITC-chitosans were not cytotoxic to the cells, since they all showed a good morphology even at higher RITC-chitosan concentrations.

We provided several controls for comparison (Figure 5-27). Cells were incubated with unlabeled chitosan for comparison. No fluorescent particles were detected using the red emission filter and fluorescent lamp. Furthermore, we also used an acid control, where the same concentration of acid used to dissolve 80% DDA chitosan overnight, was used directly on cells without chitosan. This had a cytotoxic effect on the cells, which is evident by the rounding and clumping up of the cells. Our negative control, hydrogen peroxide had a highly toxic effect on the cells. All of the cells in this well were necrotic. Cells that were incubated to close proximity to the negative control and acid control (unlabeled and labeled 40kDa 71.7% DDA) were less viable than the cells that were

further away. These data show that all 6 structurally distinct chitosans bound to, and were internalized, by the HEK293 cells.

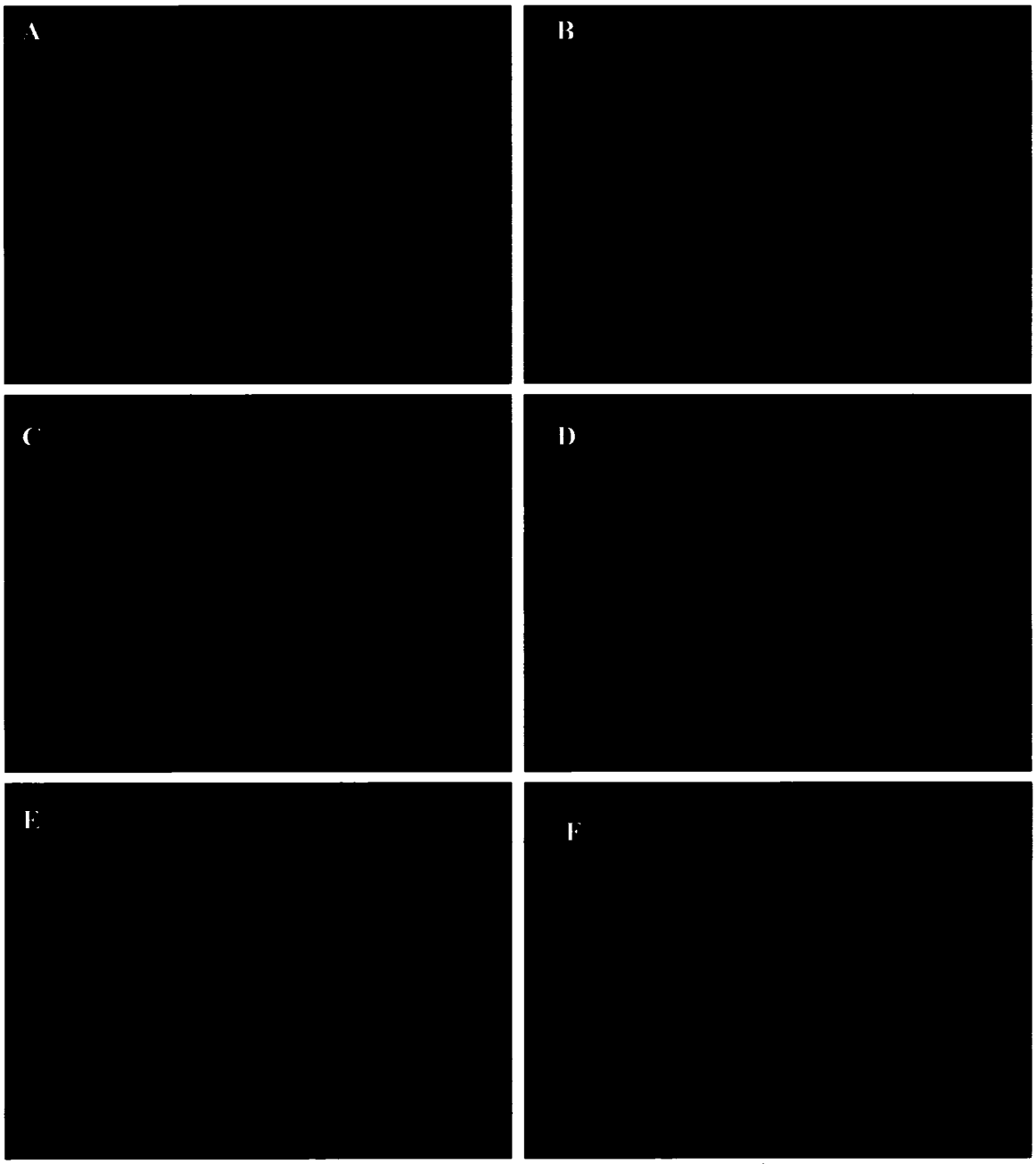

Figure 5-26. Fluorescent RITC-chitosan with HEK293 cells.
20x original magnification. Scale bar (lower right) = 100μm. 92.7%DDA (A: 152kDa, B: 40.7kda). 80%DDA (C: 143.3kDa, D 38.9kDa). 71.7%DDA (E: 140.4kDa, F 36.5kDa). The higher the DDA, the smaller the particle size.

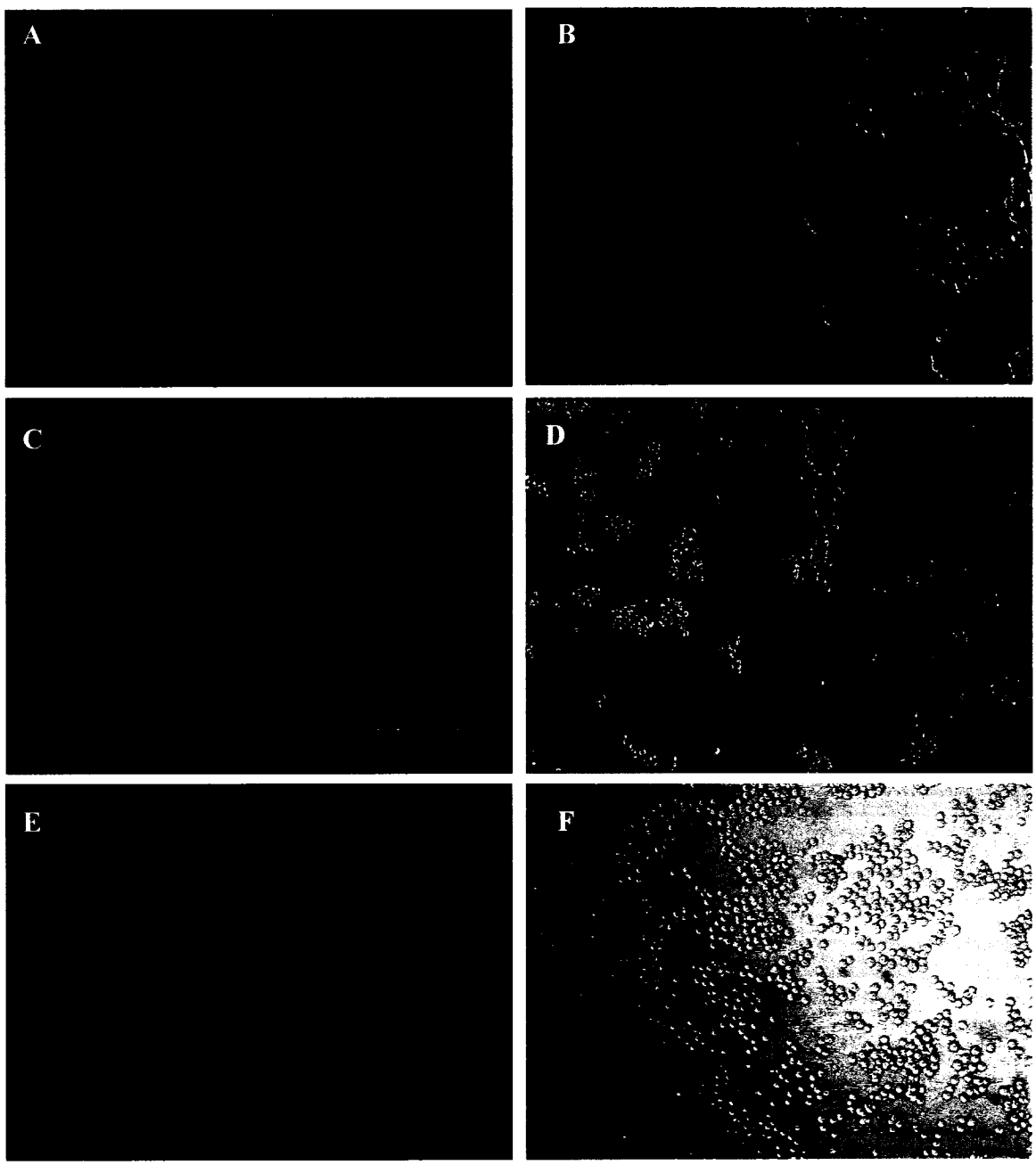

Figure 5-27. HEK cells controls

20x, scale 100μm. A: 94.6% DDA unlabeled chitosan. B: positive viability control, nothing added. C: 80% DDA unlabeled chitosan. D: 0.224 mM HCl. E: 71.7%DDA unlabeled chitosan. F: negative viability control 50% H_2O_2 in media. HCl is cytotoxic without the chitosan buffer.

Chapter 6: Discussion

6.1 Chitosan Behavior with Acid

In this study, we have generated several 1% chitosan solutions with DDAs ranging from 77% to 95% using three different acids – acetic acid, and lactic acid, and hydrochloric acid. Both lactic and acetic acid gave a relatively linear pH titration curve, while the HCl curve was precipitously sigmoidal. Acetic acid and lactic acid are both weak acids. Therefore, their behavior with chitosan resulted in a similar curve as the acid concentrations were augmented.

Lactic acid has a pKa of 3.86, which is less than that of acetic acid (pKa 4.75), making acetic acid the weaker acid. This is why acetic acid showed the least decrease in pH with increased acid (Figure 5-3, Figure 5-7). From our data, it is evident that all three acids are candidate acids for fluorophore coupling depending on the amount of fluorophore desired on chitosan. However, to achieve maximal labeling efficiency, acetic acid is the best choice as an acid solvent for several reasons, (1) chitosan solubility is better in acetic acid than HCl (Rinaudo, Pavlov, and Desbrières, 1999), (2) no precipitation of chitosan occurs in 50% volume/volume methanol even when using a minimal amount of acetic acid (70% [AcOOH]/[glucosamine]), and (3) the final reaction pH in acetic acid : methanol (1:1 vol/vol) is higher compared to chitosan-acetic acid (Figure 5-5) where even at 70% [AcOOH]/[glucosamine], the pH increased after an equal volume of methanol was added. Since the protons could be absorbed by the acetate (pKa 4.75) counterion in the presence of methanol, this indicates that more glucosamine sites will be available to react with isothiocyanate. This latter behavior, is term the "cross-over behavior" of chitosan pH in methanol-acid solutions. By contrast, for lactic acid, the solution pH was lower after an addition of equal volume methanol at 70% [LacOOH]/[glucosamine]. Since the lactate pKa is much lower, addition of methanol at

the same relative acid concentration will result in amine group protonation (changing NH_2 to NH_3^+), which is predicted to result in lower labeling efficiency.

Labeling with hydrochloric acid is expected to be the least efficient. Chitosan can be solubilized with both HCl and acetic acid at a minimum of 50% [HCl]/[glucosamine] (Rinaudo, 1999). Therefore, since acetic acid is a weak acid, it would not fully dissociate in solution, so would not give up their protons for chitosan. HCl however will fully dissociate in solution to protonate all the sites possible at that concentration. Furthermore, small pipetting errors when adding acid to dissolve chitosan could result in much greater pH variation using HCl compared to weak acids which possess a certain buffering capacity, making weak acids a such as acetic acid the best choice for targeted labeling. Around 50% to 60% of the initially added fluorophore became coupled to chitosan after 18 hours of reaction in 70% [acetic acid]/[glucosamine] in 50% v/v methanol. Theoretically, the most efficiently labeled chitosan could be achieved if 1% weight/volume chitosan were solubilized with acetic acid at 60% [acid]/[glucosamine] -- irrespective of DDA level. However, we have only tested one chitosan which was soluble at this concentration in 50% v/v methanol. For the same chitosan at 50% [AcOOH]/[glucosamine], the addition of an equal volume of methanol showed signs of precipitation. Roberts (1992) suggested that chitosan in some circumstances can remain soluble in up to 70% methanol.

The strong acid solutions exhibited very low pH values as the acid concentration was proportionally increased. Therefore, HCl at concentrations above 100% [HCl]/[glucosamine] appears unsuitable for labeling purposes since the chitosan will be fully protonated. It should be noted however, that we did achieve 1 label per 2000 monomers (which is 1 label per 1660 free glucosamine residues) for Oregon Green-ITC at a pH where chitosan is predicted to carry 100% charged glucosamine-$NH3^+$.

6.2 Labeling, Kinetics, and Efficiency

Targeted labeling would not be possible without knowing how long the process would take to reach a specific labeling efficiency. Using chitosans of three DDAs allowed us to visualize the progression of the labeling efficiency as a function of time. In the first hour (1.1h), the incorporation of RITC is varied as 71.1% DDA had an incorporation of 8.61% of the RITC, 80.2% DDA had a 14.71% incorporation, and 98.4%DDA had a 9.73% incorporation. Since the RITC concentration for 80.2% DDA was higher than for the other two experiments, it had a faster RITC incorporation. Qaqish and Amiji had labeled their chitosan with a reaction time of 1 hour in the dark and obtained 1 FITC (fluorescein isothiocyanate) label per 70 D-glucosamine residues. Just like the situations in literature, RITC was the limiting reagent in our experiments as well, where available D-glucosamine sites are more abundant than RITC. We are not certain as to why they were able to achieve a labeling a higher labeling efficiency than we have obtained in a greater amount of acid and less time to react. However, our experiments, show that within the first 4 hours, the incorporation rate can vary greatly, but not to this extent.

Other groups had solubilized chitosan at a lower pH, only to adjust the pH back up with NaOH prior to reacting chitosan with isothiocyanate-fluorophore (Yamada et al, 2001; Onishi and Machida, 1999; Ishii, et al, 2001). It is interesting to note that various groups were able to dissolve their chitosan by adjusting their pHs with NaOH at pHs, from 6.5 to 7.2, however, ending up with very different results (Yamada et al, 2001; Onishi and Machida, 1999; Ishii et al, 2001). Both Onishi and Yamada had a reaction time of 24 hours but Onishi managed a labeling efficiency of 6.4% (w/w) while Yamada et al only managed a 0.6% (w/w) labeling efficiency. Ishii had a labeling efficiency of one texas red per 40 chitosan molecules with an overnight reaction, which is a very low 0.04% (w/w) derivatization. The big difference between Yamada and Onishi's experiments is that Onishi's chitosan was 50% DDA, while Yamada's chitosan was 82% DDA. Similar to Yamada et al (1999), we have added beta glycerol-phosphate (β-GP) a bivalent disodium salt, to increase the pH after solubilizing chitosan in 60 mM acetic

acid, since chitosan will stay in solution even at a pH of 6.8-7.2 in the presence of β-GP (Chenite et al, 2000). However, chitosan-glycerol phosphate at pH 6.5, began to precipitate during of the addition of anhydrous methanol. The precipitated chitosan was less efficiently labeled that soluble chitosan, with a labeling efficiency of 0.3% mol/mol, compared to an identical reaction where chitosan remained soluble and was labeled at 0.8% mol/mol (EPRC02 vs EPRC03, Table 5-1). Our data therefore suggest that the low labeling efficiencies obtained by Ishii et al (2001) and Yamada et al (2001) were due to the fact that their labeling conditions induced chitosan precipitation. Therefore, pH plays a more critical role in determining labeling efficiency than DDA. When the pH is too low, the chemical reaction is inhibited by protonated glucosamine. When the pH is too high, the chitosan precipitates and is less efficiently labeled.

After 18 hours of reaction time, both 98.4% and 80.2% DDA had RITC incorporations around 50%. However, the 71.7% DDA only had 44% incorporation. It was suggested that the labeling lower efficiencies for the 71.7% DDA was due to the inaccurate method of taring the cryovial to weigh RITC. However, for the 98.4% and 80.2%DDA, the RITC weight was also determined using this method. Furthermore, evident in the labeling of 6 chitosan at equal efficiencies, it was necessary to increase the RITC concentration by 10% to obtain the same results. Therefore, the reason for the lower derivatization of 71.7% DDA chitosan could be due other factors, including steric hindrance by block acetyl groups, or charge state. Since 71.7%DDA has a higher pKa (pKa = 6.68) compared to 100%DDA (pKa = 6.28) (Filion et al., 2005), at the same pH, more neutral amine groups will be available for reaction with 100%DDA chitosan compared to 71.7%DDA chitosan.

6.3 Effects of Salt andpH and on RITC-Chitosan Fluorescence and Absorbance

Although RITC and RITC B carry the same fluorophore moiety, RITC was strikingly less fluorescent compared to rho B, at the same molar concentration. Absorbance was also smaller for RITC compared to rho B, at the same molar

concentration. We currently have no explanation for these findings. The extinction coefficient for RITC-chitosan was generated using rho B fluorophore standard. It was determined that RITC-chitosan had a lower fluorescence and absorbance when excess acid (pH less than pH 4.5) or salt (100 mM) was present. A similar absorbance was observed for RITC-chitosan dissolved in dilute acetic acid or dilute HCl (pH 5.0). These data suggest that for more accurate determination of labeling efficiency, RITC-chitosan should be dissolved in the same amount of acid as the concentration of glucosamine groups to ensure full solubilization of RITC-chitosan at a pH no less than pH 4.0.

6.4 Determination of the Extinction Coefficient of Rhodamine B in Water

The extinction coefficient of rhodamine B in ethanol was previously found to be 106,000 $(M \cdot cm)^{-1}$. Using standards prepared between 0.2 and 10μM, the extinction coefficient of rho B in water was determined to be 90100 $(M \cdot cm)^{-1}$. We assume that this extinction coefficient can be used to extrapolate the labeling efficiency of RITC-chitosan, despite the fact that the extinction coefficient for RITC was appreciably less than rhodamine B. An extinction coefficient 90100 $(M \cdot cm)^{-1}$ is close to that found by Dr. Kujawa (85,000 $M \cdot cm^{-1}$, personal communication).

6.5 HEK293 Cell Interaction with Chitosan

We have previously incubated HEK293 cells with various RITC labeled chitosan at a concentration of 50 μg/mL. These cells were able to survive two weeks, proliferated, and retained the fluorescent particles within them. What we have shown with the six chitosans of three DDA and two molecular weights is that the particles appear to be smaller with higher DDAs when combined with cell culture media containing serum. The labeling efficiencies of the chitosans studied are 1 RITC per 100 monomers, each 200,000 Da chain, irrespective of %DDA, is predicted to carry around 100 RITC tags with a random distribution. It is possible that since the chitosan are chains that have

blocks of alternating glucosamine groups and acetyl glucosamine groups that there is a higher concentration of RITC centered at various blocks, especially for the higher DDA chitosans. As the DDA decreases, the available sites for labeling are spread further apart, making the fluorescent chitosan appear to be larger particles under the microscope. The surrounding of the cells by smaller DDA chitosans could be a result of this effect.

We have not truly demonstrated that chitosan is indeed internalized by the cells since we have only used an inverted fluorescent microscope to observed the cells, although our data strongly suggests that both HEK293 cells and bone marrow cells internalized the 80%DDA RITC-chitosan, since cells exposed to RITC-chitosan still contained red vesicles after cell mitosis and cell passages. Confocal microscopy or live confocal microscopy would have been a better method to observe internalization. With this method, we would be able to determine the time it takes for cells to internalize chitosan, and to observe the real effect of DDA and molecular weight on chitosan internalization.

One thing to note is that the acidic content used to solublize a 80% DDA RITC chitosan is considered to be toxic to cells as evident in Figure 22D. Cells have already clumped up due to the final concentration of 0.224 mM HCl in the media. The chitosan acts as a buffer in the media to resist the change in pH. The neighboring wells of the acid control suffered due to the exchange in acidic vapor. This is why the morphology of the cells incubated with unlabeled 71.7% DDA is slightly rounded.

Chapter 7: Conclusion

In this study, our preliminary labeling experiments with rhodamine B isothiocyanate (RITC) and Oregon green (OG) allowed us to determine that efficient labeling procedures require a control of the protonation of the chitosan glucosamine monomers. Protonation is controlled by the type and amount of acid used to solubilize chitosan before the labeling procedures begin. Initially, we had hypothesized that increasing the pH by adding beta glycerol phosphate would increase the labeling efficiency. However, the presence of the bivalent salt had precipitated the chitosan after the addition of a 1 to1 (volume to volume) ratio of methanol to chitosan solution, which was necessary for full solubility during the labeling reaction of the hydrophobic fluorophores employed. Precipitated chitosan – beta glycerol phosphate – acetic acid - methanol had a lower labeling efficiency (0.3% mol/mol, 2.8% target labeling efficiency) relative to chitosan - acetic acid – methanol (0.8 % mol/mol, 2.9% target labeling efficiency). These pilot data suggested that chitosan amine groups are maximally reactive with isothiocyanate when the reaction pH is greater than pH 4.8 and when chitosan remains soluble. Previous reports of chitosan derivatization with isothiocyanate were performed at pH 6.5 (Yamada, Onishi, and Machida, 2001), pH 6.9 (Onishi and Machida, 1999), and pH 7.2 (Ishii, Okahata, and Sato, 2001) with a corresponding labeling efficiencies of 0.3%, 2.7%, and 0.01% mol/mol with a targeted efficiency of 1.3%, 3%, and 3.2%, respectively.

Due to the potential of fluorophore dimer formation (Ali, Moghaddasi, and Ahmed, 1991), the fluorophore was added to the reaction with staggered injections to avoid dimerization. Furthermore, the labeling reaction was suggested to proceed to completion at three hours and we recovered the product by dialysis, as previously performed (Dr. Kujawa, Personal Communications). Then we compared the labeling efficiency of having three staggered injections of RITC fluorophore versus one single injection and two product recovery methods – dialysis and precipitation under alkaline conditions, at two reaction times, 4 hours and 18 hours. The results showed that having

one injection in place of three produced a higher labeling efficiency. Furthermore, if targeted labeling is desired, precipitation is preferred over dialysis, since the reaction can continue under dialysis, yet at a much slower rate. To stop the reaction completely, the RITC-chitosan product must be precipitated such that the reaction does not continue. We also showed that the reaction is far from complete at 4 hours. However, at 18 hours, the reaction appears to be complete. We have achieved, a labeling efficiency of 0.5% mol/mol (4 hours, 3 injections), 1.0% (17 hours, 1 injection), and 1.3% mol RITC/mol chitosan (18 hours, 3 injection) using a starting concentration of [rho B]/[chitosan] of 3.2 % mol/mol and the precipitation recovery method. From the dialysis recovery method, we have achieved 0.8% (4 hours, 3 injections), 0.9% (18 hours, 3 injections), and 1.3% mol RITC/mol chitosan (17hours, 1 injection).

We next determined the type and quantity of acid used to solubilize chitosan in order to achieve a high and targeted labeling efficiency. We have measured the chitosan solution pH with varying quantities of acetic, lactic, or hydrochloric acid for various DDA chitosans ranging from 77.1 to 94.6% DDA. All of the pH curves (all DDAs tested) follow a single curve when the normalizing concentration is used. This factor is [acid]/[NH_2], expressed as a percentage, where [acid] is the molar concentration of acid and [NH_2] is the molar concentration of glucosamine monomers in the particular chitosan tested for a 1% wt/vol chitosan solution. We have determined that the chitosan does not precipitate after the addition of an equal volume of methanol to chitosan solution in the range of acid concentrations tested (70% -230% [acid]/[NH_2]) and that there is a cross-over point, where the pH changes from decreasing to increasing after the addition of equal volume methanol. This cross-over point is in the 90% [acid]/[/NH_2] range for lactic and hydrochloric acid and in the 60% [AcOOH]/[NH_2] range for acetic acid. The cross-over points indicate the point at which one could achieve the same labeling efficiency as predicted both before and after adding methanol.

For targeting labeling, the reaction kinetics had to be determined in order to establish the optimum reaction time. Earlier, we have verified that 4 hours is not enough for the reaction to reach completion and that 17 hours appeared to be sufficient. To resolve the doubt, and to test whether deacetylation level had an effect on labeling

efficiency, we performed reaction kinetics experiments on chitosans of varying DDAs. We have concluded that the fraction of RITC incorporated during the first few 7 hours increases considerably and that targeted labeling cannot be easily achieved during this period. After 18 hours, the fraction of RITC incorporated does not seem to vary noticeably even up to 72 hours. At 18 hours, both the 80.2% DDA and the 98.4% DDA reached ~50% incorporation of the RITC used in the reaction, while the 71.7% had reached 40% incorporation. In order to reach the same labeling efficiency, the amount of RITC used for the 70% DDA chitosans would have to be augmented by 10%.

We have determined that the molar derivatization of chitosan with RITC can be extrapolated from dilute chitosan solutions (5 to 50 μg/mL) of pH 5.0 to pH 6.0 in the absence of salt, using the extinction coefficient of rho B established at 90,100 $(M \cdot cm)^{-1}$ at λ_{abs} = 556 nm at maximal absorbance. Although fluorescence was slightly depressed at pH 2.5 and 150 mM NaCl, the RITC-chitosan was still fluorescent suggesting that RITC-chitosan internalized in endosomes or lysozomes could still be detected by live confocal microscopy.

The data presented in this thesis shows that targeted labeling of chitosan with RITC can be achieved. We have synthesized six RITC labeled chitosans of three DDA's (71.7%, 80%, and 92.7% DDA) and 2 MWs (~40 and ~140kDa) at very similar labeling efficiencies (0.9-1.0 % RITC mol/mol chitosan). Targeted labeling was achieved by using limiting amounts of acetic acid to dissolve the chitosan, and by controlling the reaction pH, temperature, and reaction time. We then used these six chitosans to determine whether DDA or MW had any influence on cell uptake.

At 50 μg/mL final concentration, the highly decorated RITC chitosans were neither toxic to rabbit bone marrow stromal cells nor human embryonic kidney cells. RITC-chitosan were seen within the cytoplasmic membrane and nearing the nucleus. We have conjectured that these particles would end up in endocytotic or lysosomal vesicles and our data suggest that the RITC-chitosans co-localized with LAMP-2-positive lysosomes. Two weeks after first incubation with RITC-chitosan, fluorescent particles were still visible in the cells after several passages, suggesting that the RITC-chitosan was metabolized and that the fluorescent breakdown products were incorporated into cell

structures. Alternatively, RITC-chitosan resistant to lysosomal degradation could persist in lysosomes and become inherited by partitioning of lysosomes to daughter cells during mitosis. Our data concerning HEK293 cells interacting with different DDA and MW indicate that higher DDA chitosans exhibit smaller particle size. However, MW does not affect particle size.

Chapter 8: Recommendations for Future Research

Future experiments using fluorescence activated cell sorting (FACS) of HEK293 cells exposed to this library of chitosans could show quantitatively whether uptake is affected by %DDA or molecular mass. Once the effects of DDA and MW are established, *in vitro* uptake of connective tissue cells and macrophages could be studied. Plans for *in vivo* fluorescent chitosan uptake studies in joint with cartilage defects are then possible.

Bibliography

ATCC. 2006. "Cell Biology Collection: Cell Biology Catalogue: CRL-1573". [Online] http://www.atcc.org/common/catalog/numSearch/numResults.cfm?atccNum=CRL-1573. (Consulted 1 February, 2006)

ALI, M.A., MOGHADDASI, J., AND AHMED, S.A. 1991. "Optical properties of cooled Rhodamine B in ethanol". *J. Opt. Soc.Am. B.* 8:9. 1807-1810.

AUSTIN, P.R. 1984. "Chitin solvents and solubility parameters". *Chitin, Chitosan, and Related Enzymes*. Zikakis, J.P. New York: Academic Press. P. 227.

BADGETT A, BONNER JC, BRODY AR. 1996. "Interferon-gamma modulates lung macrophage production of PDGF-BB and fibroblast growth". *Lipid Mediat Cell Signal.* 13. 89-97.

BASSLEER C, ROVATI L, FRANCHIMONT P. 1998. Stimulation of proteoglycan production by glucosamine sulfate in chondrocytes isolated from human osteoarthritic articular cartilage in vitro. *Osteoarthritis Cartilage*. 6. 427-34.

BAUER JA, RAO W, SMITH DJ. 1998. "Evaluation of linear polyethyleneimine/nitric oxide adduct on wound repair: therapy versus toxicity". *Wound Repair Regen.* 6. 569-77.

BECKMAN JS, BECKMAN TW, CHEN J, MARSHALL PA, FREEMAN BA. 1990. "Apparent hydroxyl radical production by peroxynitrite: implications for endothelial injury from nitric oxide and superoxide". *Proc Natl Acad Sci U S A.* 87.4. 1620-4.

BRACONNOT, H. 1811. "Sur la nature des champignons" . *Ann. Chi. Phys.* 79. 265-304.

CALDENTEY, J., HÄNNINEN, A-L., HOLOPAINEN, J.M., BAMFORD, J.K.H., KINNUNEN, P.K.J., AND BAMFORD, D.H. 1999. "Purification and characterization of the assembly factor P17 of the lipid-containing bacteriophage PRD1" *Eur. J. Biochem.* 260. 549-558.

CAPOZZA, R.C. 11 Nov 1976. *Solution of poly(N-acetyl-D-glucosamine.* [online] 8 p. Int. Cl. C08L 001/00; C07C 095/04. U.S. Patent. 3989535. http://freepatentsonline.com/3989535.html?highlight=capozza. (Consulted 1 Feb 2006)

CDC (Centers for Disease Control and Prevention). 2004. "Morbidity and Mortality Weekly Report". 53(18):388-389. http://www.cdc.gov/mmwr/preview/mmwrhtml/mm5318a3.htm. (Consulted 31 Jan 2006)

CHENITE A, CHAPUT C, WANG D, COMBES C, BUSCHMANN MD, HOEMANN CD, LEROUX JC, ATKINSON BL, BINETTE F, SELMANI A. 2000. Novel injectable neutral solutions of chitosan form biodegradable gels in situ. *Biomaterials*. 21. 2155-2161.

CHEVRIER, A., HOEMANN, C.D., SUN, J., AND BUSCHMANN, M.D. 2006. "Chitosan-glycerol phosphate/blood implants augment cell recruitment, transient vascularization and subcondral bone remodeling in drilled cartilage defects". *6th ICRS Symposium.* San Diego: International Cartilage Repair Society. P. 55-56.

CHEVRIER, A. 2005. *Application du chitosane pour la réparation de lésions du cartilage articulaire*. 205 p. Thèse de doctorat en génie biomédical, École Polytechnique de Montréal.

CUI, YL., QI, AI., LUI, WG., WANG, XH., WANG, H., MA, DM., YAO, KD. 2003. "Biomimetric surface modification of poly(L-lactic acid) with chitosan and its effects on articular chondrocytes in vitro". *Biomatierials.* 24. 3859-3868.

DOMARD, A.1987. "pH and CD measurements on a fully deacetylated chitosan: applications to Cu-polymer interactions". *Int. J. Biol. Macromol.* 9:2. 98-104.

DU, H.,F UH, R.A., LI, J.,CORKAN, A., LINDSEY, J.S. 1998. "PhotochemCAD: A computer-aided design and research tool in photochemistry," *Photochemistry and Photobiology.*68. 141-142.

DUNLOP DD, LYONS JS, MANHEIM LM, SONG J, CHANG RW. 2004. "Arthritis and heart disease as risk factors for major depression: the role of functional limitation". *Med Care*. 42:6. 502-11.

FELSON, DT. 1998. "Epidemiology of osteoarthritis". *Osteoarthritis*. Brandt, K. D, Doherty, M., and Lohmander, L. S. Osteoarthritis. New York :Oxford University Press. P. 13-22.

FELSON DT, LAWRENCE RC, DIEPPE PA, HIRSCH R, HELMICK CG, JORDAN JM, KINGTON RS, LANE NE, NEVITT MC, ZHANG Y, SOWERS M, MCALINDON T, SPECTOR TD, POOLE AR, YANOVSKI SZ, ATESHIAN G, SHARMA L, BUCKWALTER JA, BRANDT KD, FRIES JF. 2000. "Osteoarthritis: new insights. Part 1: the disease and its risk factors". *Ann Intern Med.* 133. 635–646.

FELSON DT, LAWRENCE RC, HOCHBERG MC, MCALINDON T, DIEPPE PA, MINOR MA, BLAIR SN, BERMAN BM, FRIES JF, WEINBERGER M, LORIG KR, JACOBS JJ, GOLDBERG V. 2000. "Osteoarthritis: new insights. Part 2: treatment approaches". *Ann Intern Med.* 133:9. 726-37.

FERNÀNDEZ-BUSQUETS, X. AND BURGER, M.M. 1995. "Use of Rhodamine B Isothiocyanate to Detect proteoglycan core proteins in polyacrylamide gels". *Analytical Biochemistry*. 227. 394-396.

FILION, D., LAVERTU, M., AND BUSCHMANN, M. 2005. "Titration and phase-separation of chitosan solution related to thermosensitive chitosan/glycerol-phosphate systerms". Submitted to *Biomacromolecules*. Nov 2 2005.

FOROUHAR, F., HUANG, W-N., LIU, J-H., CHIEN, K-Y., WU, W-G., AND HSIAO, C-D. 2003. "Structural Basis of Membrane-induced Cardiotoxin A3 Oligomerization" *J. Biol. Chem.*, 278:24. 21980-21988.

FRENKEL SR, SAADEH PB, MEHRARA BJ, CHIN GS, STEINBRECH DS, BRENT B, GITTES GK, LONGAKER MT. 2000. "Transforming growth factor beta superfamily members: role in cartilage modeling". *Plast Reconstr Surg*. 105:3. 980-90.

GRAHAM, F.L., SMILEY, J., RUSSELL, W.C., AND NAIRN, R. 1977. "Characteristics of a human cell line transformed by DNA from human adenovirus type 5". *J. Gen. Virol*. 36. 59-72.

GUO, T., ZHAO, J., CHANG, J., DING, Z., HONG, H., CHEN, J., AND ZHANG, J. 2006. "Porous chitosan-gelatin scaffold containing plasmid DNA encoding transforming growth factor-β1 for chondrocytes proliferation". Biomaterials. 27. 1095-1103.

HARPER, N., FARROW, S.N., KAPTEIN, A., COHEN, G.M., AND MACFARLANE, M. 2001. "Modulation of tumor necrosis factor apoptosis-inducing ligand- induced NF-kappa B activation by inhibition of apical caspases". *Journal of Biological Chemistry*. 276:37. 34743-52.

HOEMANN, C.D., HURTIG M., ROSSOMACHA E., SUN J., CHEVRIER A., SHIVE M.S., AND BUSCHMANN M.D. 2005. "Chitosan-glycerol phosphate/blood implants improve hyaline cartilage repair in ovine microfracture defects" *J Bone Joint Surg Am*. 87:12. 2671-86.

HOEMANN, C.D., HURTIG, M., ROSSOMACHA, E., SHIVE, MS., AND BUSCHMANN, MD. 2006. "Chitosan-glycerol phosphate/blood clots adhere more than marrow-derived clots to ovine microfracture defects". *6th ICRS Symposium.* San Diego: International Cartilage Repair Society. P. 113-114.

HOOTMAN JM, HELMICK CG, SCHAPPERT SM. 2002. "Magnitude and characteristics of arthritis and other rheumatic conditions on ambulatory medical care visits, United States, 1997". *Arthritis Rheum.* 47. 571-581.

HUANG, M., MA, Z., KHOR E., LIM LY. 2002. " Uptake of FITC-Chitosan Nanoparticles by A549 Cells". *Pharmaceutical Research.* 19:10. 1488-1494.

HUANG, M., KHOR, E., LIM, LY. 2004. "Uptake and Cytotoxicity of Chitosan Molecules and Nanoparticles : Effects of Molecular Weight and Degree of Deacetylation". *Phamaceutical Research.* 21:2. 344-353.

HWANG, S-M., CHEN C-Y., CHEN S-S., AND CHEN J-C. 2000. "Chitinous materials inhibit nitric oxide production by activated RAW 267.4 macrophages". Biochemical *and biophysical research communications.* 271. 229-233.

IGNOTZ RA. and MASSAGUE J. 1986. "Transforming growth-factor-beta stimulates the expression of fibronectin and collagen and their incorporation into the extracellular-matrix". J. Biol. Chem. 261:9. 4337-4345.

ISHII, T., OKAHATA, Y., SATO, T., 2001. "Mechanism of cell transfection with plasmid/chitosan complexes". *Biochimica et Biophyusica Acta.* 1514. 51-64.

KANG, K., GAPINSKI, J., LETTINGA, M.P., BUITENHUIS, J., MEIER, G., RATAJCZYK, M., DHONT, J.K.G., PATKOWSKI, A. 2005. "Diffusion of spheres in crowded suspensions of rods" *J. Chem. Phys.* 122, 044905-1-13.

KIANG T, WEN J, LIM HW, LEONG KW. 2004. "The effect of the degree of chitosan deacetylation on the efficiency of gene transfection". *Biomaterials.* 22. 5293-301.

KIM, M-S., SUNG, M-J., SEO, S-B, YOO, SU-J., LIM, W-K., KIM, H-M. 2002. "Water-soluble chitosan inhibits the production of pro-inflammatory cytokine in human astrocytoma cells activated by amyloid β peptide and interleukin -1 β". *Nanoscience Letters.* 321. 105-109.

KÖPING-HÖGGÅRD M., TUBULEKAS, I., GUAN, H., EDWARDS, K., NILSSON, M., VÅRUM, KM, and ARTURSSON, P. 2001. "Chitosan as a nonviral gene delivery system. Structure-property relationships and characteristics compared with polyethyleneimine in vitro and after lung administration in vivo". *Gene Ther.* 8. 1108–1121.

KÖPING-HÖGGÅRD M, MEL'NIKOVA YS, VÅRUM KM, LINDMAN B, ARTURSSON P. 2003. "Relationship between the physical shape and the efficiency of oligomeric chitosan as a gene delivery system in vitro and in vivo". *J Gene Med.* 5:2. 130-41.

Lakowicz, J. R. 1983. *Principles of Fluorescence Spectroscopy.* 1st edition. New York: Plenum Press. 516p.

LAMPRECHT, A., SCHÄFER, U., AND LEHR, C-M. 2000. "Structural Analysis of Microparticles by confocal laser scanning microscopy". *AAPS PharmSciTech*, 1:3. Article 17. 1-10.

LASKIN, DL AND PENDINO, KJ. 1995. "Macrophages and inflammatory mediators in tissue injury". *Annu Rev Pharmacol Toxicol.* 35. 655-77.

LEE, D-Y., CHOI, I-S., HAN, J-H., YOO, H-S. 2002. "Chitosan and D-Glucosamine Induce Expression of Th1 cytokine genes in porcine spleen cells. *J. Vet. Med. Sci.* 64:7. 645-648.

LETHBRIDGE-CEJKU M, HELMICK CG, POPOVIC JR. 2003. "Hospitalizations for arthritis and other rheumatic conditions: data from the 1997 National Hospital Discharge Survey". *Med Care.* 41:12.1367-73.

LU, J.X., PRUDHOMMEAUX, F., MEUNIER, A., SEDEL, L., AND GUILLEMIN, G. 1999. "Effects of chitosan on rat knee cartilages". *Biomaterials.* 20. 1937-1944.

LUCKACHAN, G.E. AND PILLAI, C.K.S. 2006. "Chitosan/oligo L-lactide graft copolymers: Effect of hydrophobic side chains on the physico-chemical properties and biodegradability". *Carobohydrate Polymers* xx 1-13. Article in Press.

MILLIS MB, MURPHY SB, POSS R. 1996. "Osteotomies about the hip for the prevention and treatment of osteoarthritis". *Instr Course Lect.* 45:209-26.

MOLECULAR PROBES. 2005. "Amine Reactive Probes". [Online] http://probes.invitrogen.com/media/pis/mp00143.pdf?id=mp00143. (Consulted 1 February, 2006)

MOLECULAR PROBES. 2005. "Introduction to Amine Modification" [online] http://probes.invitrogen.com/handbook/sections/0101.html. (Consulted 1 February, 2006)

MOLECULAR PROBES. 2006. "Long-wavelength Rhodamines, texas red dyes and QSY quenchers". [Online] http://probes.invitrogen.com/handbook/sections/0106.html. (Consulted 2 February, 2006)

MONCADA S, HIGGS A. 1993. "The L-arginine-nitric oxide pathway". *N Engl J Med.* 1993 329:27. 2002-12.

MUN S, DECKER EA, MCCLEMENTS DJ. 2005. "Effect of molecular weight and degree of deacetylation of chitosan on the formation of oil-in-water emulsions stabilized by surfactant-chitosan membranes". *J Colloid Interface Sci.* xx 1-10. Article in Press.

NAIRN, R.C. 1976. *Fluorescent Protein Tracing.* 4th edition. Edingburgh: Churchill Livingstone. 648p.

NAKAJIMA, M., ATSUMI, K., AND KIFUNE, K. 1985. Effects on wound healing acceleration by chitin absorbable suture. *Saishin Igaku* 40. 1958-1960.
NAKAJIMA, M., ATSUMI, K., KIRUNE, K., MIURA, K., AND KANAMARU, H. 1986. "Chitin is an effective material for sutures". *Japanese Journal of Surgery.* 16. 418-424.

NIAMS (National Institute of Arthritis and Musculoskeletal and Skin Disease). 2002. "Handout on health: Osteoarthritis." [online] http://www.niams.nih.gov/hi/topics/arthritis/oahandout.htm. (Consulted 31 January 2006)

ONISHI, H. AND MACHIDA, Y., 1999. "Biodegradation and distribution of water-soluble chitosan in mice". *Biomaterials.* 20. 175-182.

PALAPURA, S. and KOHN, J. 1992. Trends in the development of bioresorbable polymers for medical application. *Journal of Biomaterial Applications.* 6. 216-250.

PANCHUCK-VOLOSHINA, N., HAUGLAND, R.P., BISHOP-STEWART, J. BHALGAT, M.K., MILLARD, P.J., MAO, F. LEUNG, W-Y., HAUGLAND, R. 1999. "Alexa dyes, a series of new fluorescent dyes that yield exceptionally bright, photostable conjugates". *The Journal of Histochemistry & Cytochemistry.* 47:9. 1179-1188.

PARK, J.W., CHOI, K-H. AND PARK, K.K. 1983. "Acid-base Equilibria and Related Properties of Chitosan". *Bull. Korean Chem. Soc.* 4. 68-72.

POLA E, PAPALEO P, POLA R, GAETANI E, TAMBURELLI FC, AULISA L, LOGROSCINO CA. 2005. "Interleukin-6 gene polymorphism and risk of osteoarthritis of the hip: a case-control study". *Osteoarthritis Cartilage.* 13:11.1025-8.

PRUDDEN, J.F., MIGEL, P., HANSON, P., FREIDRICH, L., AND BALASSA, L. 1970. "The discovery of a potent pure chemical wound-healing accelerator". *American Journal of Surgery.* 119. 560-564.

PUBLIC HEALTH AGENCY OF CANADA. 1999. "Canada's Seniors A growing population". [Online] http://www.hc-sc.gc.ca/seniors-aines/pubs/factoids/1999/pdf/entire_e.pdf. (Consulted 6 February, 2006)

QAQISH, R., AMIJI M. ,1999. "Synthesis of a fluorescent chitosan derivative and its application for the study of chitosan-mucin interactions". *Carbohydrate Polymers.* 38. 99-107.

RAO JK, MIHALIAK K, KROENKE K, BRADLEY J, TIERNEY WM, WEINBERGER M. 1999. "Use of complementary therapies for arthritis among patients of rheumatologists". *Ann Intern Med.*131. 409-16.

RHAZI, M., DESBRIERES, J., TOLAIMATE, A., ALAGUI, A., VOTTERO, P. 2000. "Investigation of different natural sources of chitin: influence of the source and deacetylation process on the physicochemical characteristics of chitosan". *Polym Int.* 49. 337-344.

RINAUDO, M., AUZELY, R., VALLIN, C., AND MULLAGALIEV, I. 2005. "Specific interactions in modified chitosan systems". *Biomacromolecules.* 6. 2396-2407.

RINAUDO M, PAVLOV G, DESBRIERES J. 1999. "Solubilization of chitosan in strong acid medium". *International Journal Of Polymer Analysis And Characterization.* 5:3. 267-276.

RINAUDO M, PAVLOV G, DESBRIERES J. 1999. "Influence of acetic acid concentration on the solubilization of chitosan". *Polymer.* 40:25. 7029-7032.

ROBERTS, George AF. 1992. *Chitin Chemistry*, ed. G.A.E. Roberts, Macmillan Press, Ltd, London, pp. vii, 224-227.

ROTH A, MOLLENHAUER J, WAGNER A, FUHRMANN R, STRAUB A, VENBROCKS RA, PETROW P, BRAUER R, SCHUBERT H, OZEGOWSKI J, PESCHEL G, MULLER PJ, KINNE RW. 2005. "Intra-articular injections of high-molecular-weight hyaluronic acid have biphasic effects on joint inflammation and destruction in rat antigen-induced arthritis". *Arthritis Res Ther.* 7:3. R677-86.

SAPELLI P.L., BALDASSARRE, V., MUZZARELLI, R.A.A., AND EMANUELLI, M. 1986. "The use of chitosan in densitry". *Chitin Nature and Technology.* MUZZARELLI, R.A.A., JEUNIAX, C. AND GOODAY, G.W. New York: Plenum Press. 507-512.

SASHIWA, H. and SHIGEMASA, Y. 1999. "Chemical modification of chitin and chitossan 2: preparation and water soluble property of N-acylated or N-alkylated partially deacetylated chitins". *Carbohydrate Polymers.* 39. 127-138.

SEO, H. 1990. "Processing and Utilization of Chitin and Chitosan". *Sen-i Gakkaishi.* 46. 564-569.

SEO, S-B., JEONG, H-J., CHUNG, H-S., LEE, J-D., YOU, Y-O, KAJIUCHI, T., KIM, H-M. 2003. "Inhibitory effect of high molecular weight water-soluble chitosan on hypoxia-induced inflammatory cytokine production". *Biol. Pharm. Bull.* 26:5. 717-721.

SHEARER JD, RICHARDS JR, MILLS CD, AND CALDWELL MD. 1997. "Differential regulation of macrophage arginine metabolism: a proposed role in wound healing". *Am J Physiol.* 272:2 Pt 1. E181-90.

SHEPHERD, R., READER, S., AND FALSHAW, A. 1997. "Chitosan functional prorperties". *Glycoconjugate Journal.* 14. 535-542.

SIGMA ALDRICH. 2006. "Fluorescein Isiothiocyanate Product Information". [Online] http://www.sigmaaldrich.com/sigma/product%20information%20sheet/f7250pis.pdf. (Consulted 2 February, 2006)

SKOOG, DOUGLAS A., HOLLER, F JAMES, NIEMANN, TIMONTHY A. Principles of Instrumental Analysis. Fifth Edition. Harcourt. 1999. 849p

STAHL S, KARSH-ZAFRIR I, RATZON N, ROSENBERG N. 2005. "Comparison of intraarticular injection of depot corticosteroid and hyaluronic acid for treatment of degenerative trapeziometacarpal joints". *J Clin Rheumatol.* 11:6. 299-302.

STASTICS CANADA. 2005. "Persons with arthritis or rheumatism by age and sex". http://www40.statcan.ca/l01/cst01/health51a.htm?sdi=arthritis. (Consulted the 31 January 2006)

STATISTICS CANADA. 2005. "Population by sex and age group". [Online]. http://www40.statcan.ca/l01/cst01/demo10a.htm?sdi=age%20sex. (Consulted the 6 February 2006)

STUEHR DJ, NATHAN CF. 1989. "Nitric oxide. A macrophage product responsible for cytostasis and respiratory inhibition in tumor target cells". *J Exp Med.* 169:5. 1543-55.

THANOS S, VIDAL-SANZ M, AGUAYO AJ. 1987. "The use of Rhodamine-B-isothiocyanate (RITC) as an anterograde and retrograde tracer in the adult rat visual system". *Brain Res.* 406:1-2. 317-321.

TOKURA, S., NISHI, N., NISHIMURA, S. AND SOMORIN, O. 1983. "Lysozyme-Accessible Fibers from Chitin and its Derivatives". *Sen-i Gakkaishi.* 39. 507-511.

TOMMERAAS K, STRAND SP, TIAN W, KENNE L, VARUM KM. 2001. "Preparation and characterization of fluorescent chitosans using 9-anthraldehyde as fluorophore". *Carbohydrate Research.* 336. 291-296.

UEBELHART D, THONAR EJ, ZHANG J, WILLIAMS JM. 1998. "Protective effect of exogenouschondroitin 4,6-sulfate in the acute degradation of articular cartilage in the rabbit". *Osteoarthritis Cartilage.* 6(Suppl A). 6-13.

UENO, H., MURAKAMI, M., OKUMURA, M., KADOSAWA, T., UEDE, T., AND FUJINAGA, T. 2001a "Chitosan accelerates the production of osteopontin from polymorphonuclear leukocytes". Biomaterials. 22. 1667-1673.

UENO, H., NAKAMURA, F., MURAKAMI, M, OKUMURA, M., KADOSAWA, T., FUJINAGA, T. 2001b. "Evaluation effects of chitosan for the extracellular matrix production by firborblasts and the growth factors production by macrophages". *Biomaterials.* 22. 2125-2130.

U.S. Census Bureau. 2004. "Projected Population of the United States, by Age and Sex: 200 to 2050". [online]. http://www.census.gov/ipc/www/usinterimproj/. (Consulted 6 January 2006)

VACHOUD L, ZYDOWICZ N, DOMARD A. 1997. "Formation and characterisation of a physical chitin gel". *Carbohydrate Research.* 302:3-4. 169-177.

VERHAEGH, N.A.M. AND VAN BLAADEREN. 1994. "Dispersions of rhodamine-labeled silica spheres: synthesis, characterization, and fluorescence confocal scanning laser microscopy". *Langmuir.* 10:5. 1427-1438.

VON WIEMARN, P.P., 1927. "Conversion of fibroin, chitin, casein, and similar substances into the Ropy-Plastic State and Colloidal Solution". *Ind. Eng. Chem.* 19. 109-110.

VULT VON STEYERN, F., JOSEFSSON, J-O., AND TÅGERUD, S. 1996. "Rhodamine B, a fluorescent probe for acidic organelles in denervated skeletal muscle". *The Journal of Histochemistry and Cytochemistry.* 44:3. 267-274.

WALSTON J, ARKING DE, FALLIN D, LI T, BEAMER B, XUE Q, FERRUCCI L, FRIED LP, AND CHAKRAVARTI A. 2005. "IL-6 gene variation is not associated with increased serum levels of IL-6, muscle, weakness, or frailty in older women". *Exp Gerontol.* 40:4.344-52.

YAMADA, T., ONISHI, H., MACHIDA, Y. 2001. "In Vitro and in Vivo Evaluation of Sustained Release Chitosan-Coated Ketoprofen Microparticles". *Yakugaku Zasshi.* 121:3. 239-245.

YANO, H., IRIYAMA, K., NISHIWAKI, H. AND KIHUNE, K.1985. "Effects of N-Acetyl-D-glucosamine on Wound Healing in Rats". *Mie Medical Journal.* 35. 53-56.

ZHAO, Q., AGGER, M.P. FITZPATRICK, M., ANDERSON, J.M., HILTNER, A., STOKES, K. and IRANSKI, P. 1990. "Cellular interactions with biomaterials: in vivo cracking of prestressed Pellethane 2363-80A". *Journal of Biomedical and Materials Research.* 24. 621-637.

ZHU, A., LUI, J., YE, W. 2006. "Effective loading and controlled release of camptothecin by O-carboxymethylchitosan aggregates". *Carbohydrate Polymers*. 63.89-96.